

The production of foot-and-mouth disease virus-like particles in the plant *Nicotiana benthamiana*: a potential candidate vaccine for foot-and-mouth disease

By

Steven Patrick O'Connor



Thesis presented for the
Degree of MASTER OF SCIENCE
In the
Department of Molecular and Cell Biology
UNIVERSITY OF CAPE TOWN

The copyright of this thesis vests in the author. No quotation from it or information derived from it is to be published without full acknowledgement of the source. The thesis is to be used for private study or non-commercial research purposes only.

Published by the University of Cape Town (UCT) in terms of the non-exclusive license granted to UCT by the author.

Abstract

Foot and mouth disease virus (FMDV) infects cloven-hoofed animals causing the highly contagious foot and mouth disease. It is spread by contact or through aerosol. The disease is often debilitating for infected animals and can be fatal. Severe measures are taken to contain outbreaks; quarantine and trade restrictions are imposed and herds with infected individuals are culled to prevent the spread of the disease. Consequently, outbreaks of the disease have drastic implications for agriculture and social economies which can be devastating for affected countries. There are seven serotypes of the virus; of which SAT1, SAT2, and SAT3 are endemic to Africa. South African buffalo populations such as those in the Kruger National Park, are natural carriers of FMDV (Thomson 1995). Careful monitoring and regular vaccination are necessary to detect and prevent outbreaks and the spread of the disease to livestock of neighbouring areas and farms. The vaccines currently used are inactivated FMDV virions. These are produced in cell culture, an expensive process that requires high levels of biosafety. Furthermore, inactivated virions present non-structural proteins (NSPs) and thus cannot be distinguished from the infectious virus by imported ELISA kits that utilise the NSPs as coating antigens and conventionally produced detecting antibodies.

We aimed to use recombinant constructs encoding the FMDV capsid and protease genes, cloned into the different vectors; pRIC, pEAQ and pTRAc, for transient expression in *Nicotiana benthamiana* to generate virus-like particles as an alternative vaccine candidate. Using a plant based expression system presents numerous advantages over the traditional cell culture production of the vaccine currently used.

After having synthesised the FMDV genes P12A and 3C, the fusion gene P1-2A-3C (required for the vaccine) was cloned into these different plant expression vectors available in our laboratory. With *Agrobacterium* mediated infiltration of *N. benthamiana*, we demonstrated expression of recombinant protein by western blotting; and Coomassie stain, for each of the different constructs. Analytical ultra-centrifugation through a sucrose gradient was used to purify protein extracts. Comparison against a dilution series of bovine serum albumin was used to quantify the yield for each respective vector construct by densitometry. Transmission Electron Microscopy (TEM) imaging was used to qualitatively determine virus-like particle (VLP) assembly.

In conclusion, we demonstrate proof of concept for a viable alternative approach for the production of a candidate vaccine for FMDV.

Declaration

I, Steven O'Connor, declare that this dissertation is my own work.

I know the meaning of plagiarism and declare that all of the work in the document, save for that which is properly acknowledged, is my own.

I have used the Harvard (author, date) convention to cite other sources of information.

Steven O'Connor

Acknowledgments

A Master's thesis is a feat not accomplished in an individual capacity; I thus wish to thank and acknowledge the following people without whose contributions this thesis would not have materialised:

My supervisors, Dr Ann Meyers and Professor Edward Rybicki for providing me the opportunity to embark on this journey of learning, and for the assistance offered every step along the way. I thank you especially for your patience particularly when not all those steps were taken in the right direction.

All the members of the MCB BRU, both seasoned academics and students who all contribute to an amazing learning environment and welcoming atmosphere. A special mention of thanks to Aleyo Chebada and Francisco "Pedro" Pera whose constant presence over the two years from their neighbouring benches were the source of invaluable knowledge, advice, and the greatest humour. Varusha Veerpan and Scot DeBeer, working on related projects, generously provided help, assistance and good advice whenever called upon. Alta van Zyl and Sandiswa Mbewana as senior members in the lab provided sound advice and frequent assistance, especially with ultracentrifugation.

Mr Mohammed Jaffer and Innocent at the Electron Microscopy Unit for assisting with microscopic analysis of my samples

Instituto de Virología, C.I.C.V., INTA-Castelar, Buenos Aires, Argentina: the collaborating Argentinian lab for providing the anti-FMDV antiserum and original FMDV DNA and GenScript for sequencing the DNA

Vanessa Ruiz for preliminary work cloning the P12A3C gene into pEAQ and pRIC3.0 plasmids that were used for comparison in this project

My parents Jo-Anne Stevens -O'Connor and Tim O'Connor, for their support and encouragement through the time on this project.

Poliomyelitis Research Foundation, for providing me with the funding to do this project.

Table of Contents

Abstract.....	i
Declaration	ii
Acknowledgments.....	iii
Table of Contents	iv
Frequently used Abbreviations.....	vi
Chapter 1	1
Introduction and Literature Review	1
1.1 Economic importance and burden of Foot-and-Mouth Disease	1
1.2 Virology.....	2
1.2.1 <i>Distribution</i>	2
1.2.2 <i>Virus Structure</i>	4
1.3 Vaccines	6
1.3.1 <i>Current vaccines for FMD</i>	6
1.3.2 <i>Aftovax vaccine</i>	7
1.3.3 <i>Virus like particles</i>	8
1.4 Protein Expression.....	9
1.4.1 <i>Expression in a bacterial system</i>	9
1.4.2 <i>Expression in Yeast system</i>	10
1.4.3 <i>Expression in insect cell culture systems</i>	11
1.4.4 <i>Mammalian cell culture expression system</i>	12
1.4.5 <i>Expression in plant systems</i>	13
1.5 Project aims	16
Chapter 2:	17
Bacterial Expression of FMDV P12A in E. coli.....	17
2.1 Overview.....	17
2.2 Materials and Methods.....	19
2.2.1 <i>PCR amplification of P12A fragment</i>	19
2.2.2 <i>Cloning of P12A into pProEx HTa E. coli expression vector</i>	22
2.2.3 <i>P12A induced expression</i>	24
2.2.4 <i>Protein analysis by SDS PAGE, Western Blot, Coomassie Blue stain</i>	24
2.2.5 <i>Scaled up induction of P12A expression</i>	25
2.2.6 <i>Purification of P12A using affinity chromatography</i>	26
2.3 Results.....	28
2.3.1 <i>PCR amplification of P12A and restriction enzyme digest of pProEX</i>	28
2.3.2 <i>cloning of P12A into pProEX and transformation</i>	29
2.3.3 <i>Induced expression of P12A with IPTG</i>	30

2.3.4	<i>Protein purification of up scaled expression</i>	31
2.4	Discussion	34
Chapter 3	35
Plant expression and yield quantification of FMDV structural proteins and VLP formation		35
3.1	Overview	35
3.2	Materials and methods	36
3.2.2	<i>Transformation of pTRAc-P12A3C into E. coli and A. tumefaciens</i>	39
3.2.3	<i>Small scale syringe infiltration of N. benthamiana leaves</i>	41
3.2.4	<i>Large scale vacuum infiltration of N. benthamiana</i>	42
3.2.5	<i>Processing of large-scale infiltrated leaves</i>	42
3.2.6	<i>Sucrose gradient purification of VLPs</i>	43
3.2.7	<i>Analysis of gradient fractions</i>	43
3.2.8	<i>Protein quantification</i>	44
3.3	Results	46
3.3.1	<i>Plant expression vector construction – pTRAc-P12A3C</i>	46
3.3.2	<i>Syringe Infiltration Plant expression protein analysis</i>	47
3.3.3	<i>Up-scaled plant protein analysis comparing different vectors</i>	49
3.3.4	<i>Sucrose gradient purification protein analysis</i>	49
3.3.5	<i>Transmission electron microscopy</i>	55
3.4	Summary and discussion	60
Chapter 4	65
References	69
Appendices	77
Appendix A:	<i>P12A3C Nicotiana optimised DNA sequence</i>	77
Appendix B:	Composition of Buffers and Solutions	81
Appendix C:	FMDV capsid protein quantification	85
Protein yield calculations by SynGene™ software for pTRAc-P12A3C produced protein		85
Protein yield calculations by SynGene™ software for pRIC3.0--P12A3C		99

Frequently used Abbreviations

BSA	bovine serum albumin
DNA	deoxyribonucleic acid
Dpi	days post-infiltration
ELISA	enzyme-linked immunosorbant assay
FMD	Foot and mouth disease
FMDV	Foot and mouth disease virus
His-tag	6 x histidine sequence
LB	Luria-Bertani Broth media (composition detailed in appendix)
LLB	Luria – Lennox Broth media (composition detailed in appendix)
NSP	non-structural protein
ORF	open reading frame
PBS	phosphate buffered saline
PCR	polymerase chain reaction
P12A	oligopeptide of FMDV structural protein precursor
<i>P12A</i>	<i>Gene encoding the P12A oligopeptide</i>
P21A3C	oligopeptide of FMDV structural protein precursor with 3C protease included
<i>P12A3C</i>	<i>Gene encoding the P12A3C oligopeptide</i>
RNA	ribonucleic acid
SAB	sample application buffer (composition detailed in appendix)
SAT	Southern African territories serotype
SDS	sodium dodecyl sulphate
SDS-PAGE	sodium dodecyl sulphate - polyacrylamide gel electrophoresis
TEM	transmission electron microscope
VLP	virus-like particle
SP	structural protein
VP	viral protein

Chapter 1

Introduction and Literature Review

1.1 Economic importance and burden of Foot-and-Mouth Disease

Foot and Mouth Disease (FMD) is the most economically devastating viral disease of domestic livestock (Wernery & Kaaden 2004). FMD infects ruminants and other cloven hoofed animals; of particular importance are livestock such as cattle, sheep, and pigs (Domingo et al. 2003). The disease is both highly infectious and contagious; spreading rapidly from one animal to another through air by inhalation of aerosols, by contact, either directly or via fomites, or ingestion (Parthiban et al. 2015; Bravo De Rueda et al. 2014; Canadian Food Inspection Agency n.d.; Arzt et al. 2010). The rate of morbidity of this disease will often approach or reach 100% in immunologically naive animals (Jemberu et al. 2014). Because of the infectious and highly contagious nature of the disease, farmers in many areas are forced to cull entire herds of livestock in order to prevent the spread of the disease in the case of an infection (Bravo De Rueda et al. 2014). Outbreaks of foot and mouth disease thus have dire consequences; causing large numbers of livestock to be culled, entire regions to be quarantined, and trade bans to be implemented. The resulting financial toll on the farmers can be devastating, so too are the major impacts on the agricultural industries and economies of affected countries (Segarra & Rawson 2001; Robinson et al. 2016a). The outbreak of FMD in the United Kingdom during 2001 is estimated to have cost up to 8 billion Pounds and necessitated the slaughter of approximately 10 million sheep and cattle (Segarra & Rawson 2001). Quarantine measures taken in order to restrict the movement of infected animals and contain the disease also have an environmental impact on ecological conservation, limiting the movement of other animals in these areas (Somers & Hayward 2012).

Animals infected by the disease can be symptomatic to varying degrees, among and within species. Symptoms include: fever, blisters and calluses, or lesions on the feet, as well as lips, tongue, gums,

palate, and throat. Ruptured vesicles or blisters can be the source of much pain and discomfort for the animals. The severity of these ailments can be severely debilitating and will often render the animal lame. In some cases, infection can prove fatal, although the disease is not necessarily considered lethal. The mortality rate does not typically exceed 5% in adult livestock, although this varies among species and mortality may reach levels of over 75% in infant animals – suckling piglets may exhibit mortality rates of as much as 100% (Brown 1995). Death from FMD may come as a result of myocarditis (Stenfeldt et al. 2014). Infection can also drastically hamper milk production and this may persist indefinitely beyond the duration of the infection. The lesions created by the disease are also susceptible to secondary bacterial infections. In addition to this, those animals with ruptured lesions in the mouth, or rendered lame by the disease, cannot eat and typically also suffer from starvation. Studies characterising the pathogenesis of FMD have been conducted predominantly in cattle and pigs. Cattle become infected most typically by aerosolized virus through the respiratory tract.

1.2 Virology

1.2.1 *Distribution*

The disease is caused by the foot and mouth disease virus (FMDV) of the *Aphthovirus* genus from the family Picornaviridea (Domingo et al. 2003). There are seven serotypes of this virus: type O, A, C, Southern Africa Territories 1 (SAT-1), SAT-2, SAT-3, and Asia-1 (Domingo et al. 2003). The distribution of each respective strain is illustrated in Figure 1.1. Infections by this virus have been recorded throughout the globe and it is regarded as endemic to areas in Africa, Asia and South America. The Buffalo (*Syncerus caffer*) populations of Southern Africa, such as those in the Kruger National Park, are typically natural and asymptomatic hosts of FMDV, specifically stereotypes SAT-1, 2, and 3. Buffalo thus act as reservoirs of the virus (Robinson et al. 2016a; Robinson et al. 2016c; Thomson 1995). Animal containment with strict and rigorous screening and vaccination is necessary to

prevent the spread of the virus into the neighbouring farming regions. The continual screening and vaccination is costly for farmers and government.

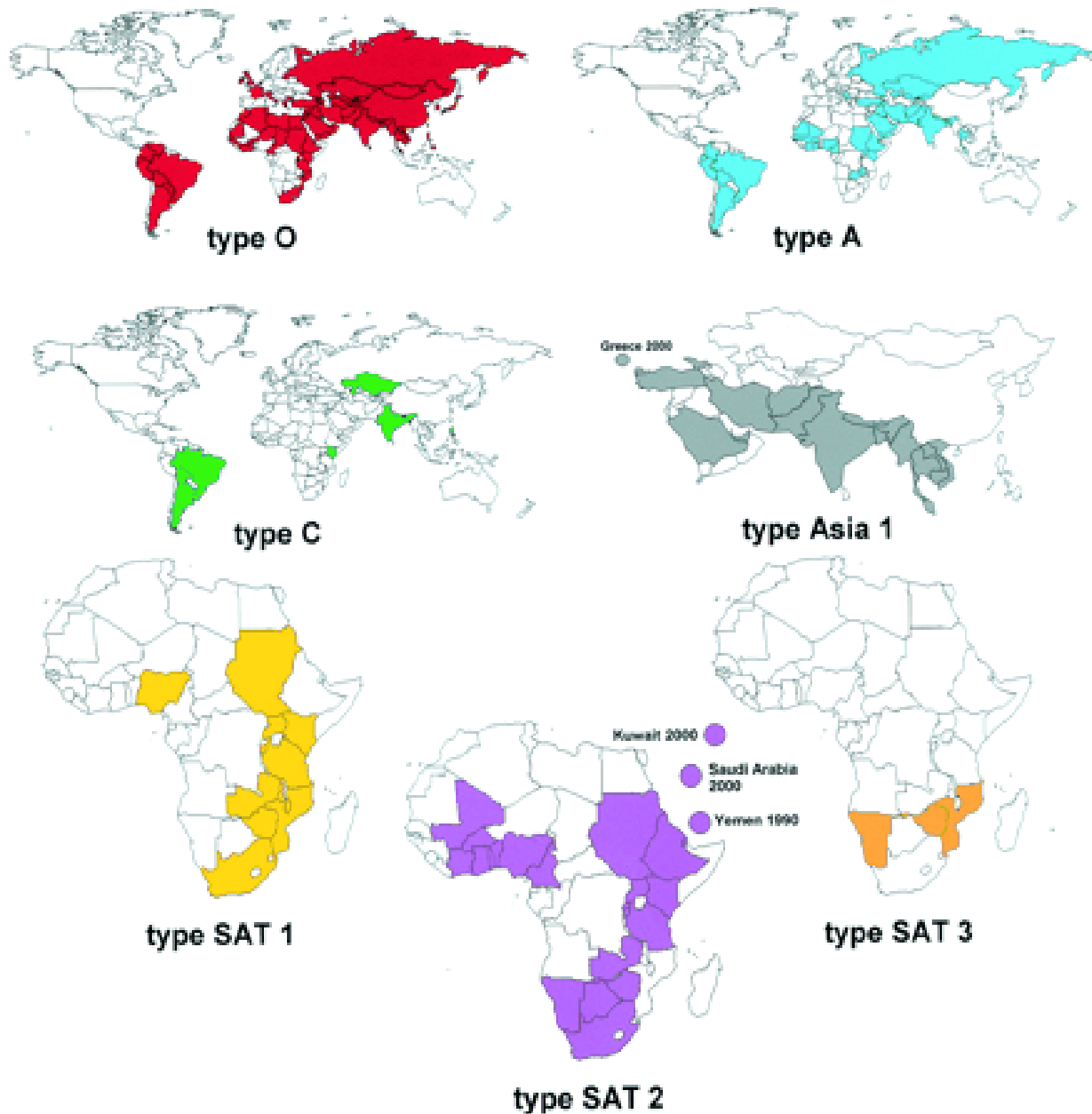


Figure 1.1: Countries in which respective serotypes of FMD were reported to the OIE between 1990 and 2002. The data and maps were compiled by Nick Knowles and can be found at www.iah.bbsrc.ac.uk/virus/picornaviridae/aphthovirus. Image sourced from the review by Grubman and Baxt and reproduced with permission (Grubman & Baxt 2004)

1.2.2 Virus Structure

FMDV is a single stranded RNA virus. The RNA is encapsulated in an icosahedral capsid constructed from 60 protomeric assemblies of four structural proteins, arranged in 12 pentameric copies. The capsid is typically 25 to 30 nm in diameter (Cao et al. 2009). The structure described is illustrated in Figure 1.2. The positive sense strand of RNA is translated into a single oligopeptide of the viral proteins upon entering the host cell. During translation, cleavage by the 2A protease yields the P12A subunit, subsequent cleavage by the 3C protease generates the VP0, VP1, and VP3. Finally upon assembly of the capsid; the VP0 precursor is cleaved to yield the VP2 and VP4 structural proteins (reviewed by Jamal & Belsham 2013). VP1, VP2, VP3 and VP4 thus comprise the structural proteins of FMDV derived from the P12A portion of the oligopeptide (Carrillo et al. 2005; Domingo et al. 2003). However, VP4 exists within the interior of the viral capsid, unexposed, and consequently is not antigenic. Two documented sites that are of immunogenic importance are the GH loop and C terminus of the polypeptide, which both occur on VP1. The GH loop binds to the host cell surface via an integrin receptor to enable the entry of the virus (Logan et al. 1993; K. Strohaimeier 1982; Martinez-Salas & Belsham 2017; Robinson et al. 2016d). The remaining P2 and P3 portions of the original oligopeptide comprise the precursors for the other non-structural proteins of FMDV. The virus induces high levels of translation of these viral proteins, which assemble into vast numbers of FMDV particles with encapsulated RNA within the host cell, thereby causing cell lysis, and thus releasing more live virus particles into the host. FMDV is likely the most rapidly replicating virus infecting mammalian cells; levels of viral RNA within cells equal that of cellular mRNA within a few hours (Martinez-Salas & Belsham 2017). Cell lysis can occur within 4 hours in infected ovine, bovine and porcine species (Grubman & Baxt 2004).

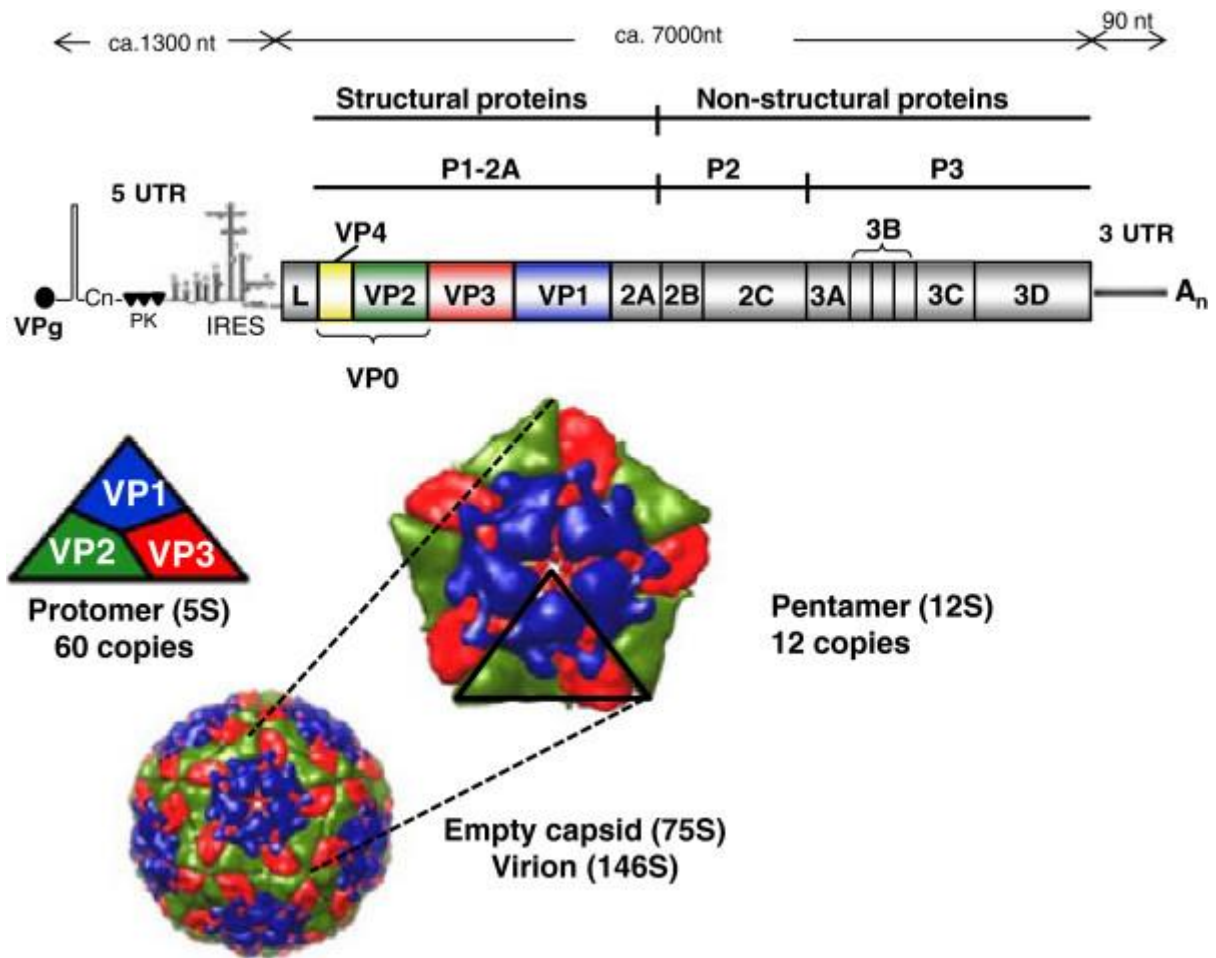


Figure 1.2. FMDV genome arrangement and particle structure morphology, presented in a review by Jamal and Belsham and reproduced with permission (Jamal & Belsham 2013).

1.3 Vaccines

A vaccine is typically a protective inoculation prepared from a biological source that serves to induce a cellular and humoral immune response in the host animal against a specific pathogen. This provides the host with active acquired immunity to protect it against future exposure to the same pathogen. Such a vaccine that prevents future infection is referred to as a prophylactic vaccine. Traditionally these vaccines were developed by the inactivation of virulent pathogens to impede their infectious nature, and are hence termed inactivated vaccines. Inactivation is achieved through either radiation, antibiotic, chemical, or heat destruction of the virulent pathogen (Ebert 1998). Further research in the field of Immunology, and the underlying mechanisms and principles upon which vaccines induce protection, has led to the development of other forms of vaccines. These include attenuated vaccines, sub-unit vaccines, conjugate vaccines, as well as other experimental forms of vaccines. An attenuated vaccine is a cultivated form of a pathogen which has been modified, usually at a nucleic acid and amino acid level, in order to reduce the virulence of the pathogen. These are typically viral vaccines (Jane Flint 2009; Ebert 1998). Inactivated and attenuated vaccines constitute whole agent vaccines. A subunit vaccine, by comparison, introduces only a representative protein or portion of the pathogen to the host immune system. Recognition of the relevant epitopes confers future immune protection against the parent pathogen. Similarly, a conjugate vaccine is a molecular fusion of a poorly immunogenic molecule endogenous to a pathogen (often a polysaccharide) with a more immunogenic protein, in order to induce the necessary immune response and memory against pathogen molecular epitopes that are otherwise not typically immunogenic (Jane Flint 2009).

1.3.1 *Current vaccines for FMD*

Current vaccines in use against FMDV are live inactivated virus particles (Mignaqui et al. 2013; Li et al. 2016; Robinson et al. 2016b; Smitsaart & Bergmann 2017). These are expensive to produce and

require a high level of biosafety for their production prior to the point at which they are deactivated. Furthermore, the use of the live inactivated virus carries the risk of accidental spread of the infectious diseases. This can result from escape of the virus from production facilities, or by vaccination with incompletely inactivated vaccine virus particles that results instead in viral infection (Doel 2003; Robinson et al. 2016b). It is suspected that a confirmed case of infection in Normandy, Surrey in the United Kingdom during 2007 was caused by such an escape. The strain of the virus was identified to be the same 01 BFS 67-like strain (De Clercq et al. 2008; BBC 2007a) that was being used in a nearby animal health Institute facility for vaccine production (BBC 2007b). The strain is not commonly found in animals and was otherwise not seen since an outbreak in 1967. Following confirmation of the disease, all animals in the vicinity were culled the next day and a nationwide ban across Britain was imposed on the movement of cattle and pigs. A protection zone and increased surveillance zone was established and, in the next month, two more cases of FMD were confirmed in the Egham area 20km away (DEFRA 2007). All at risk animals in the Egham area were also culled. This is but one incident that emphasises the legitimacy for concern of biosafety and the severity of the implications associated with such a vaccine. In addition to these concerns of biosafety, and the high cost of production; another problem presented by the current vaccines used is that the live inactivated virus particles cannot be effectively distinguished from the infectious version of the virus by standard imported ELISA test kits (Mignaqui et al. 2013; Blanco et al. 2017). This is because the ELISA test kits use antibodies developed against the non-structural proteins, and the whole inactivated live virus also contains these non-structural proteins and so these proteins are present in vaccinated animals as well as infected animals.

1.3.2 Aftovax vaccine

Despite the prevalence of FMD in South Africa and the resulting demand for a vaccine against FMDV, no commercially available vaccines are produced within this country's borders. Efforts to control

FMD in this country currently rely on importing vaccines from neighbouring Botswana where they are produced by the Botswana Vaccine Institute in conjunction with Merial (Joemat-Pettersson 2014). The produced vaccine is sold commercially branded as Aftovax. Aftovax is an inactivated foot and mouth disease virus composed of the five serotypes relevant to the region and incorporates the adjuvants aluminium hydroxide and saponin. The production process for Aftovax requires a period of 41 days to develop the vaccine, complete with product testing (Botswana Vaccine Institute 2013). The vaccine is administered in young animals by injection and boosters are required every four to six months until the animal reaches adulthood (Merial 2013).

1.3.3 Virus like particles

Virus like particles (VLPs) are empty capsids that are structural and immunological replicas of the original virus, but do not contain the genomic DNA and non-structural proteins that makes the virus infectious and virulent, but are equally immunogenic (Li et al. 2016). Consequently, VLPs are not infectious and thus do not present the same safety concerns as using live inactivated virus. Hence production facilities for VLPs will not require the same level of biosafety precautions. VLPs thus offer huge potential as alternative vaccine candidates. VLPs can induce an immunogenic response, without presenting the non-structural proteins of the parent virus, thus enabling them to be distinguished from the live infectious forms of the virus. These reasons contribute to the growing popularity towards using VLPs as an alternative vaccination method. VLPs are produced via recombinant protein expression of the viral capsid structural proteins, with subsequent folding and self-assembly of these proteins into a complete virus capsid.

1.4 Protein Expression

The production of VLPs thus requires an expression system for the expression of the recombinant protein. Various protein expression systems exist and each presents its own advantages and shortcomings. More specifically relevant to this project, FMDV structural, non-structural, and indeed, as is our aim, entire viral capsids have been successfully expressed in a range of different expression systems. These systems include bacterial, yeast, insect and mammalian cell culture.

1.4.1 *Expression in a bacterial system*

A bacterial expression system is a well-established system and remains a typical favourite for the production of recombinant proteins in the pharmaceutical industry because of its low cost and high productivity. Bacterial expression systems have been used successfully for the production of recombinant protein in a number of bacterial species but are most well characterised by the species *Escherichia coli*. Bacteria such as *E. coli* can easily be cultured in large volumes and at high densities very rapidly to produce desired recombinant protein (Terpe 2006). This particular platform of expression is appealing because the *E. coli* can easily be transformed to include the genes for the recombinant protein. The extensive research done on *E. coli* has produced numerous strains specific for various purposes and has enabled the process to be well optimised. Specific strains and vectors compatible with *E. coli* have been designed to allow for selective induced expression by various selective promoters such as the araBAD promoter (PBAD), the L-rhamnose inducible rhaPBAD promoter and, relevant to work done in this project, the lac promoter (discussed later).

A major shortcoming of bacterial expression systems is that bacterial cells are not eukaryotic and consequently do not perform the same post-translational modifications of proteins as those of eukaryotic cells. There is no glycosylation of proteins and no chaperone proteins to assist in the nature of folding as it would in natural eukaryotic cells (Terpe 2006). This presents a major problem for expressing proteins, such as virus proteins to be used in vaccines; these require precise shape and confirmation in order to induce the required response in a host organism's immune system.

Recognition of these viral proteins is essential for an immune response to recognise the appropriate antigen, and hence is essential to the working of a vaccine. Thus a bacterial expression system is limited in its ability to produce proteins capable of functioning as an effective candidate vaccine. In spite of the theoretical shortcomings of a bacterial expression system, FMDV VLPs have been successfully produced in *E.coli* with the ability to induce an immune response in cattle sufficient for protection against viral challenge (Xiao et al. 2016).

1.4.2 Expression in a Yeast system

Other platforms such as mammalian cell culture, insect cell culture, and yeast cell culture expression systems have been developed for the production of recombinant proteins, and have also been successful in the production of VLPs. Each of these expression systems make use of eukaryotic cells and thus avoid the shortcomings of a bacterial expression system, which fail to produce proteins with appropriate post-translational modification in heterogeneous recombinant proteins of eukaryotic origin. Proteins expressed in *Saccharomyces cerevisiae*, a yeast expression system, however show high levels of glycosylation and often hyperglycosylation (Punt et al. 2002). This level of glycosylation can effectively alter the topography of the protein surface and consequently impede the efficacy with which antibodies react to the protein since the sugar molecules mask original protein epitopes for which the antibodies are to be designed. Since vaccine efficacy relies on the recognition of the vaccine by the immune response-generated antibodies, this presents a major flaw in the use of a yeast expression system for the production of recombinant proteins and VLPs to serve as a candidate vaccine. Some strains of yeast have been developed that have decreased levels of glycosylation to address this shortcoming (Balamurugan et al. 2007). Rotavirus VP8, expressed in yeast, has been recorded to have successfully generated an immune response in mice and protected them from viral challenge (Andrés et al. 2006). The structural proteins of FMDV have also been successfully expressed in *Pichia pastoris*, a methylotrophic yeast, and used to protect guinea pigs against a viral challenge of the disease (Balamurugan et al. 2007). Few studies have successfully produced VLPs with yeast cells; a study developing rotavirus VLPs, after much vector modification,

was one such study (Rodríguez-Limas et al. 2011). The yeast expression platform is better suited to the production of non-enveloped VLPs (Kushnir et al. 2012). Improper particle formation and protein degradation are further problems encountered when using a yeast expression system for the production of VLPs. The low level of protein expression in individual cells fails to promote particle assembly. It has been further speculated that protein degradation becomes preferential when particle formation is limited (Rodríguez-Limas et al. 2011).

1.4.3 Expression in insect cell culture systems

A baculovirus-insect cell expression system presents an alternative eukaryotic expression system capable of complex post-translational modifications, protein folding and oligomerisations, while also accommodating high levels of accumulated heterologous protein. For the expression of recombinant protein in such a system; an insect cell is infected with the recombinant baculovirus containing the gene for the protein of interest: for the purpose of VLP production these will be the genes encoding the structural proteins of the virus. Once infected, the insect cell will then produce the desired protein encoded in the recombinant baculovirus genome. The cellular environment of insect cells will however vary from that of mammalian cells, the natural host environment of FMDV. Strict conditions are required for the correct assembly of VLPS which may not be met with the varying pH buffer capacity and other nutritional requirements of the insect cell (Cao et al. 2009; Mena et al. 2006). Although a number of studies have successfully demonstrated the production of assembled VLPs by insect cell culture, the VLPs do not assemble within the insect cells, possibly on account of inappropriate pH of the insect cells (Cao et al. 2009). High Five™ cells (HF cells) were used for the expression of FMDV P12A3C, generating empty capsid like particles that successfully elicited an immunogenic response in guinea pigs which produced vast levels of FMDV specific antibodies as determined by ELISA tests (Cao et al. 2009).

The baculovirus-insect cell approach does however have the major disadvantage of requiring expensive culture media - thus making it expensive to scale up to an industrial scale. In addition to this, insect cells do not proliferate to the same extent as bacterial cells and so protein production is not as rapid in these cultures. This presents a problem for using this technology for the production of a commercial product. Another problem encountered with the use of an insect expression system for the production of recombinant protein is that not all species will reliably produce the desired protein. Only one out of three lepidopteran species tested was capable of producing VLP forming FMDV capsid proteins (Kumar & Jalali 2016)

FMDV Serotype O is globally predominant, but Serotype O capsids are acid sensitive and as such Serotype O VLPs are not stable within the acidic conditions of insect haemolymph, thus presenting a further challenge with using insect expression. Though this challenge has been successfully addressed with the creation of a chimeric VLP harbouring VP1 of serotype O that is less acid sensitive and which successfully induced an immune response in guinea pigs with similar efficacy to the standard FMDV inactivated vaccine (Li et al. 2016)

1.4.4 Mammalian cell culture expression system

Mammalian cell culture expression platforms similarly present a eukaryotic expression system capable of the appropriate post-translational modifications, identical to that of the cellular environment of the natural virus host in the case of FMDV. This platform was used to successfully produce empty capsid VLPs in human embryonic kidney cells/ 293-6E cells (Mignaqui et al. 2013). This same study reported that the 293-6E cells achieved similar levels of expression to those currently achieved in operating vaccine production facilities with baby hamster kidney-21 (BHK-21) cell suspensions infected with live FMDV. Furthermore, it was reported that the transiently expressed capsid particles were recognised by serum from vaccinated cattle, and also induced an immunogenic response in mice equal to that induced by the same amount of inactivated virus,

which had been sufficient to surpass a viral challenge. The study demonstrated the technical viability of using empty capsid VLPs, transiently expressed in mammalian cell culture, as a next generation FMDV vaccine. Mammalian cell culture is however expensive, limiting the technology's potential for broader industrial application as a more cost effective alternative to that of bacterial cultures, insect cell culture or plant expression systems. The authors argue that the use of serum-free suspension-growing 293-6E cells makes the technology inexpensive, but this is in the context of comparison with the current method of FMDV vaccine production which typically uses suspension growing BHK21 cells. (Mignaqui et al. 2013)

1.4.5 Expression in plant systems

Plant expression systems have gained much recognition as platforms for expressing recombinant proteins (Rybicki 2009; Rybicki 2010). The plant expression platform presents many advantages over other expression platforms, particularly insect and mammalian cell culture expression systems, with the main advantage being the low cost and ease of upscaling production. A plant, being autotrophic, essentially requires primarily carbon dioxide, sunlight, and water, sources of nitrogen and phosphorous. These are inexpensive or freely available. It does not require expensive sugar based media substrate for growth and protein expression. Using a plant expression system is thus competitively advantageous on a financial basis, over the other protein expression systems discussed. Plant expression systems do not require the expensive media substrates for the production of recombinant proteins that are required by these alternative platforms. Plant based recombinant protein expression thus provides a promising, financially viable means of large scale production for industrial application (Sainsbury & Lomonossoff 2008; Rybicki 2009; Regnard et al. 2010).

One of the major shortcomings of a bacterial expression platform, as discussed previously, is the failure to produce the correct post-translational modifications of recombinant proteins native to

eukaryotic cells, as bacteria lack the same mechanisms of protein glycosylation and folding. Consequently, many recombinant proteins of eukaryotic origin, expressed in bacterial systems, do not present the correct tertiary and quaternary structures, as well as chemical properties, identical to the original protein. A plant system, by comparison, is eukaryotic and therefore does not have this same disadvantage; on the contrary many heterologous proteins expressed in plants are nearly identical to the original proteins (Kushnir et al. 2012). As a consequence of this, the plant expression platform is capable of producing VLPs, as these require specific conformational arrangement of the constituent proteins (Scotti & Rybicki 2013; Chen et al. 2012). This is particularly favourable since VLPs present a highly efficient vaccine approach (Kushnir et al. 2012). The full extent of the potential economic advantages of using a plant based expression system for the production of recombinant proteins has been comprehensively reviewed (Nandi et al. 2016) and provides a compelling argument for the use of the technology in the future of vaccine development and production.

A plant expression system provides a highly rapid production platform for the expression of heterologous protein; these proteins can be expressed at high quantities to accumulate at high levels, alternatively they can also be secreted owing to the endomembrane system and secretory pathways present in plants (Lico et al. 2008).

Another significant advantage to using a plant expression system in the context of vaccine production (and other products destined for human and/or animal use), is that it is free of mammalian pathogens (Kushnir et al. 2012).

The use of plant expression systems for the production of FMDV proteins has already gained significant attention, and consequently is being intensively explored. Initial research efforts focused on a transgenic approach whereby the actual genome of the plants would be altered to introduce the exogenous recombinant protein genes. Transgenic *Arabidopsis thaliana* leaf extract containing VP1 has been used to elicit a protective antibody response in immunized mice (Carrillo et al. 1998). Mice have also demonstrated protection against the virus after receiving vaccinations with leaf

extract from inoculated *N. benthamiana* (Wigdorovitz & Pe 1999) and transgenic alfalfa containing VP1 (Escribano & Borca 1999). Similarly the gene for the P1 polyprotein was expressed in transgenic alfalfa (Dus Santos et al. 2005). Guinea pigs have been vaccinated with tomato plant produced FMDV antigens derived from expression of the *P12A* gene, and then demonstrated full protection against a viral challenge with FMDV (Pan et al. 2008). More recently, however, the focus of most research has shifted to investigating transient expression in plants, since this approach is not complicated with growing multiple generations, and can produce the recombinant proteins far more rapidly: transient expression employs transformed *Agrobacterium tumefaciens* to transfect plant cells and thereby induce expression of with the desired recombinant genes. Recombinant protein will be produced within a few days of infiltration, instead of waiting several weeks for transgenic plants to grow sufficiently for protein production. VP1 and VP4 epitopes of FMDV have already been successfully expressed in the plant expression system *Nicotiana benthamiana* as a potential candidate vaccine, which successfully induced an immunogenic response in guinea pigs (Andrianova et al. 2011). The same system has successfully produced FMDV VLPs (Veerapen et al. 2018). VLPs for other viruses, including the human papillomavirus have also been successfully produced through the plant expression system *N. benthamiana*. This promising new technology for the rapid production of recombinant proteins is still in its infancy – few commercial operations have adopted and implemented this approach and the majority of industrial protein is still produced by cell-culture approaches.

1.5 Project aims

The aim of this project was twofold:

- To generate anti-P12A antibody used as a reagent for detection purposes of recombinantly expressed FMDV P12A. This was carried out by cloning FMDV P12A in an *E. coli* expression vector, purifying expressed P12A and injecting rabbits with it to yield serum for use as the detection reagent.
- To compare the expression of FMDV P12A-3C in *Nicotiana benthamiana* using 3 different plant expression vectors and determine whether VLPs could be assembled with the expressed protein. FMDV P12A-3C was cloned into pEAQ-HT, pTRAc, and PRIC3.0 expression vectors. The gene for the FMDV capsid proteins was cloned into these respective vectors which were then used to transform *Agrobacterium tumefaciens* for transfection and expression of recombinant protein in plant leaf cells. Plant leaves were harvested, the protein extracted, purified, and analysed.

Chapter 2:

Bacterial Expression of FMDV P12A in *E. coli*

2.1 Overview

The well characterised method of recombinant protein expression in bacteria is the most well-established of the different expression systems. The rapid expression afforded by the fast growth of the bacteria contributes to the appeal of this expression system. Additionally; the refined motifs within available vector plasmids, which enable the specific induction and strict regulation of expression, further contribute to the favourability of this expression system for pharmaceutical industrial application. Non-hydrolysable lactose analogue isopropyl- β -D-1-thiogalactopyranoside (IPTG) can be used to induce expression via the *lac*, *trc*, and *tac* promoters. These promoter regions are located in the region immediately prior to the multiple cloning site (MCS) of the pProEX vector (Figure 2.1) allowing for inducible expression of genes cloned into the vector at a position within the MCS. The *lac* promoter is relatively weak and is not particularly effective for protein production at high levels, but the neighbouring *trc* and *tac* promoters are strong synthetic promoters capable of very efficient expression and high levels of protein accumulation (Terpe 2006). T7 RNA polymerase delivers far more rapid transcription elongation of mRNA than *E. coli* RNA polymerase, further enhancing the rate of protein expression (Terpe 2006). The gene for T7 RNA polymerase is itself also under the control of the L8-UV5 *lac* promoter and is thus also induced by IPTG; ensuring that the entire expression system is strictly and synergistically regulated by the addition of IPTG.

In the present study, the lactose analogue IPTG was used for the activation of the *lac* promoter to induce *P12A* expression. After the *lac* promoter and immediately prior to the MCS, the pProEX vector includes a gene that translates to a short peptide sequence of 6 histidine amino acid residues followed by a space linker motif of amino acid residues that are expressed with the inserted gene. This feature of the pProEX vector means the *E. coli* expresses the recombinant protein with a His-tag.

The His-tag enables the produced protein to be purified with Nickel tagged affinity resin, and also enables the protein to be detected using anti-his antibodies.

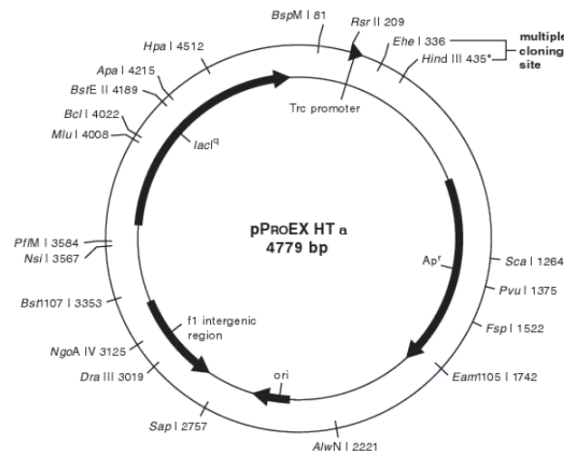


Figure 2. 1. pProEX HT α vector map, illustration position of lac and trc promoter regions before the MCS.

The main objective of this project was to express FMDV type A1 capsid proteins in a plant system for the purpose of VLP production. However, we had no continual supply of any commercial, or other, antibodies specific for FMDV Type A1 in order to use for the detection of recombinant proteins to confirm their expression. To address this matter, this project also included an endeavour to produce the P12A oligopeptide in the *E. coli* bacterial expression system with the use of the pProEX vector, and to develop a purification protocol in order to ultimately develop antiserum in rabbits against FMDV P12A.

2.2 Materials and Methods

A *Nicotiana* . codon optimised version of the FMDV A/Arg/01 (serotype A, Argentinian 1) *P12A* gene sequence, with the gene for the 3C protease incorporated at the 3' terminus of the sequence of the sequence (P12A3C), was synthesized and cloned into pUC57 by GenScript (Inc) USA.

2.2.1 PCR amplification of *P12A* fragment

E. coli containing the pUC 57-P12A3C plasmid were cultured in Luria-Bertina broth (LB) with ampicillin (100 µg/mL) at 37 °C overnight. DNA necessary for amplification was extracted using the plasmid preparation QIAprep Spin "Miniprep Kit" (QIAGEN) according to the manufacturer's instructions.

Forward and reverse nucleotide primers were designed for the select amplification of the 2767 bp *P12A* fragment of the gene received from GenScript, excluding the 3C protease gene. The binding site of the reverse primer was located prior to the portion of the gene encoding the 3C protease thus ensuring amplification excluded the 3C protease, schematically illustrated with green markers in Figure 2.2 (entire DNA sequence with primer binding annotation in appendix A).

These primers were designed to incorporate *Nco*I and *Xho*I restriction endonuclease cleavage sites (highlighted in blue, Table 2.1. Primers *designed for amplification of P12A gene fragment* PCR with Phusion® Taq polymerase (New England BioLabs) was used for high fidelity amplification of this fragment in order to clone it into the *E. coli* expression vector pProEX - HTa (Life Technologies, Ontario, Canada). Reaction volumes and PCR parameters for gene amplification are detailed in Tables 2.2 and 2.3, respectively. The PCR product was run on a 0.8 % (w/v) agarose gel at 120 V for 45 min to verify that the reaction had generated a fragment of the appropriate size.

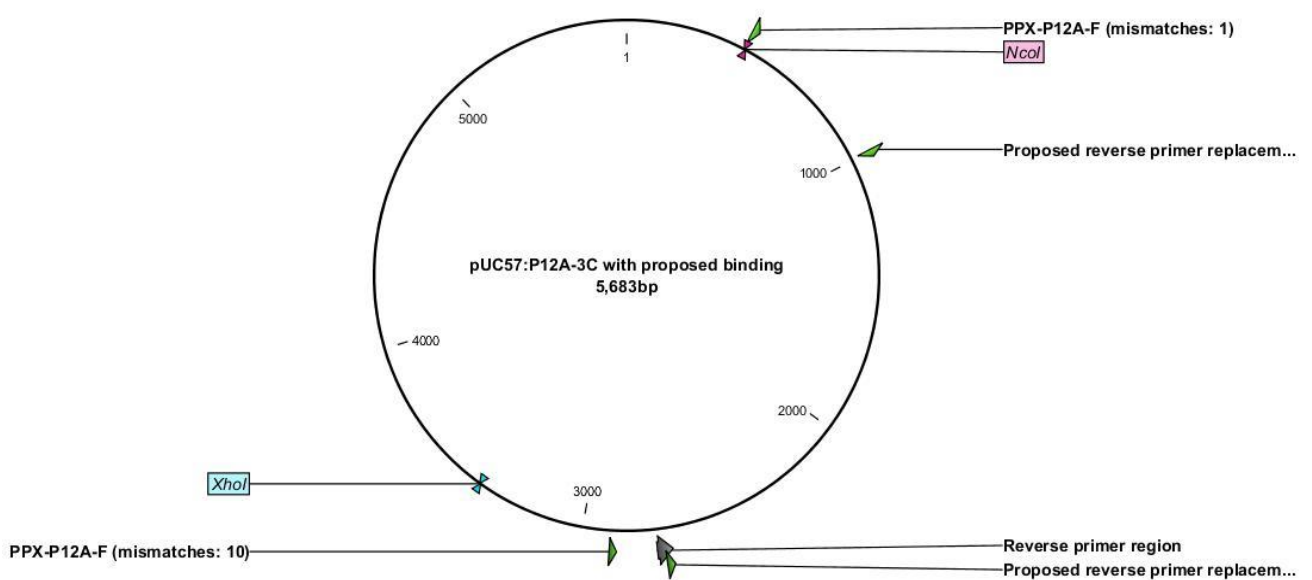


Figure 2.2. Schematic diagram of pUC57-P12A3C storage plasmid with labelled binding sites of relevant PCR primers and restriction endonuclease sites.

Table 2.1. Primers designed for amplification of P12A gene fragment. Position of added endonuclease restriction site highlighted in blue.

	Orientation	5'-3' Nucleotide sequence	Restriction site added
PPX-P12A-F	forward	ttc/catgggagcaggatcaatcaagt	NcoI
PPX-P12A-R	reverse	ctgac/tcgagttatgggtagattc	XhoI
Screening	Reverse	caagtttgaagatgaccgaaag	-

Table 2.2. PCR components and volumes for 50 μ L reactions

Component	Volume in 50 μ L Reaction	Final Concentration
5X Phusion HF Buffer	10 μ L	1X
10 mM dNTPs	1 μ L	200 μ M
10 μ M PPX-P12A-F Forward Primer	2.5 μ L	0.5 μ M
10 μ M PPX-P12A-R Reverse Primer	2.5 μ L	0.5 μ M
pUK57-P12A3C DNA	2.5 μ L	250 ng
Phusion [®] DNA Polymerase	0.5 μ L	1.0
Nuclease-free water	31 μ L	

Table 2.3. PCR step parameters

PCR step	Initial Denaturation	Denaturation	Annealing	Extension	Final Extension	Hold
Temp ($^{\circ}$ C)	98	98	68	72	72	4
Duration	30 sec	10 sec	30 sec	3 min	10 min	
		Number of cycles = 30				

2.2.2 Cloning of P12A into pProEx HTa *E. coli* expression vector

E. coli cells harbouring the empty pProEX HTa vector were grown in 10 mL LB containing ampicillin (100 µg/mL) at 37 °C with shaking overnight. DNA for the pProEX vector was extracted from *E. coli* cells using the DNA extraction miniprep kit (QIAGEN) as per the manufacturer's instructions.

Amplified P12A and extracted vector DNA were digested using the restriction endonuclease enzymes NcoI and XhoI (Thermo Fischer Scientific). Reactions were incubated at 37 °C for 1 hour. Correctly linearized pProEX DNA was separated by electrophoresis on a 0.8 % (w/v) agarose gel, at 100 V for 1 hour. The DNA was retrieved from the agarose gel using a gel extraction kit (QIAGEN) as per the manufacturer's instructions. The DNA was dephosphorylated with Shrimp Alkaline Phosphatase (New England Biolabs) prior to the ligation reaction using T4 DNA ligase (Thermo Fischer Scientific). Competent DH5α *E. coli* cells (Lucigen) were transformed with successfully cloned recombinant pProEX - P12A plasmids by means of heat shock. Recombinant plasmid DNA and competent cells were placed in the same reaction tube and placed on ice for 2 minutes before being placed in a 37 °C water bath for 1 minute then returned to ice. Three hundred microlitres (300 µL) LB media was added to the reaction tube and the tube was returned to 37 °C water bath for 1 hour. After 1 hour, transformed cells were centrifuged in a benchtop centrifuge (Eppendorf 5424) at $17933.4 \times g$ for 5 minutes. Two-hundred µL of the supernatant media was removed from the tube and the cells were re-suspended in the remaining 100 µL. Fifty microliters (50 µL) of transformed cells were plated onto Luria agar containing ampicillin (100 µg/mL). The plates were incubated overnight at 37 °C.

An additional nucleotide primer was designed to amplify a 500 bp internal fragment of the inserted gene for the purpose of screening transformed bacterial colonies (identified by a green arrow, Figure 2.3). Random *E. coli* colonies were selected from the agar plates and screened by PCR amplification of the internal gene specific 500 bp fragment, using ppx-p12a-f and screening primers, to confirm successful transformation (colony PCR). Positively transformed colonies were then used to inoculate 10 mL LB media and incubated at 37 °C with shaking overnight. DNA was again extracted from the *E. coli* using the miniprep extraction kit (QIAGEN). A double restriction digest, with XhoI and NcoI

enzymes, of the DNA retrieved from the *E.coli* transformed with pProEX-P12A, further verified that the *E. coli* had been successfully transformed with the recombinant pProEX - P12A plasmid. Aliquots of transformed *E. coli* containing the pProEX - P12A plasmids were stored at -80 °C in a 50 % glycerol solution.

DNA fragments generated through cloning and PCR procedures were run on agarose gels for the purpose of visualising the experimental results. Four microliters of ethidium bromide (0.1g/mL) were added to 100 mL agarose gels, in order to visualise the DNA when viewed under UV light. Gels were photographed with short wavelength (280 nm) UV-B light.

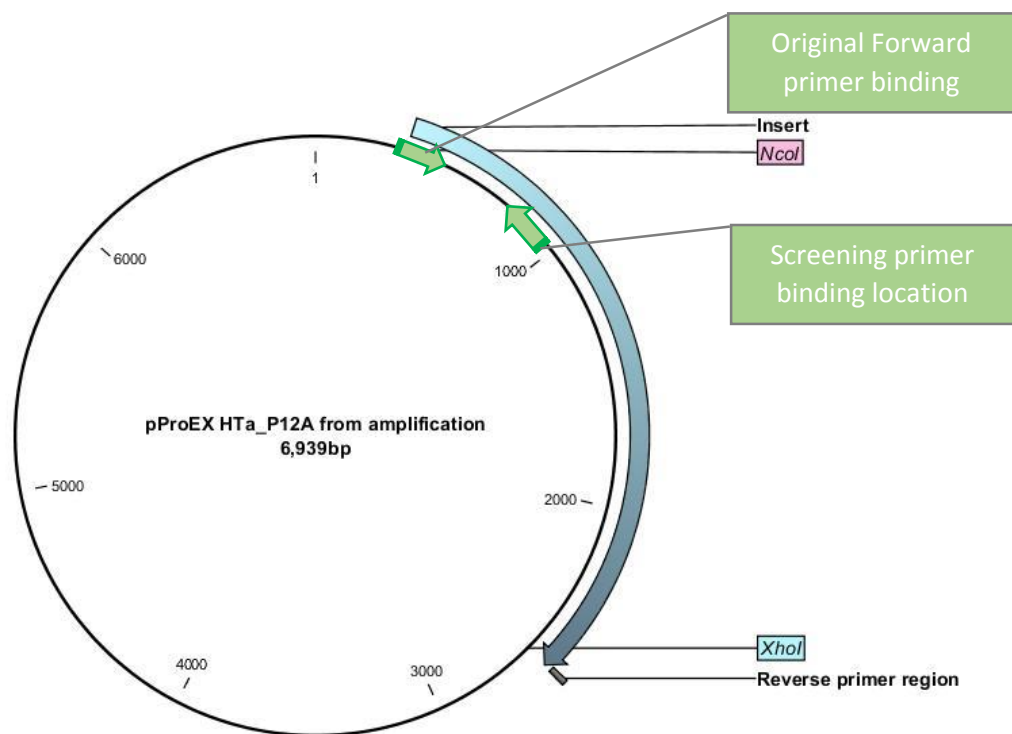


Figure 2.3. Schematic diagram of cloned pProEX – P12A construct with labelled PCR amplified insert and relevant restriction endonuclease sites, and location of forward and screening primers.

2.2.3 *P12A induced expression*

After successfully transformed *E. coli* were verified by means of colony PCR and restriction enzyme digests, for the recombinant pProEX - P12A plasmids, 10 mL volumes of Luria broth media (LB) were inoculated with 1 mL glycerol stock of transformed *E. coli* and cultured at 37 °C with shaking overnight for protein expression. IPTG was added to a final concentration of 0.6 mM once the culture had reached an optical density of between 0.5 and 1. A time trial was conducted to establish the amount of time necessary for optimal protein expression; 1 mL samples were removed from the culture, prior to induction by addition of IPTG, and every hour for 3 hours post the addition of IPTG. Cells were pelleted with a benchtop centrifuge at $17933.4 \times g$ for 2 minutes, the supernatant was discarded and the cells re-suspended in 200 μ L Phosphate buffered saline (PBS) for protein extraction. 50 μ L 5 \times sample application buffer (SAB), (composition detailed in appendix C), was added to the cell re-suspension and samples incubated at 95 °C for 10 minutes to denature proteins prior to analysis by SDS-PAGE and western blot.

2.2.4 *Protein analysis by SDS PAGE, Western Blot, Coomassie Blue stain*

10% SDS Polyacrylamide gels were made up as described in appendix B. Thirty microliters (30 μ L) of protein samples prepared in section 2.2.3 were loaded in gel wells, one lane was loaded 5 μ L NEB Broad range protein marker ladder. Gels were submerged in 1 \times running buffer (composition of 10 \times concentrated running buffer detailed in appendix B) for electrophoresis and run at 120 V for ≥ 2 h using Bio-Rad equipment.

For western blotting, the gels were placed on nitrocellulose membranes pre-soaked in transfer buffer (composition detailed in appendix B), which were sandwiched between blotting paper also soaked in transfer buffer. The blot sandwich was transferred at 15V for ≥ 2 h using a transblotter (Bio-Rad). After transfer the membrane was washed in blocking buffer (+ 5 % m/v fat-free milk powder in 1 \times PBS, composition detailed in appendix B) with shaking for 30min at room

temperature. The membrane was probed with guinea pig or rabbit anti FMDV antibodies (kindly donated by Andrés Wigdorovitz, INTA, Buenos Aries) diluted 1 in 100 in blocking buffer (+ 5% m/v fat-free milk powder in 1 × PBS), and incubated at 4 °C with shaking overnight. The membrane was then washed with blocking buffer four times for 15 min. After washing the membrane was probed with alkaline-phosphatase-conjugated anti-guinea pig/ rabbit secondary antibody, diluted 1 in 10 000 in blocking buffer for 1 hour at 37 °C, after which the membrane was again washed with blocking buffer lacking milk four times for 15 min. The blot was developed with 3 mL BCIP/NBT (Sigma-Aldrich) for 1 h.

Polyacrylamide gels used for Coomassie staining, instead of western blotting, were placed in Coomassie blue stain solution (appendix B) after electrophoresis, and left shaking at room temperature overnight. Coomassie blue stain solution was discarded and replaced with de-stain solution (appendix B) and the gel was left shaking in de-stain solution, until protein bands had become distinct.

2.2.5 Scaled up induction of P12A expression

Overnight cultures of recombinant *E. coli* were used to inoculate fresh 100 mL volumes of LB media. Cultures were grown at 37 °C with shaking until the optical density reached between 0.5 and 1.0, at which time IPTG was again added to a final concentration of 0.6 mM to induce the expression of P12A. The culture was incubated at 37 °C with shaking for 3 hours. After 3 hours the culture was centrifuged at 10 000 ×g (Beckman Coulter centrifuge) for 10 minutes, the supernatant was discarded and the pellet was stored at – 80 °C. In order to determine whether the expressed P12A was soluble or insoluble, 100 µL samples of the stored cells were transferred to a clean Eppendorf tube and re-suspended in 1 mL lysis buffer (QIAGEN). To achieve cell lysis, the re-suspended cells were sonicated at 14 µm amplitude for 1 minute. The suspension was centrifuged at 17933.4 ×g for 2 minutes to pellet the cell debris. The supernatant was transferred to a clean Eppendorf tube this

was the soluble fraction; the cell pellet that remained was re-suspended in another 1 mL of lysis buffer – this was the insoluble fraction. To each of the 100 μ L fractions 25 μ L of 5 \times SAB was added, and denatured at 95 $^{\circ}$ C for 10 minutes. The samples were analysed by SDS-PAGE and western blot as described in 2.2.4. After confirmation that the expressed protein was insoluble, cell lysis of the remaining stored pelleted cells was performed using the Bug Buster[®] (Novogen) protocol. These cells were re-suspended with 5 mL of Bug Buster[®] reagent per gram of cells. Benzonase[®] nuclease was added to the buffer at 1 μ L per mL. Lysozyme was added at 1000 units per mL of buffer. The re-suspended cells were incubated at 4 $^{\circ}$ C with shaking for 30 minutes, and the cell suspension was then centrifuged at 16000 \times g for 20 minutes – the supernatant (soluble fraction) was discarded. A portion of the pellet was re-suspended in 100 μ L of 1 \times PBS and denatured with 25 μ L of 5 \times SAB at 95 $^{\circ}$ C for 10 minutes to represent the unpurified protein sample when analysed by western blot and SDS-PAGE. Purification of the protein inclusion bodies was performed using the Bug Buster[®] protocol as per its instructions. The final pellet was again re-suspended in PBS with 0.1 % Triton, in a volume equal to that of 1/10th of the original culture volume. The suspension was centrifuged at 16000 \times g at 4 $^{\circ}$ C for 10 minutes to collect inclusion bodies. Re-suspension and centrifugation of the inclusion body pellet was repeated five times, and the final pellet was re-suspended in 2 mL of PBS with 0.1 % Triton. 25 μ L of 5 \times SAB were added to 100 μ L of the sample and denatured at 95 $^{\circ}$ C for 10 minutes prior to analysis by SDS-PAGE and western blot as described in 2.2.4.

2.2.6 Purification of P12A using affinity chromatography

Immobilized metal affinity chromatography, with Nickel chelate (Ni-NTA) (Sigma-Aldrich) resin columns, was used in an attempt to further purify the protein inclusion bodies. Pelleted inclusion bodies were re-suspended in 14 mL denaturing equilibration buffer (DEB(appendix B)) containing two protease Inhibitor tablets (cOmplete[™], Mini, EDTA-free, Sigma-Aldrich). The suspension was left to shake for 10 minutes and then centrifuged at 8595.3 \times g in a benchtop centrifuge for 10 minutes.

The supernatant was discarded and the pellet re-suspended in 2 mL DEB prior to being run through a pre-equilibrated column and collecting the flow-through. The column was then washed with three column volumes of washing buffer (appendix B) and then three 1 mL fractions of washing buffer, each fraction was collected. Four 1 mL fractions of elution buffer (appendix B) were then run through the column and elution fractions collected. 100 μ L of each fraction sample was denatured with 25 μ L of 5 \times SAB at 95 $^{\circ}$ C for 10 minutes for analysis by SDS-PAGE and western blot as described in 2.2.4.

In an effort to resolve poor binding of expressed P12A to Ni-NTA resin, treatment with 8 M urea was used to solubilize the inclusion bodies. The pelleted inclusion bodies were resuspended in 8 M urea, vortexed and left shaking for 15 minutes. The suspension was centrifuged at 16000 \times g at 4 $^{\circ}$ C for 10 minutes. The final pellet was again re-suspended in PBS with 0.1 % Triton and the suspension was again centrifuged at 16000 \times g at 4 $^{\circ}$ C for 10 minutes. Re-suspension and centrifugation of the urea treated pellet was repeated 5 times, and the final pellet was re-suspended in 2 mL of PBS with 0.1% Triton prior to metal affinity chromatography.

Persistent absence of any detectable P12A protein band from metal affinity chromatography required a cognate anti-his blot to clarify whether the lack of P12A was possibly due to cleavage of the his tag, in which case the six histidine residue tag might have been binding successfully to the resin, but without P12A which was being probed for with anti-FMDV antibodies.

This protocol was adapted by fellow student Varusha Veerapen for the production and purification of the P12A oligopeptide to obtain amounts sufficient to inject into rabbits for the generation of anti – P12A rabbit anti serum capable of detecting both the *E. coli* produced P12A and the plant produced protein from the P12A3C construct.

2.3 Results

2.3.1 PCR amplification of P12A and restriction enzyme digest of pProEX

The pProEX plasmid was successfully digested with NcoI and XhoI evident from the 4663 bp band visible in Figure 2.4 (lane 1). P12A was successfully amplified from pUC57 - P12A3C and digested with NcoI and XhoI, which generated a 2276 bp gene insert (Figure 2.4, lane 2)

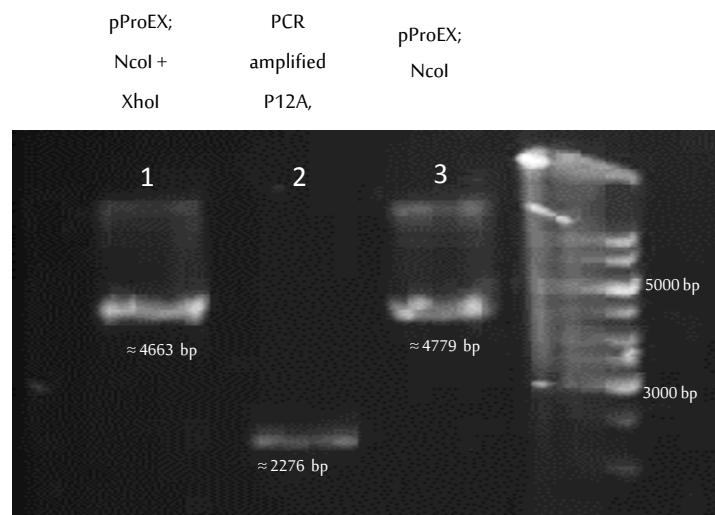


Figure 2.4. pProEX Digested with NcoI and XhoI(4663 bp) lane 1; PCR amplified P12A fragment (2276 bp) lane 2, digested with NcoI and XhoI ; pProEX linearized with NcoI lane 3 (4779).

2.3.2 Cloning of P12A into pProEX and transformation

Successful cloning of the *P12A* gene fragment into the pProEx vector plasmid, and subsequent transformation of the pProEX-P12A construct into *E. coli* was verified by colony screening PCR and restriction enzyme digest. Figure 2.5 shows that 3 of 8 colonies screened with primers to generate a 500 bp band were positive. Gels showing restriction enzyme digest of colony 1 (Figure 2.6) showed fragments with the appropriate sizes for the insert (2276 bp) and vector (4663 bp) as opposed to the empty vector which only displayed a single band (4779 bp), therefore further confirming that the ligation and cloning of the insert into the vector had been successful.

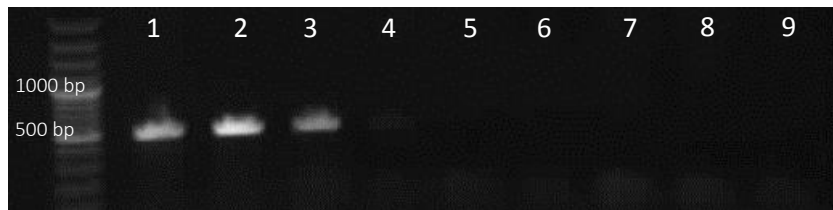


Figure 2.5. pProEX-P12A colony PCR amplification of 500 bp fragment with internal screening primer. Lanes 1 – 8 randomly selected colonies from agar plate. Lane 9 = negative control colony with empty pProEX. Ladder used = O'GeneRuler™ 100 bp Plus

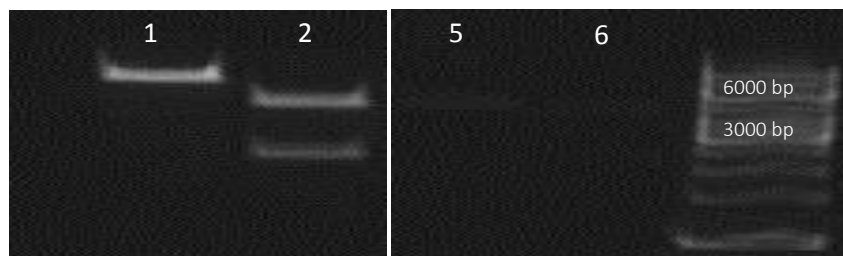


Figure 2.6. Restriction endonuclease linearization of pProEX-P12A using restriction enzyme XhoI (lane 1); double digestion of pProEX-P12A using restriction enzyme XhoI & NcoI (lane 2) linearization of pProEX-empty using restriction enzyme XhoI (lane 5); double digestion of pProEX-empty using restriction enzymes XhoI & NcoI (lane 6).

2.3.3 Induced expression of P12A with IPTG

The expression of P12A was successfully induced with IPTG. Western blot analysis of the samples obtained from the protein expression time trial (Figure 2.7) showed the most prominent band in the region of the expected 81kDa P12A peptide in the lane corresponding to the sample taken 3 hours post induction. The blot indicates that the best levels of expression were achieved at least 3 hours post induction with IPTG, although low levels of expression were already evident in the sample taken one hour post induction.

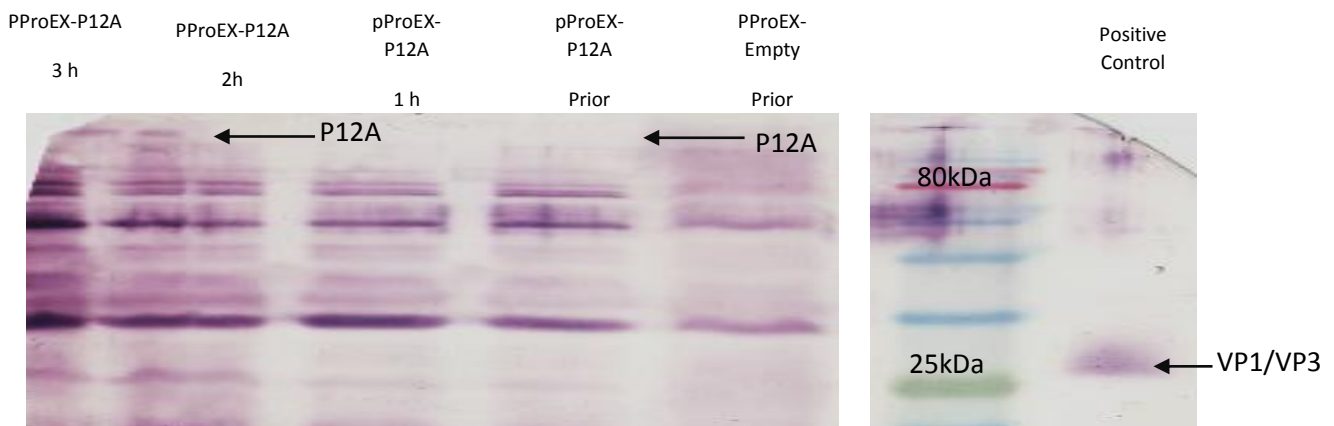


Figure 2.7. Western blot of P12A \approx 81kDa, indicated by an arrow, induced expression time trial in *E. coli* probed with Guinea pig anti-FMDV antiserum. Positive control shows VP1/VP3, indicated by an arrow.

2.3.4 Protein purification of up scaled expression

Having established that the highest level of expression occurred 3 hours post infiltration, tests were carried out to determine whether the expressed protein was soluble or insoluble. P12A was detected in both soluble and insoluble fractions. Western Blot analysis revealed the more prominent (darker) band of 80 kDa in the lane corresponding to the sample of the insoluble fraction (Figure 2.8).

The western blot of the purified inclusion bodies showed a distinct prominent band of approximately 81 kDa (Figure 2.9). The insoluble fraction was concentrated further by repeated washes with BugBuster™ reagent and then PBS, results of which are shown in figure 2.10. The 80 kDa band is faint in the crude extract sample from lysed cells compared to the concentrated insoluble sample.

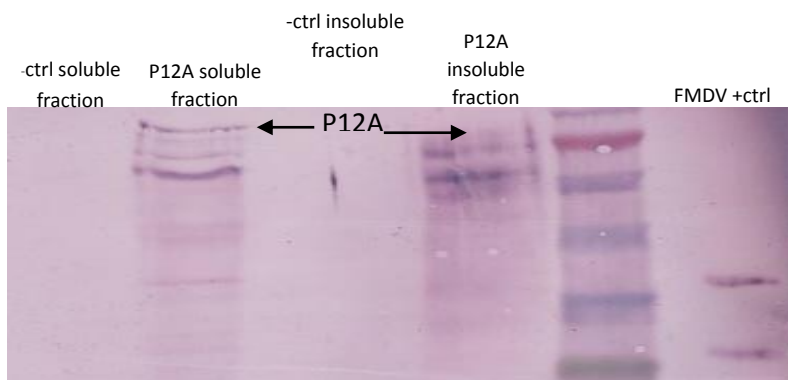


Figure 2.8. Western blot comparing samples of pProEX-empty soluble protein extract (lane 1), pRoEX-P12A soluble protein extract (lane 2), pProEX-empty insoluble protein extract (lane 3), pRoEX-P12A insoluble protein extract (lane 4), FMDV + ctrl (lane 6); ladder used = NEB #P7712S broad range protein marker.

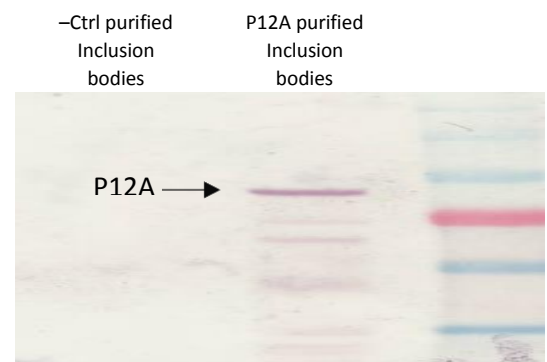


Figure 2.9. Western blot of gel comparing purified inclusion bodies of insoluble P12A indicated with arrow, expressed in E.coli, via pProEX, induced with IPTG. Lane 1 = pProEX-empty purified inclusion bodies; lane 2 = pProEX-P21A purified inclusion bodies; Ladder used = NEB #P7712S broad range protein marker.

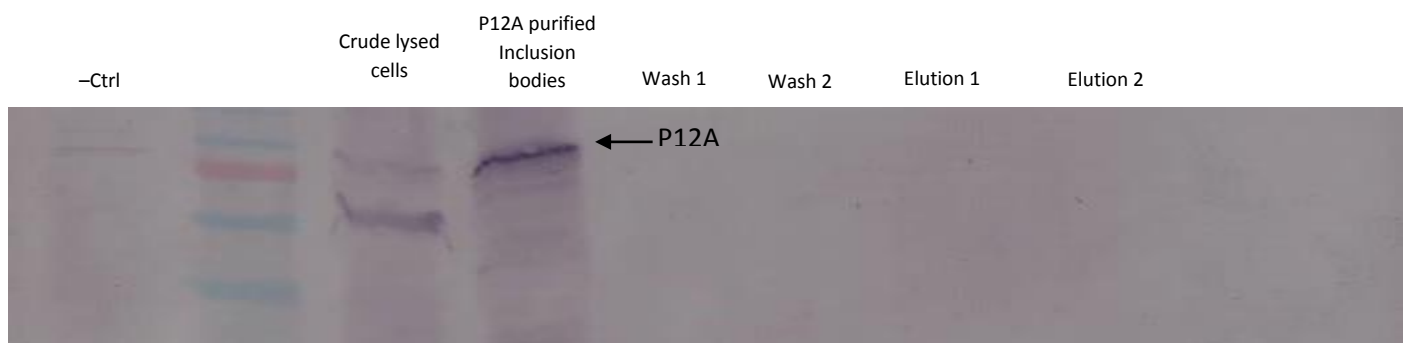


Figure 2.10. Western blot of gel comparing purified inclusion bodies of insoluble P12A, indicated with arrow, expressed in E.coli, via pProEX, inuced with IPTG. Lane 1 = pProEX-empty pre-induced; lane 3 = pProEX-crude lysed cells; lane 4 = pProEX-P12A purified inclusion bodies; lane 5 = Wash 1; lane 6 = wash 2; lane 7 = Elution 1; lane 8 = elution 2; Ladder used = NEB #P7712S broad range protein marker.

An attempt to further purify the protein was made with Nickel affinity chromatography using Ni-NTA resin columns to bind the His-tagged P12A protein of the insoluble fraction. However, no P12A band of 81 kDa was evident in the elution fractions (Figure 2.10). The hydrophobic nature of the inclusion bodies is likely a significant factor contributing to the resin's inability to bind the protein. To address the possibility that the hydrophobic nature of insoluble protein in the inclusion bodies was hindering binding to the resin, the P12A protein was treated with 8 M urea prior to chromatography in order to solubilize the protein so that it might increase binding with the Ni-NTA resin. This proved to be unsuccessful. No band corresponding to the 81 kDa size of P12A could be seen in the elution fractions (Figure 2.11). This was not resolved despite treatment with 8 M urea intended to solubilize the expressed P12A (Figures 2.10, 2.11, 2.13). Instead, the first wash fractions showed a band of the appropriate size indicating that the protein was still not binding to the Ni-NTA resin effectively and was being lost in both the flow-through and wash fractions.

The western blot was repeated; Anti-His antibodies were used for the primary antibody probe as an alternative to anti-FMDV antiserum (Figures 2.12) in order to verify that the results observed were not in fact caused by cleavage of the His-tag. The blot revealed the same P12A band in the 81 kDa region of the wash and flow through fractions as did the anti-FMDV primary antibodies, but not the elution fractions, dispelling the possibility that the His-tag at the N terminus of the protein had been lost or cleaved.



Figure 2.11. Western blot with anti-FMDV 1 antibodies, of gel comparing purified inclusion bodies of insoluble P12A expressed in *E.coli*, via pProEX, induced with IPTG for 3 h. The expressed protein was purified with BugBuster inclusion body purification protocol followed by 8M urea denaturation and NTA resin column purification. Lane 1 = pProEX-empty; lane 3 = pProEX-P21A purified inclusion bodies elution 2; lane 4 = pProEX-P21A purified inclusion bodies elution 1; lane 5 = pProEX-P21A purified inclusion bodies Wash 1; lane 6 = Flow through; lane 7 = solubilized Inclusion bodies with 8M Urea; lane 8 = re-suspended pellet from 8M urea treatment; lane 9 = BugBuster purified Inclusion bodies; lane 10 = Soluble fraction from initial extraction. Ladder used = NEB #P7712S boad range protein marker.

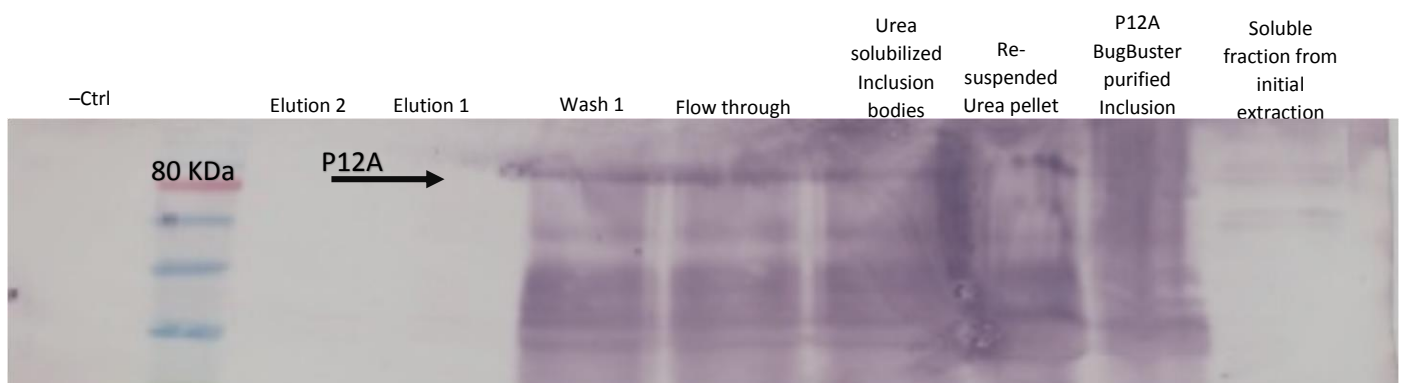


Figure 2.12. Western blot with anti-His 1 antibodies, of gel comparing purified inclusion bodies of insoluble P12A expressed in *E.coli*, via pProEX, induced with IPTG for 3 h. The expressed prtein was purified with BugBuster inclusion body purification protocol followed by 8M urea denaturation and NTA resin column purification. Lane 1 = pProEX-empty pre-induced; lane 3 = pProEX-P21A purified inclusion bodies elution 2; lane 4 = pProEX-P21A purified inclusion bodies elution 1; lane 5 = pProEX-P21A purified inclusion bodies Wash 1; lane 6 = Flow through; lane 7 = solubilized Inclusion bodies with 8M Urea; lane 8 = re-suspended pellet from 8M urea treatment; lane 9 = BugBuster purified Inclusion bodies; lane 10 = Soluble fraction from initial extraction. Ladder used = NEB #P7712S boad range protein marker.

2.4 Discussion

The gene for the P12A oligopeptide was successfully cloned into the pProEX expression vector which was subsequently transformed into competent *E. coli* for protein expression. Induction of the recombinant *E. coli* with IPTG resulted in P12A expression after 1 to 3 hours, visualised as an 80 kDa sized protein band on western blots. The highest observed expression was after 3 hours induction and this time was subsequently used for further expression. Although P12A was present in both soluble and insoluble fractions of the cells, the higher levels appeared to be in the insoluble fraction, and so further work was carried out with this fraction. The insoluble fraction was repeatedly washed with BugBuster™ Protein Extraction Reagent and PBS in efforts to increase the concentration of P12A by removing impurities.

Further attempts to purify P12A with Ni-NTA resin were unsuccessful. This was not surprising. The protein was from the insoluble fraction and the resin is known to have poor binding with insoluble proteins. Insoluble proteins have hydrophobic chemical groups exposed, and the charged histidine groups are inaccessible to the nickel chelating complex of the resin. The challenge of recombinant protein aggregating into inclusion bodies, as a consequence of incomplete protein folding, when expressed with *E. coli* is frequently encountered (Singh et al. 2015).

Consequently, treatment with 8 M urea was used in an attempt to solubilize the insoluble P12A protein so that it might bind to the resin. Urea is a widely recognized denaturing agent aiding solvation of proteins through stabilizing peptide and non-polar groups, thereby denaturing the proteins by decreasing hydrophobic effects and forming hydrogen bonds, binding with amide groups (Wei et al. 2010; Zou et al. 1998; Duke & Carolina 1963). Urea treatment however also proved ineffective in binding the His-tag of P12A with Ni-NTA resin.

Chapter 3

Plant expression and yield quantification of FMDV structural proteins and VLP formation

3.1 Overview

In the past, virus-like particles (VLPs) of FMDV serotype O and Asia 1 have been successfully expressed with a baculovirus expression system (Li et al. 2016; Mohana Subramanian et al. 2012; Cao et al. 2009). Other expression systems have also been used to express FMDV VLPs such as silkworm larvae (Li et al., 2012), *E. coli* (Lewis et al., 1991; Xiao et al., 2016), insect cells (Cao et al., 2009; Porta et al., 2013b; Roosien et al., 1990), mammalian cells via recombinant vaccinia virus (Abrams et al., 1995) and in transfected mammalian cells (Mignaqui et al., 2013). In addition to these, various FMDV structural proteins and VLPs have been expressed in plants as an expression system. These include transgenic alfalfa plants and tomato fruits (Dus Santos et al., 2005; Dus Santos and Wigdorovitz, 2005). Carrillo et al. (1998), document the expression of FMDV structural protein VP1 in transgenic *Arabidopsis thaliana*, the earliest account of a virus antigen expressed in a transgenic plant, conferring protective immunity. This was used as a subunit vaccine to immunize mice against virulent FMD. In a similar fashion, the polyprotein VP1 with the 3C protease was expressed in transgenic Alfalfa, and also induced a protective immune response in mice (Dus Santos et al. 2005). Polyepitope proteins including B-cell epitopes of FMDV VP1 and VP4 with T-cell epitopes from 2C and 3D proteins, have also been successfully expressed in *E. coli* and *N. benthamiana*, and demonstrated to induce an efficient immune response in guinea pigs (Andrianova et al. 2011). In addition, Veerapen *et al.* (Veerapen et al. 2018) showed the expression of FMDV structural proteins and VLP assembly using transient expression mediated by agroinfiltration of a recombinant plant expression vector. However, yields of VLPs were low.

The primary objective of this project was to compare the transient expression of FMDV structural proteins and VLP formation in *N. benthamiana* using two additional plant expression vectors to determine whether the VLP yield could be increased. The three different plant expression vectors; pEAQ-HT, pTRAc, and pRIC3.0 (schematically illustrated in Figure 3.1) have distinguishing features: the pEAQ-HT vector allows for the easy and quick expression of recombinant proteins in plants and is based on the Cow Pea Mosaic Virus derived from pBINPLUS but with over half of the vector backbone removed. The reduced size of the vector can be transcribed and translated more quickly, thereby greatly improving yields (Sainsbury et al. 2009); pTRAc by contrast is a plant expression vector created using the Cauliflower Mosaic virus (CaMV) 35S promoter and to improve expression of foreign genes it includes duplicated transcriptional enhancer chalcone synthase 5' UTR and CaMV 35S polyadenylation signal (Maclean et al. 2007); pRIC3.0 was created from the pTRAc backbone with the incorporation of intergenic regions based on the Bean Yellow Dwarf Virus (BeYDV), which creates DNA replicons containing the inserted gene that can be transcribed and thus translated independently, thus providing higher expression (Regnard et al. 2010).

The principle of this approach to create a vaccine candidate, was to introduce the P12A3C gene encoding the FMDV structural proteins into *N. benthamiana* plants via *Agrobacterium*-mediated transformation of the recombinant vectors by infiltration. The significance of incorporating the 3C protease is that it facilitates cleavage of the P12A oligopeptide into component structural proteins: VP0, VP1, and VP3, necessary for VLP formation; whether this also happened with expression via the pTRAc vector was of particular interest in this project. Infiltrated plant leaves were harvested several days post infiltration and screened for FMDV protein expression.

3.2 Materials and methods

The methods are summarised in a stepwise procedure presented in the Work-Flow chart 3.1 at the end of the section (Pg 46).

3.2.1 Cloning of recombinant plant expression vector pTRAc-P12A3C

The same *Nicotiana*. codon optimised *P12A3C* (section 2.2), was cloned into the pTRAc plant expression vector (Maclean et al. 2007) for expression of the FMDV viral capsid proteins in *N.benthamiana*.

Alternative vector constructs pEAQ-HT-P12A3C and pRIC3.0-P12A3C, were provided by the BRU. The vector maps for pTRAc, pRIC3.0 and pEAQ-HT are illustrated in Figure 3.1.

The XhoI and NcoI restriction enzymes were used for the excision of the gene from the pUC 57-P12A3C plasmid. NcoI and AflIII, with restriction sites complementary to NcoI and XhoI respectively, were used for the digestion linearization of the destination pTRAc vector to generate compatible sticky ends for ligation of the vector construct. Since the pTRAc expression vector does not contain an NcoI site; AflIII and XhoI restriction enzymes (Thermo Fischer Scientific) were used to linearize the pTRAc vector in order to enable the complementary insertion of the *P12A3C* gene. Endonuclease restriction digest reactions were performed according to the manufacturer's instructions (Thermo Fisher Scientific) at 37 °C for 1 hour.

DNA fragments were separated by electrophoresis in a 1 % (w/v) agarose gel at 120 V for 1 hour. The gel was viewed under longwave UV A light (400nm) to reduce potential damage to the DNA while enabling the excision of the DNA bands. The precise portions of gel containing the relevant 2952 bp DNA bands were manually excised using a scalpel blade and DNA extracted according to the instructions of the QIAquick® Gel Extraction Kit (QIAGEN). DNA was de-phosphorylated with Shrimp Alkaline phosphatase (rSAP by New England Biolabs). A ligation reaction was performed to clone *P12A3C* into linearized pTRAc using T4DNA ligase (Thermo Fischer Scientific) to generate pTRAc-P12A3C (Figure 3.2).

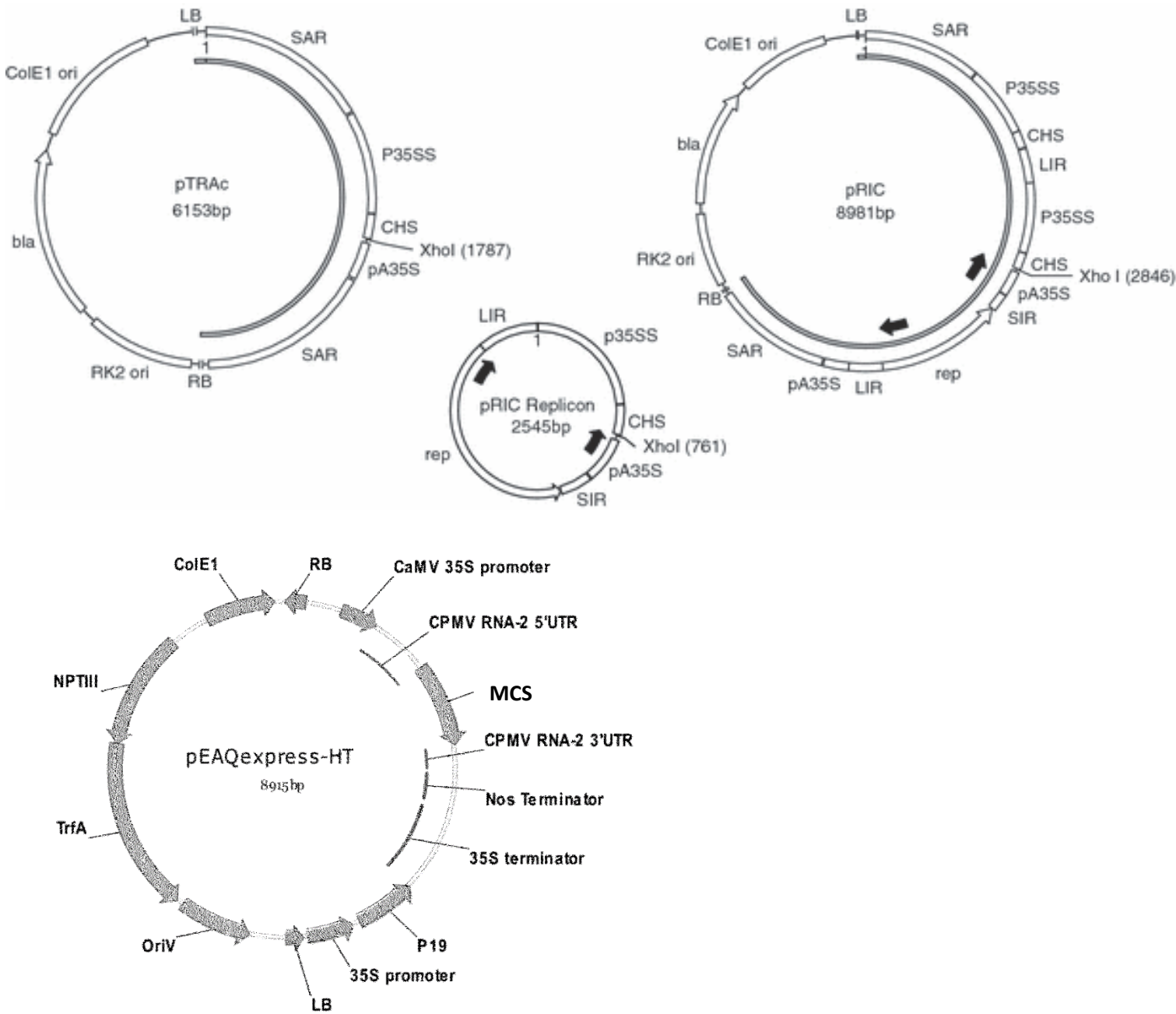


Figure 3.1. Vector maps of pTRAc (top left), pRIC (top right with pRIC replicon (centre)) (Maclean et al. 2007), and pEAQ-HT (bottom left) (Sainsbury & Lomonossoff 2008).

3.2.2 Transformation of pTRAc-P12A3C into *E. coli* and *A. tumefaciens*

The newly constructed pTRAc-P12A3C (Figure 3.2) was transformed into *E. coli* by heat shock (see section 2.3.2). These cells were plated on media containing 100 µg/mL ampicillin and then incubated at 37 °C overnight. Transformed *E. coli* cells were verified by a means of DNA digest reactions using endonuclease restriction enzymes EcoRV (Thermo Fischer Scientific) which recognises two restriction sites, one of which is situated within P12A3C, and another present in the vector (Figure 3.2) to yield two bands of approximately 6.2 kb and 2.9 kb. Colony PCR using the same primers described in section 2.3.3 was also performed for confirmation. Transformed *E. coli* cells from the plate were used to inoculate 10 mL LB and grown in culture overnight at 37°C with agitation. Recombinant *E.coli* DNA was extracted using QIAprep Spin Miniprep Kit (QIAGEN), according to the manufacturer's instructions.

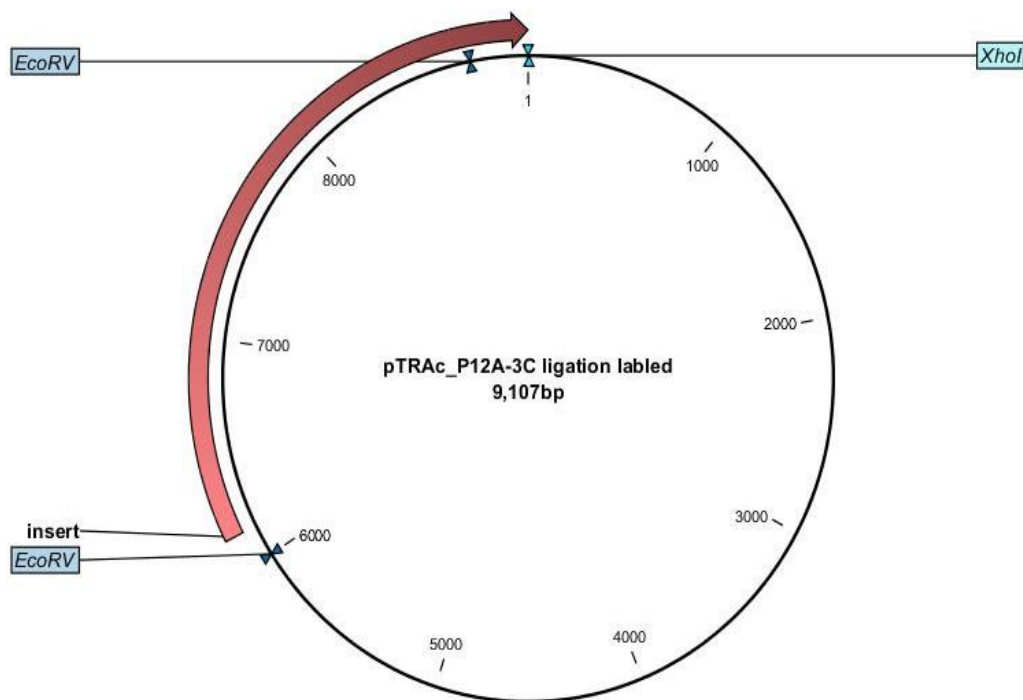


Figure 3.2. Schematic diagram of pTRAc-P12A3C vector construct indicating position of EcoRV and XhoI endonuclease restriction sites in relation to the gene insert size.

Electrocompetent *A. tumefaciens* cells were prepared by inoculating 100 mL LB containing 30 µg/mL kanamycin, and 50 µg/mL rifampicin with 1 mL *A. tumefaciens* GV3101::pMP90RK and incubated overnight at 27 °C with agitation. The 100 mL overnight culture was then centrifuged at 2448.5 × *g* for 10 min to pellet cells. The supernatant was discarded and the cell pellet resuspended in 2 mL sterile water, then tubes refilled and re-centrifuged for 10 min at 2448.5 × *g*. The rinse step was repeated, and then the cell pellet was resuspended in 10 % glycerol and washed again as described above. The wash with 10 % glycerol was also repeated. The final pellet was resuspended in a volume of 5 mL 10 % glycerol.

Electrocompetent *A. tumefaciens* GV3101::pMP90RK cells were transformed by electroporation (1.8 kV; 25 µF; 200 Ω) with the pTRAc-P12A3C plasmid DNA purified from *E. coli*. Transformed cells with pTRAc-P12A3C were selectively grown on plates of LB media containing kanamycin (50 µg/mL), carbenicillin (100 µg/mL) and rifampicin (100 µg/mL), then verified by EcoRV endonuclease restriction digest and colony PCR amplification using the same screening primers described in section 2.2.2 (Table 3.1), with same parameters (Table 3.2). Recombinant agrobacteria were used for infiltration of *N. benthamiana* plants.

Table 3.1. P12A3C screening primers for PCR amplification of 500 bp internal gene fragment

	Orientation	5'-3' Nucleotide sequence
PPX-P12A-F	forward	ttccatgggagcaggtcaatcaagt
P12A-screening R	reverse	caagtttggaagatgaccgaaag

Table 3.2. Colony screening PCR cycle parameters

PCR step	Initial Denaturation	Denaturation	Annealing	Extension	Final Extension	Hold
Temp (°C)	95	95	63	72	72	10
Duration	3 min	30 sec	30 sec	3 min	15 min	
		Number of cycles = 30				

3.2.3 Small scale syringe infiltration of *N. benthamiana* leaves

In an attempt to optimise protein expression with the pTRAc-P12A3C vector construct, an optical density trial was performed to estimate the best concentration of bacteria to use for infiltration, and simultaneously a time trial was conducted to provide some indication of the best time at which to harvest leaves for optimal protein expression. Three × 10 mL LBB (composition detailed in appendix B) vials were inoculated with 500 µL pTRAc-P12A3C and the cultures grown overnight at 27 °C with agitation. Infiltration medium (appendix B) was added to each 10 mL culture to dilute the cultures to optical densities (OD_{600}) of 0.25, 0.5 and 0.75. *Nicotiana benthamiana* plants were infiltrated with *Agrobacterium* suspensions; by injecting into the abaxial air spaces from the underside of the leaf, using a 1 mL syringe and left to grow under conditions of 24°C, 55% humidity and an 16h:8h light:dark cycle. Three leaf discs, approximately 1 cm (size of an Eppendorf tube cap) in diameter were harvested (closing an Eppendorf tube cap to punch the holes/discs out of the leaves) from plants at 3, 4, 5, 6, and 7 days post infiltration. Leaf discs were ground to a fine powder in liquid nitrogen using a micro pestle. Protein extraction was performed using 400 µL (PBS) with 0.5 % Triton X-100, and one protease inhibitor tablet (Roche EDTA free mini cocktail tablets) (1/10 mL) to reduce protein degradation resulting from the release of endogenous protease enzymes during leaf processing. Samples were vortexed for 2 minutes then centrifuged in a benchtop centrifuge (Eppendorf 5424) at $17933.4 \times g$ for 5 minutes. After centrifugation the supernatant was transferred to a clean tube. The soluble proteins were denatured with the addition of 5 × sample application buffer (SAB) (appendix B) and incubated at a temperature of 95 °C for 10 minutes. Samples were then analysed by SDS-PAGE and western blot, as described in section 2.2.4, with guinea pig or rabbit anti FMDV antiserum (kindly donated by Andres Wigdorovitz, INTA, Buenos Aries) diluted 1 in 100 in blocking buffer (+ 5 % m/v fat-free milk powder in 1 × PBS), and incubated at 4°C with shaking overnight for primary antibody probing.

3.2.4 *Large scale vacuum infiltration of N. benthamiana*

Large-scale expression involved infiltration of up to 25 plants, approximately four weeks old. For this scale of infiltration, 1L volumes of LBB media were inoculated with an 11 mL pre-culture of recombinant *Agrobacterium* strain. Transformed *A. tumefaciens* contained either pTRAc-P12A3C; pRIC3.0-P12A3C, or pEAQ-P12A3C, grown overnight at 27 °C containing respective antibiotics (kanamycin, rifampicin and carbenicillin for GV3101 agrobacteria and only kanamycin and rifampicin for pEAQ containing LBA4404 Agrobacteria, at concentrations described in section 3.2.2), with agitation. The 1 L inoculated culture was also grown overnight at 27 °C and then diluted with infiltration medium to an OD₆₀₀ of 0.5. The plants were infiltrated by vacuum infiltration at -100 kpa. Plants were returned to growth rooms to continue growing and allow for expression of the heterologous protein. These rooms had the same growing conditions as described above.

3.2.5 *Processing of large-scale infiltrated leaves*

Plant leaves were harvested 3 days post infiltration. Sixty grams of plant leaves were homogenised with 180 mL of buffer solution, (buffer solution volume (ml) = 3 × leaf mass (g): 1 × PBS (pH 7.0) supplemented with 1% Triton-X100 and three protease inhibitor cocktail tablets (Roche), using a homogenizer). The homogenous liquid was left to shake at 4 °C for 30 minutes to allow for protein extraction. The liquid was then filtered through a double layer of Miracloth™ to remove leaf debris, after which it was centrifuged (Beckman Coulter) at 3098.8 × *g* for 15 minutes, removing any remaining cellular debris. The supernatant was pipetted on to a 5 mL cushion of 30 % sucrose (w/v in PBS), and centrifuged (Beckman Coulter ultra-centrifuge) at 125755 × *g* for 3 hours at 20 °C.

One millilitre fractions were taken from the supernatant, the 30 % (w/v) sucrose cushion, and a sample from the pellet respectively, for analysis by SDS-PAGE and western blot as described in 2.2.4.

The remaining pellet was then re-suspended with 3 mL PBS containing 1 % Triton X-100 and 5 µL Benzonase® nuclease, in a mortar with a pestle. The pellet suspension was left overnight at 4 °C

allowing time for maturation to promote particle formation before being separated by rate-zonal centrifugation.

3.2.6 Sucrose gradient purification of VLPs

A continuous sucrose density gradient ranging from 5 to 20 % sucrose (w/v) was set up in a volume of 34 mL in a 40 mL ultracentrifuge tube. The re-suspended pellet matured overnight was loaded on top of the sucrose gradient. A further 2 mL of PBS was used to rinse the mortar of residual pellet suspension adhering to the sides, and added to the ultracentrifuge tube, bringing the total volume of pellet suspension to 5 mL, once the 5 mL of re-suspended pellet had been laid on top of the sucrose gradient, it was centrifuged at $125755 \times g$ for 3 hours. The procedure was repeated, centrifuging the pellet suspension through a 15 – 40 % sucrose gradient for 2 hours instead of 3 hours. The gradient was fractionated into 1 mL fractions.

3.2.7 Analysis of gradient fractions

Dot blots were performed with the gradient fractions. A 2 μ L aliquot from each fraction was pipetted onto a piece of nitrocellulose membrane. The membrane was washed in blocking buffer (appendix B) containing 1 % Tween20 and 5 % (m/v) milk powder for 15 minutes. The membrane was then probed with guinea pig anti-FMDV polyclonal antiserum (1:100 dilution), overnight. Following the probing with primary antibodies, the membrane was again washed with blocking buffer and then probed with alkaline phosphatase conjugated rabbit anti-guinea pig secondary antibodies (Sigma-Aldrich) developed in rabbits (diluted 1 in 10000), after which the dot-blot membrane was washed and developed over 1 hour with BCIP/NBT substrate (KPL). Those fractions that generated the darkest dots were selected for further analysis by SDS-PAGE and western blot (performed as described in section 2.3.4).

To determine whether expressed proteins assembled into VLPs, transmission electron microscopy (TEM) was used for viewing of selected fractions. Glow discharged carbon/copper grids were placed on 10 μ L of the protein extracts and left for 2 min before being washed 6 times with sterile distilled water. Grids were then floated on 20 μ L of 2 % uranyl acetate for 1 min, dried and then viewed with a Zeiss 912 OMEGA Energy Filter Transmission Electron Microscope, University of Cape Town, to evaluate whether the expressed proteins were able to assemble into VLPs, and hence determine the fraction of the gradient in which the VLPs could be found.

3.2.8 Protein quantification

Fractions containing putative VLPs were also separated by SDS-PAGE together with a standardised bovine serum albumin (BSA) dilution series, from 3.13 μ g – 0.20 μ g, and then stained with Coomassie blue in order to quantify the relative amount of the expressed protein by gel densitometry. The quantification estimates were performed using SynGene™ computer software, to calculate the approximate total protein yield.

The FMDV capsid protein genes *P12A3C* were cloned into the pTRAc expression vector from pUC 57



Competent *E. coli* cells were transformed with recombinant pTRAc-P12A3C by heat shock and grown in culture to amplify the quantity of recombinant plasmid DNA.



A. tumefaciens were transformed by electroporation with recombinant pTRAc-P12A3C DNA amplified and extracted from *E. coli*



Plants were infiltrated with media containing the transformed *A. tumefaciens*. Syringe infiltration was used for small scale (<5 plants) while vacuum infiltration was used for large scale (≥ 20 plants)



Leaf material was harvested after at least 3 days growth post infiltration.



Harvested leaf material was processed for protein extraction.



Protein extract was purified by ultra centrifugation through a sucrose cushion and sucrose gradient.



samples were analysed by SDS-PAGE with western blot and commasie stain, and samples were also prepared on grids for TEM viewing.

Work-Flow chart 3.1

3.3 Results

3.3.1 Plant expression vector construction – pTRAc-P12A3C

P12A3C was successfully cloned into the pTRAc plant expression vector to yield pTRAc-P12A3C. The construct was successfully transformed into *A. tumefaciens* pMP90::RK90 as demonstrated by PCR of putatively transformed colonies and double restriction digest. Figure 3.3 shows the expected 500 bp band amplified from P12A3C insert of all colonies selected. Figure 3.4 shows two bands, of approximately 2900 bp and 6200 bp, appropriately sized for the EcoRV double digest of the pTRAc containing the *P12A3C* insert, compared with linearized empty pTRAc of 6107 bp.

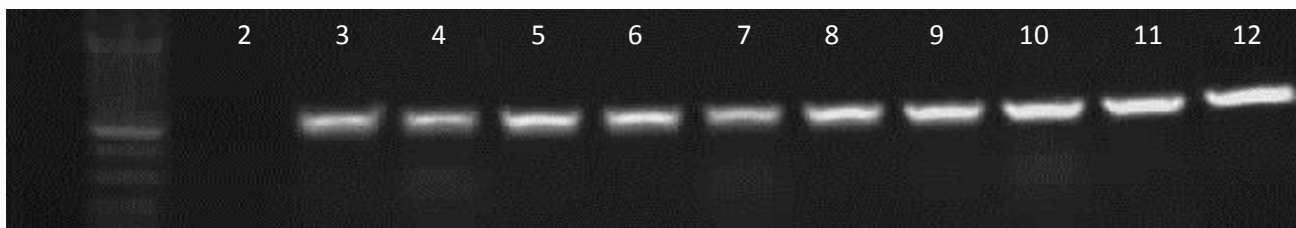


Figure 3.3. Agarose gel electrophoresis showing results of the colony screening PCR amplification of a 500 bp internal gene fragment. The presence of a band verifies successful insertion and subsequent ligation of the *pTRAc-P12A3C* vector construct. Lane 2 = pTRAc-empty (negative control); lane 3 – lane 11 = selected colonies 1 – 10; lane 12 = pUC57 storage plasmid of P12A3C (positive control). Ladder used = O'GeneRuler™ 100 bp Plus DNA Ladder.

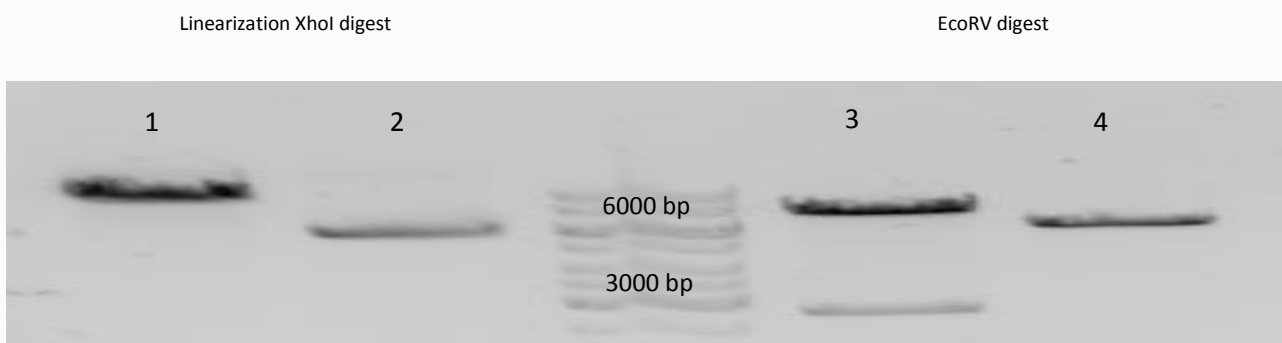


Figure 3.4. Restriction endonuclease digestion to linearize pTRAc-P12A3C construct and empty pTRAc with XhoI (lanes 1 & 2 respectively), and with EcoRV (lanes 3 & 4 respectively). Ladder used = O'generuler 1kb.

3.3.2 Syringe Infiltration of pTRAc-P12A3C to assess protein expression

Small scale syringe infiltration served to evaluate on which day it was best to harvest leaves to achieve, qualitatively, the highest level of protein expression, and similarly at what bacterial concentration (OD_{600}) expression was most effective. It also served to verify whether the P12A3C polypeptide expressed with pTRAc-P12A3C would in fact be cleaved into its component structural proteins (VP0, VP1, VP3) in plant host cells. Western Blot analysis of protein samples taken 3, 5, and 7 days post infiltration, from plants infiltrated with infiltration medium of OD_{600} 0.5, revealed bands in line with the 25 kDa marker, which is approximately the size of the FMDV VP1 and VP3 proteins which are of similar size, thus confirming cleavage of P12A (Figure 3.5). A second band in lane 2 was also observed between 32 KDa and 48 KDa markers appropriate for the size of VP0. A band in the region of the 80 KDa marker was also seen, which may possibly be uncleaved P12A. The VP3/VP1 bands were most apparent in the samples harvested on day 3 and day 5; this is similar to expression of pRIC3.0-P1-2A3C and pEAQ-HT-P1-2A3C in plants – shown in previous work done in the BRU. Based on this observation, whole plant leaves were all harvested at 3 days post infiltration in subsequent large-scale plant expression experiments using vacuum infiltration. The optical density of the infiltration medium did not influence protein expression particularly significantly as seen by

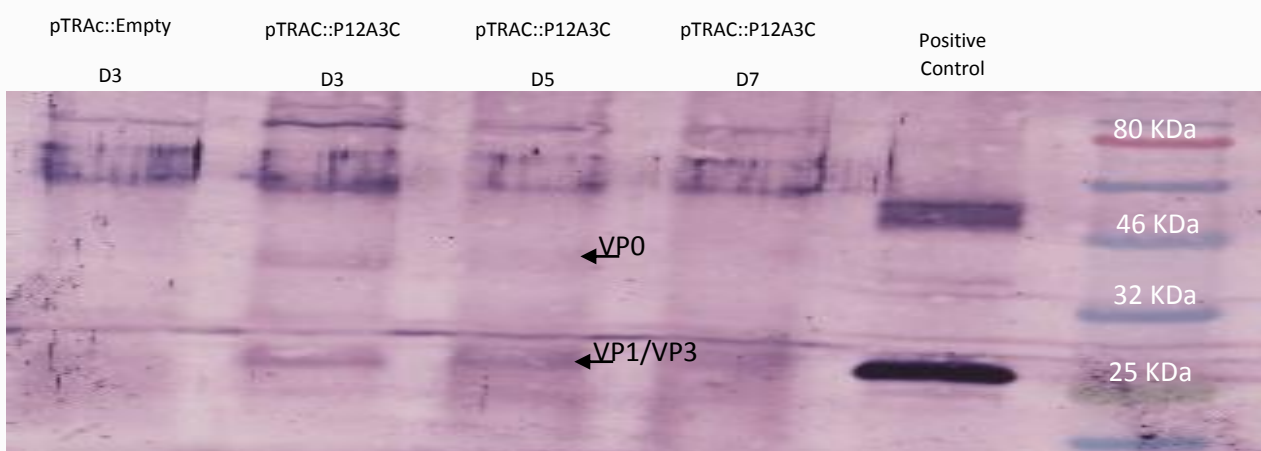


Figure 3.5. Western blot of gel comparing P12A-3C extracted from *N.benthamiana* leaf discs harvested 3, 5, and 7 days post infiltration lanes 2 – 4. Lane 1 = pTRAc-empty (negative control); lane 5 = Isolated FMDV positive control. Ladder used = NEB # P7712S boad range protein marker.

similar band intensities (data not shown), with the exception of the observation that the highest optical density of approximately 0.75 resulted in more severe and more rapid leaf necrosis.

3.3.3 Comparison of scaled up protein expression using different vectors

Having established that, like pRIC3.0-P12A3C and pEAQ-HT-P12A3c, expression of pTRAc-P12A3C also results in the FMDV VP0, VP1, and VP3 component proteins; infiltration using all three was scaled up for purification necessary for comparative purposes.

3.3.4 Sucrose gradient purification protein analysis

Protein purification involved a two-step ultracentrifugation procedure of the protein extract from the expression vectors pEAQ-HT-P12A3c, and pTRAc-P12A3C. The first ultracentrifugation step was carried out through a 30 % sucrose cushion to concentrate the FMDV proteins/VLPs in a pellet. Fractions from the supernatant, the 30% cushion region and the pellet separated on a SDS polyacrylamide gel showed the presence of VP0 and VP1/3 predominantly in the pellet for pTRAc-P12A3C (figure 3.7) and pEAQ-HT-P12A3C (figure 3.9) suggesting that VLPs were present in these samples (comparison with pRIC3.0-P12A3C expression was only introduced later, with the adjustment of parameters for rate-zonal centrifugation).

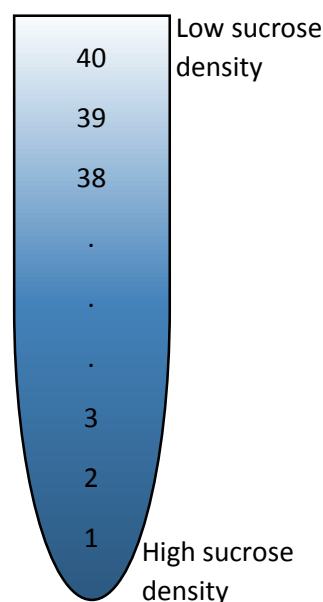


Figure 3.6: Schematic representation of rate-zonal sucrose gradient 1 mL fractions in ultracentrifuge tube.

The re-suspended pellet was subsequently centrifuged through a rate-zonal sucrose gradient, initially 5 – 20 %, which was fractionated (40 fractions per construct). The position of each fraction relative to the rate-zonal gradient in the ultracentrifuge tube is illustrated schematically in figure 3.6.

To minimise the number of fractions across which to sample for detection of the FMDV structural proteins by western blot, fractions were first dot-blotted (data not shown). The fractions displaying the darkest dots ranged from 1 to 10 for preparations from pTRAc-P12A3C and pEAQ-P12A3C vector constructs, and these were selected for analysis by SDS-PAGE and TEM.

No obvious VP0 or VP1/3 bands were observed in the subsequent rate-zonal gradient fractions derived from the pTRAc-P12A3C construct (Figure 3.7 and 3.8), although a very faint band for VP0 could be seen in fraction 2. By comparison, the band corresponding to VP3/VP1, as well as VP0 to a lesser extent, was clearly visible in the rate-zonal fractions 1, 2, 4, and 5, from the bottom of the tube (fraction 3 lost because of broken wells), expressed with the pEAQ-HT-P12A3C construct (Figure 3.9 and 3.10).

The re-suspended pellet was then loaded onto a rate-zonal sucrose gradient, which was then fractionated. The position of each fraction relative to the rate-zonal gradient in the ultracentrifuge tube is illustrated schematically in figure 3.6. Each of these fractions, for each respective vector construct, was compared subject to a dot blot to indicate which fractions contained most of the expressed FMDV capsid proteins (data not shown). Fractions displaying the darkest dots, along with the respective neighbouring fractions that also showed significant reaction with anti-FMDV antibodies, were selected for analysis by SDS-PAGE and TEM viewing. Rate-zonal fraction samples 1 – 10 were selected for comparison against each of the three fractions of the first centrifugation step through the 30 % sucrose cushion, by SDS-PAGE. Ten rate-zonal fractions were run against the crude supernatant, 30% cushion, and pellet, across two gels to accommodate all samples with controls and reference markers for both the pTRAc-P12A3C (Figure 3.7 and 3.8) and pEAQ-HT-P12A3C vector constructs (Figures 3.9 and 3.10).

pTRAc-P12A3C expression

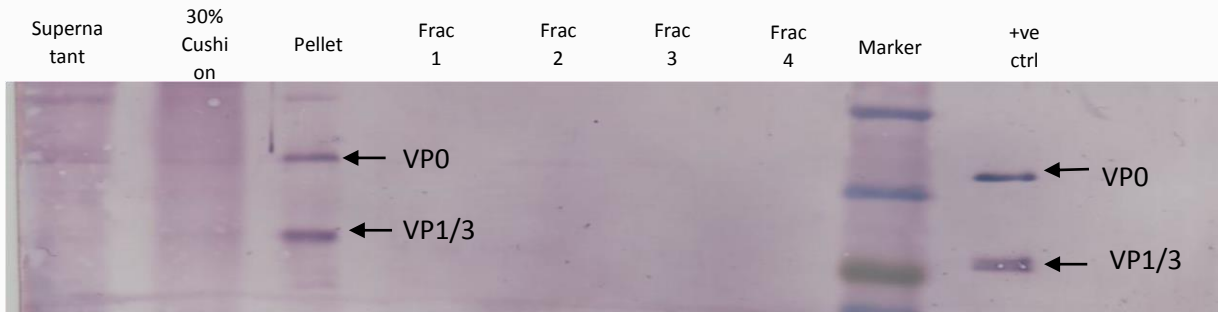


Figure 3.7. Western blot of gel showing crude samples, and fractionated samples of protein extract from pTRAc-P12A3C infiltrated plants, centrifuged through 5-20% rate zonal sucrose gradient. Lane 1 = supernatant, lane 2 = 30% sucrose cushion, lane 3 = pellet, lane 4 = fraction 1, lane 5 = fraction 2, lane 6 = fraction 3, lane 7 = fraction 4, lane 8 = fraction 5, lane 9 = Isolated FMDV positive control. Ladder used = NEB # P7712S broad range protein marker.

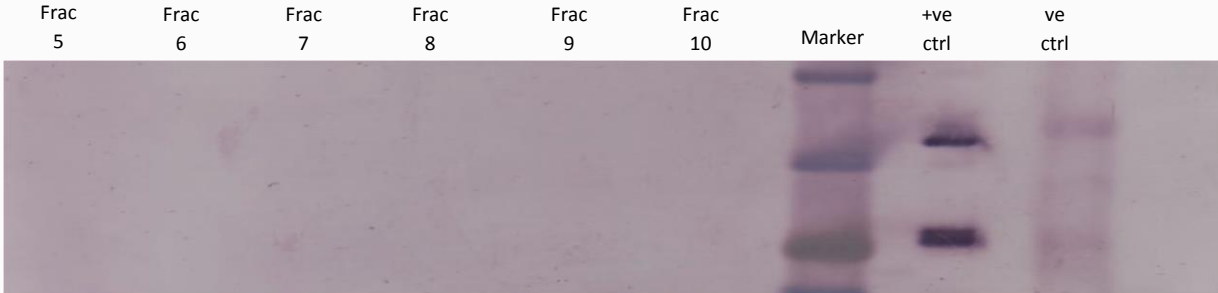


Figure 3.8. Western blot of gel showing crude samples, and fractionated samples of protein extract from pTRAc-P12A3C infiltrated plants, centrifuged through 5-20% rate zonal sucrose gradient. Lane 1 = fraction 5, lane 2 = fraction 6, lane 3 = fraction 7, lane 4 = fraction 8, lane 5 = fraction 9, lane 6 = fraction 10, lane 7 = fraction 4, lane 8 = fraction 3, lane 9 = Isolated FMDV positive control, lane 10 = pTRAc:empty (negative control). Ladder used = NEB # P7712S broad range protein marker.

pEAQ-HT-P12A3C expression

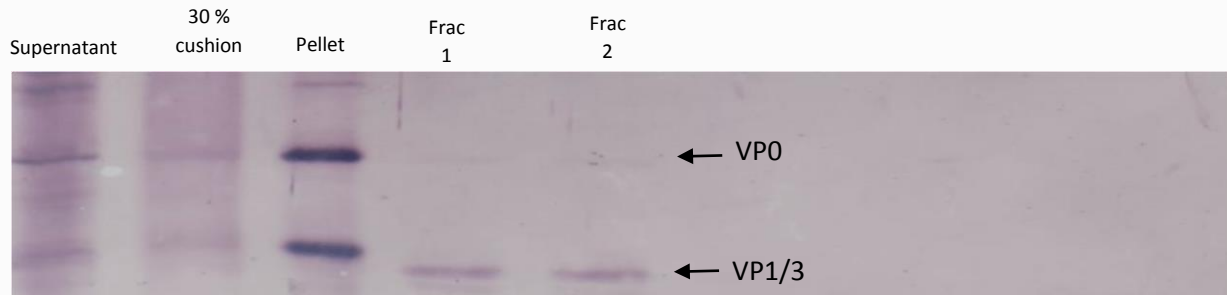


Figure 3.9. Western blot (of gel2) showing crude and fractionated samples centrifuged through 5-20% rate zonal sucrose gradient from protein extract of pEAQ-HT:P12A-3C infiltrated plants. Lane 1 = supernatant from 30% sucrose cushion, lane 2 = 30% sucrose cushion, lane 3 = pellet, lane 4 = fraction 1, lane 5 = fraction 2, lane 6 -10 = broken wells. Ladder used = NEB # P7712S broad range protein marker.

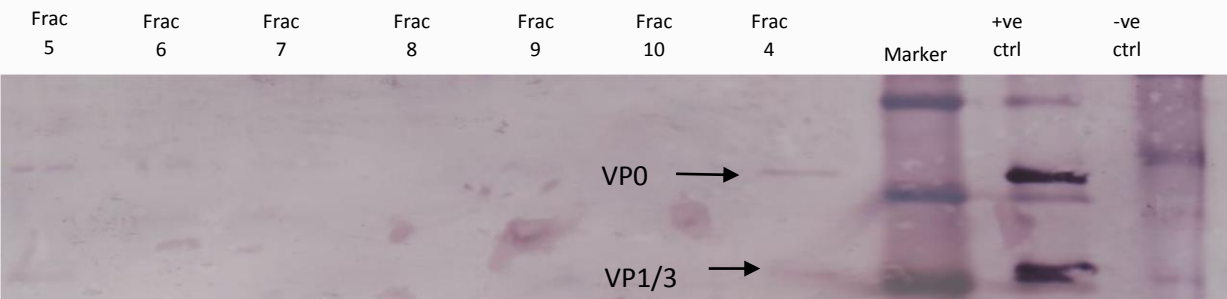


Figure 3.10. Western blot of gel showing fractionated samples from protein extract of pEAQ-HT:P12A-3C infiltrated plants, centrifuged through 5-20% rate zonal sucrose gradient. Lane 1 = fraction 5, lane 2 = fraction 6, lane 3 = fraction 7, lane 4 = fraction 8, lane 5 = fraction 9, lane 6 = fraction 10, lane 7 = fraction 4, lane 8 = fraction 3, lane 9 = positive control with ladder over-lap, lane 10 = pEAQ:empty crude. Ladder used = NEB # P7712S broad range protein marker.

FMDV proteins were enriched by pelleting them through the 30% sucrose cushion; Figures 3.7 and 3.9 demonstrate the effective removal of most unwanted proteins during this purification step, evident when comparing the absence of non-specific bands and protein smear in the lane of the pellet, against the lanes of the 30% cushion and the supernatant which present cross reactivity with unwanted proteins – a protein smear throughout the lanes. Similarly, the effective removal of any residual unwanted proteins during purification through the sucrose gradient can also be observed when comparing the lane of fractions 1 and 2 displaying a distinct bands absent of any smear, against the lane of the pellet (Figure 3.9). Concentrations of the desired FMDV capsid proteins were perhaps slightly higher for pEAQ than for pTRAc, which may have been really low since the band for VP0 was really faint in fraction 2 and otherwise absent, while bands for VP0 and VP1/3 were comparatively easily discernible for pEAQ.

Bands for both VP0 and VP1/3 are prominent in the pellet from the 30% cushion of pTRAc-P12A3C extract (Figure 3.7, lane 3), which was used for purification through the rate-zonal gradient, but these bands are absent in the subsequent rate-zonal fractions. This suggests the absence of any obvious VP1/3 bands in the rate-zonal fractions from pTRAc-P12A3C expressed protein (Figure 3.7 and 3.8) was possibly a result of the FMDV particles pelleting at the base of the tube during the rate-zonal ultracentrifugation step, instead of being suspended midway in the gradient. As the pellet was not collected this hypothesis could not be tested. To prevent the desired FMDV proteins or VLPs from pelleting during the rate-zonal gradient purification step, the rate-zonal centrifugation was repeated using a 15 – 40 % sucrose gradient with a reduced ultracentrifugation duration of 2 hours instead of 3 hours, adjusting the parameters to be more similar to those described by Cao et al. in their purification of FMDV capsid particles (Cao et al. 2009). Expression of FMDV capsid proteins with the vector construct pRIC3.0-P12A3C was introduced for comparison with pTRAc-P12A3C at this point. The gradient was fractionated and dot blots used to assess the predominant positions of the FMDV proteins as described above (data not shown). They were markedly different in that the predominance of the FMDV proteins in the gradient were shifted from fractions 1 to 10 to fractions

24 to 28. For pRIC3.0-P12A3C, fraction 28 (two thirds up the gradient from the bottom of the tube) displayed the darkest spot, fraction 24 displayed the darkest spot for pTRAc-P12A3C and fraction 26 displayed the darkest spot for pEAQ-HT P12A3C.

Fractions 24 -28 for both pTRAc-P12A3C and pRIC3.0-P12A3C, purified through the 15 – 40 %, were selected then compared by western blot (Figure 3.12 and 3.13). Protein expressed with pEAQ, purified through 15 – 40 % sucrose gradient was not reanalysed by western blot as had already been done with 5 – 20 %, and was instead only compared by dot blot and then TEM (section 3.3.5).

All five fractions (F24 to F28) from pTRAc-P12A3C, purified through a 15 – 40 % sucrose, displayed distinct bands of the sizes 25 kDa and 37 kDa appropriate for VP1/3 and VP0 respectively (Figure 3.11). Only fractions 25, 27 and 28 of pRIC3.0-P12A3C expressed protein, purified through 15 – 40 % sucrose gradient presented discernible bands of the sizes appropriate for VP1/3 and VP0 (Figure3.12).

pTRAc-P12A3C (15-40%)

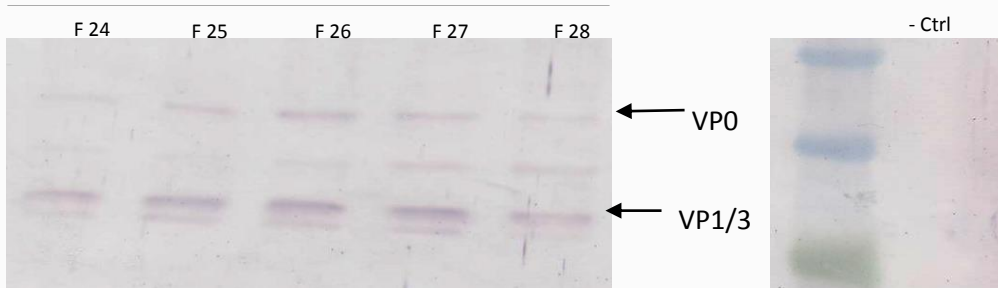


Figure 3.11. Western blot of gel comparing selected fractions of P12A3C expressed in *N. benthamiana*, using pTRAc purified with a 15% - 40% sucrose gradient (lanes 1-5), and pTRAc purified with a 5% - 20% sucrose gradient (Lane 1 = pTRAc-P12A3C Fraction 24; lane 2 = pTRAc-P12A3C Fraction 25; lane 3 = pTRAc-P12A3C Fraction 26; lane 4 = pTRAc-P12A3C Fraction 27; lane 5 = pTRAc-P12A3C Fraction 28; lane 10 = pTRAc-empty. Ladder used = NEB # P7712S boad range protein marker.

pRIC3.0-P12A3C (15-40%)

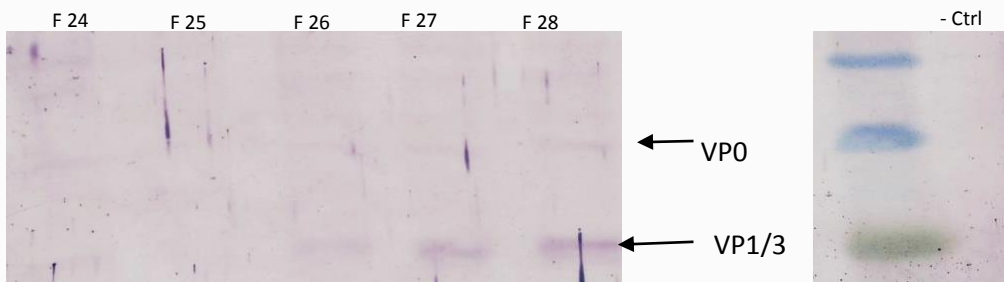


Figure 3.12. Western blot of gel comparing selected fractions of P12A3C expressed in *N. benthamiana*, using pRIC3.0 purified with a 15% - 40% sucrose gradient (lanes 1-5), Lane 1 = pRIC3.0-P12A3C Fraction 24; lane 2 = pRIC3.0-P12A3C Fraction 25; lane 3 = pRIC3.0-P12A3C Fraction 26; lane 4 = pRIC3.0-P12A3C Fraction 27; lane 5 = pRIC3.0-P12A3C Fraction 28; lane 10 = pRIC3.0-empty. Ladder used = NEB # P7712S boad range protein marker.

3.3.5 Transmission electron microscopy

Samples from the 15 to 40% gradients fractions described above were examined by TEM for the presence of particles: pTRAc-P12A3C - fraction 28, pRIC3.0-P12A3C - fraction 27 and pEAQ-HT-P12A3C, fraction 28. In all cases, VLPs of 25 ± 5 nm in diameter were observed (Figures 3.13 - 3.15). These resembled FMDV and VLPs depicted in electron micrographs from literature (McKenna et al. 1996; Li et al. 2012; Cao et al. 2009; Kotecha et al. 2015; Li et al. 2016; Liu et al. 2017; Xiao et al. 2016; Veerapen et al. 2018). The VLPs uniformly appear as distinct, regular spherical/circular structures contrasting against the background debris, ranging slightly in size from 23 to 30 nanometres in diameter (the length of the line drawn across the diameter is displayed in images 3.13a, 3.14b, and 3.15a). Sizes of 23 – 30 nm are consistent with the size of FMDV virus particles and VLPs cited in literature (K. Strohaimeier 1982; Grubman & Baxt 2004; Liu et al. 2017).

Figure 3.13 displays sample derived from pEAQ-P12A3C with VLPs present; individual particle diameter lines were measured to be 27.77 and 28.59 nm. Figure 3.13 b displays a duplicate image of 3.13a, with increased magnification. Figure 3.14 presents sample expressed with pRIC3.0-P12A3C, Figure 3.14b is a magnified image of the same sample, with particle diameters measuring 24.74, 25.43, 26.94 nm. A sample of protein expressed with pTRAc-P12A3C is displayed in figure 3.15 with particle diameter measuring 23.71 nm, Figure 3.15b is a magnified image of the same sample. Figure 3.16a and 3.16b display negative control samples of purified protein extract from plants infiltrated with pTRAc-empty and pEAQ-HT-empty respectively. No VLPs are present in these samples.

These images provide supporting evidence that plant expressed FMDV viral capsid proteins were indeed able, with the presence of the 3C protease, to cleave appropriately into the respective individual structural proteins and self-assemble into VLPs. The sample derived from the plants infiltrated with pRIC3.0-P12A3C seemed to show many VLPs in the frame viewed (Figure 3.19a). However, it must be noted that TEM imaging was used solely for the qualitative assessment of particle formation and was not used as a means of quantifying the number of particles formed.

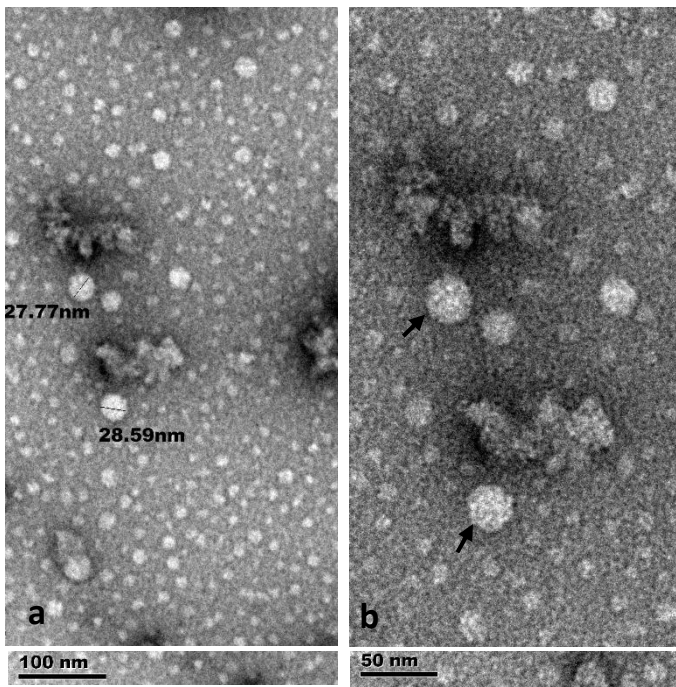


Figure 3.13a: TEM image displaying VLPs (Identified by black arrows, with figures indicating the precise length of the line drawn across the diameter) derived from a sample expressed by pEAQ-P12A3C fraction 28. Reference scale bar = 100 nm.

Figure 3.13b: Magnified TEM image displaying VLPs (Identified by black arrows) derived from same sample expressed by pEAQ-P12A3C fraction 28. Reference scale bar = 50 nm.

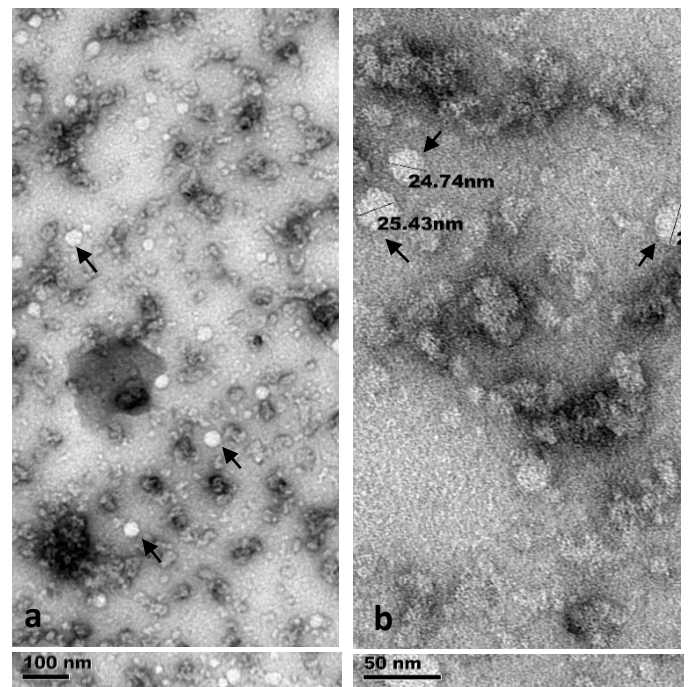


Figure 3.14a: TEM image displaying VLPs (Identified by black arrows) derived from a sample expressed by pRIC-P12A3C fraction 27. Reference scale bar = 100 nm.

Figure 3.14b: Magnified TEM image displaying VLPs (Identified by black arrows, with figures indicating the precise length of the line drawn across the diameter) derived from same sample expressed by pRIC-P12A3C fraction 27. Reference scale bar = 50 nm.

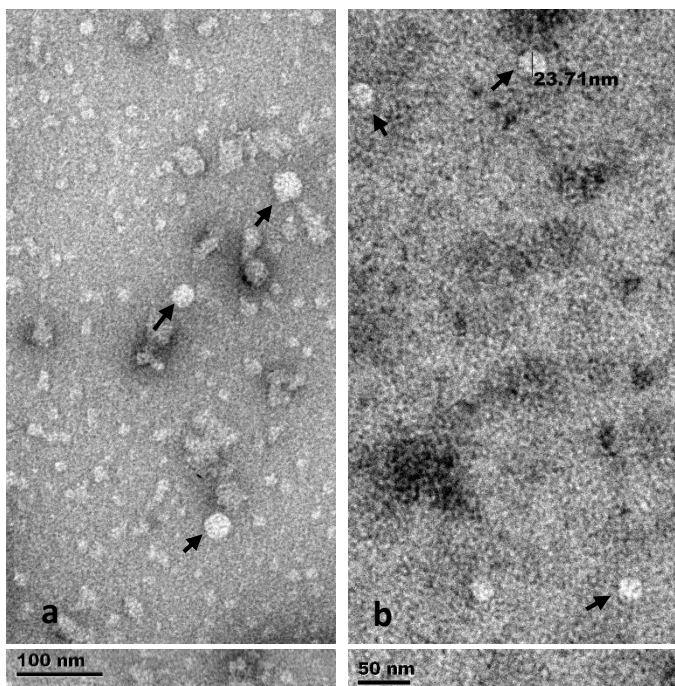


Figure 3.15a: TEM image displaying VLPs (Identified by black arrows) derived from a sample expressed by pTRAc-P12A3C fraction 28. Reference scale bar = 100 nm.

Figure 3.15b: Magnified TEM image displaying VLPs (Identified by black arrows, with figures indicating the precise length of the line drawn across the diameter) derived from same sample expressed by pTRAc-P12A3C fraction 28. Reference scale bar = 50 nm.

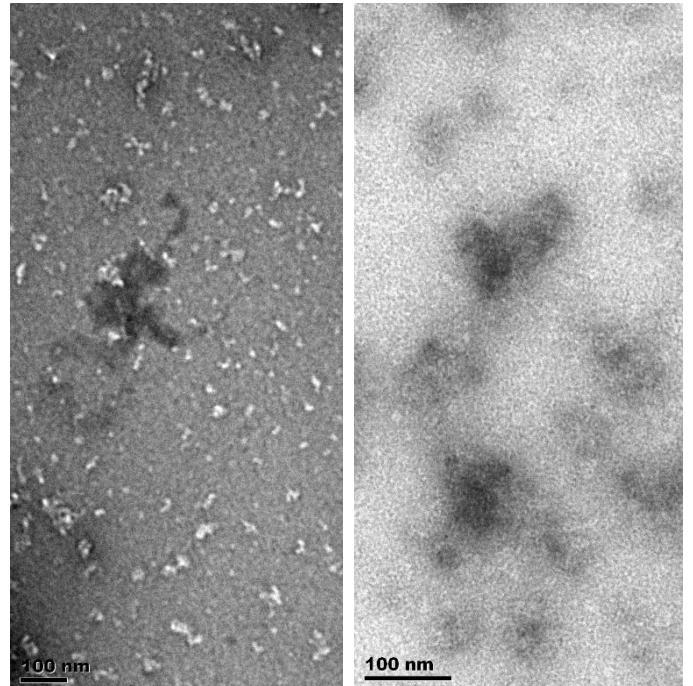


Figure 3.16a: TEM image displaying absence of VLPs derived from a sample expressed by pTRAc-empty (negative control,) fraction 28. Reference scale bar = 100 nm.

Figure 3.16b: TEM image displaying absence of VLPs derived from a sample expressed by pEAQ-empty (negative control), fraction 18. Reference scale bar = 100 nm.

3.3.6 Protein yield quantification

Quantification of expressed FMDV protein using all three expression vectors was done by densitometric analysis of Coomassie stained gels. Fractions were selected for each of the respective three constructs, and were independently quantified against a dilution series of Bovine serum albumin (BSA) ranging from 0.20 to 3.13 μg .

Figures 3.19, 3.20 and 3.21 show the Coomassie-stained gels of proteins expressed using pTRAc-P12A3C, pEAQ-HT-P12A3C and pRIC3.0-P21A3C, respectively, and Table 3.3 displays the estimated quantity of each. For pTRAc-P21A3C (Figure 3.19), fractions 24 and 25 showed distinct bands of 25 kDa corresponding to VP1/3, while those of fractions 27 and 28 were comparatively faint; the 37 kDa band of VP0 was more visible in fractions 27 and 28 than in fractions 24 and 25. These bands correspond to those detected by western blot, shown in figure 3.11.

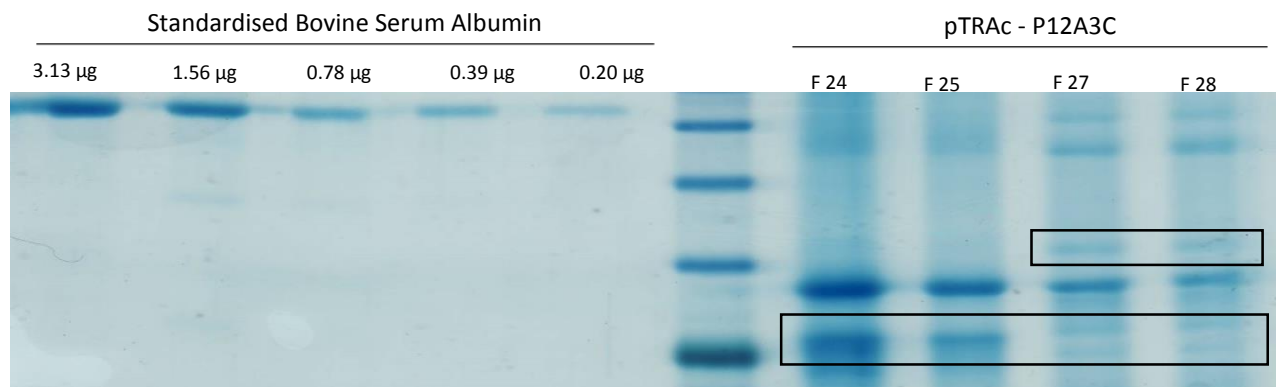


Figure 3.19. Coomassie stain comparing selected fractions of P12A3C expressed in *N. benthamiana*, using pTRAc- P12A3C (lanes 7-10), purified with a 15% - 40% sucrose gradient. Lane 1 = Bovine Standard Albumin 3.13 μg ; lane 2 = Bovine Standard Albumin 1.56 μg ; lane 3 = Bovine Standard Albumin 0.78 μg ; lane 4 = Bovine Standard Albumin 0.39 μg ; lane 5 = Bovine Standard Albumin 0.20 μg . lane 7 = pTRAc-P12A3C Fraction 24; lane 8 = pTRAc -P12A3C Fraction 25; lane 9 = pTRAc -P12A3C Fraction 27; lane 10 = pTRAc -P12A3C Fraction 28; Ladder used = NFB # P7712S broad range protein marker.

For pEAQ-HT-P12A3C, no bands corresponding to the VP1/3 and VP0 proteins were detectable in any of the fractions tested (figure 3.20).

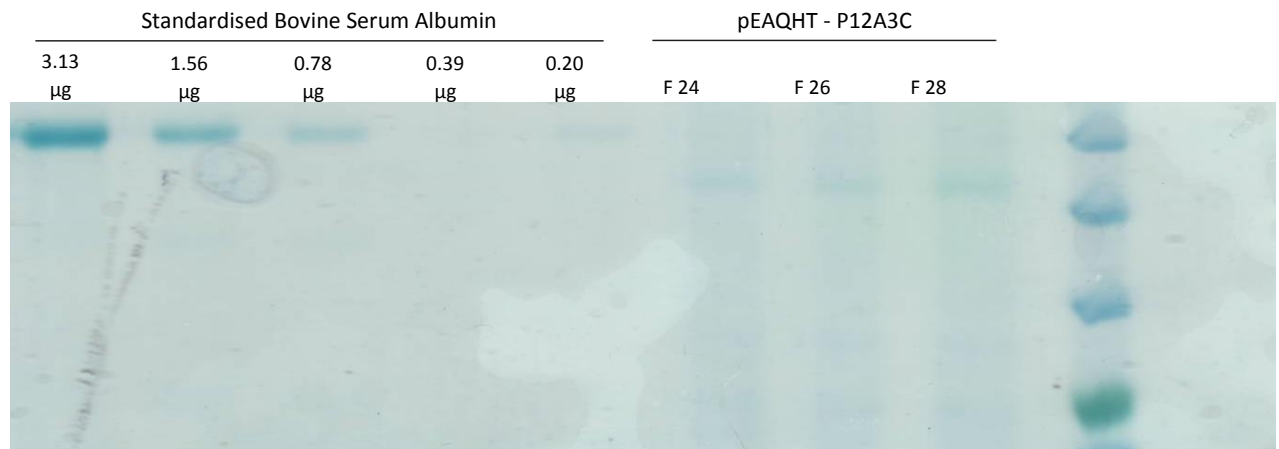


Figure 3.20. Coomassie stain comparing selected fractions of P12A3C expressed in *N. benthamiana*, using pEAQ- P12A3C (lanes 7-10), purified with a 15% - 40% sucrose gradient. Lane 1 = Bovine Standard Albumin 3.13 µg; lane 2 = Bovine Standard Albumin 1.56 µg; lane 3 = Bovine Standard Albumin 0.78 µg; lane 4 = Bovine Standard Albumin 0.39 µg; lane 5 = Bovine Standard Albumin 0.20 µg. lane 7 = pEAQ -P12A3C Fraction 24; lane 8 = pEAQ -P12A3C Fraction 25; lane 9 = pEAQ -P12A3C Fraction 27; lane 10 = pEAQ -P12A3C Fraction 28; Ladder used = NEB # P7712S boad range protein marker.

For pRIC3.0-P12A3C, bands of 25 kDa were visible in fractions 23, 25, and 27 but not in 28. No VP0 band of 37 kDa was visible in any fraction (figure 3.21).

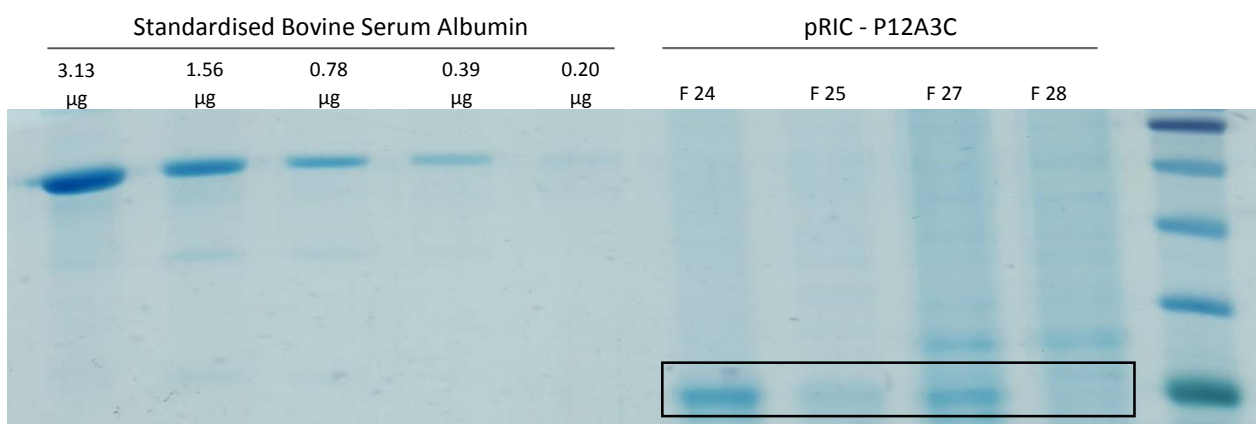


Figure 3.21. Coomassie stain comparing selected fractions of P12A3C expressed in *N. benthamiana*, using pRIC- P12A3C (lanes 7-10), purified with a 15% - 40% sucrose gradient. Lane 1 = Bovine Albumin Standard 3.13 µg; lane 2 = Bovine Albumin Standard 1.56 µg; lane 3 = Bovine Albumin Standard 0.78 µg; lane 4 = Bovine Albumin Standard 0.39 µg; lane 5 = Bovine Albumin Standard 0.20 µg. lane 7 = pRIC-P12A3C Fraction 24; lane 8 = pRIC -P12A3C Fraction 25; lane 9 = pRIC -P12A3C Fraction 27; lane 10 = pRIC -P12A3C Fraction 28; Ladder used = NEB # P7712S boad range protein marker.

Quantification of FMDV protein was performed using densitometric SynGene™ software. pEAQ-HT-P12A3C was not quantitated as the bands could not be visualised, nor was VP0 of pRIC3.0. The 25

kDa VP1/3 and 33 kDa VP0 bands visualised on Coomassie stained gels of pTRAc-P12A3C-expressed proteins, as well as the 25 kDa VP1/3 band visualised for pRIC3.0-P12A3C-expressed proteins were quantified. The respective bands selected for quantification are outlined with a black box (Figure 3.19 and 3.21). The resulting data generated are presented in appendix C with accompanying calculations.

Samples generated by the pTRAc-P12A3C vector, obtained from fractions 24, 25, 27 and 28 (Figure 3.19), produced yield estimates of 1.25 µg/ g fresh leaf mass for the 25 kDa VP1/VP3 band (relevant calculations displayed in appendix C). Yield estimates for the 37 kDa VP0 band from the same fractions amounted to only 0.155 µg / g (appendix C).

The estimated quantities for the band of VP1/3, generated by the pRIC3.0 vector (Figure 3.21), only amounted to 0.16 µg/ g of fresh leaf mass, (appendix C).

Table 4

Construct	VP1/VP3 (µg/g fresh weight)	VP0 (µg/g fresh weight)
pTRA	1.25	0.155
pEAQ	ND	ND
pRIC	0.16	ND

ND Not determined

These results suggest that the pTRAc-P12A3C vector was the best vector for generating higher yields of the desired FMDV capsid proteins.

3.4 Discussion and summary

The full *P12A* gene for the FMDV structural proteins and 3C protease was successfully cloned into the pTRAc plant expression vector. FMDV structural proteins were successfully expressed in plant leaf tissue with each of the different recombinant vector constructs pTRAc, pEAQ, and pRIC3.0.

Furthermore, electron microscopy provided images of virus-like particles (VLPs) resembling other TEM images of FMDV and VLPs presented in literature (McKenna et al. 1996; Kotecha et al. 2015), which confirmed that the expressed proteins were able to self-assemble into VLPs.

Quantification was done by densitometry of a standardized dilution series instead of quantification by ELISA on account of not having a quantified control sample with a known concentration of FMDV proteins. A limitation of quantification using a Bradford assay, it could not distinguish plant expressed FMDV proteins from the other endogenous plant proteins still present after purification through the sucrose gradient, and would thus present an over estimate reflecting the total yield of all proteins present. Quantification by densitometry allowed the specific band of the appropriate size for the FMDV capsid proteins (VP1 and VP3, in the region of 25 kDa, being the most distinct) to be quantified relative to the bands of standardised BSA of a known concentration, thus providing a more accurate and specific yield estimate. The one limitation of the method is that it is dependent on effective Coomassie staining.

Coomassie stain and densitometric comparison of protein expressed with each of the vectors used, suggested that the pTRAc-P12A3C vector is the most useful or effective vector for obtaining high yields of the recombinant P12A3C protein. No bands for the FMDV capsid proteins expressed with the pEAQ-HT vector were detectable with Coomassie staining for quantification despite positive detection with western blot. Antibodies used for protein detection by western blot are more sensitive and specific to the target protein and are thus capable of positive detection of the expressed protein even when the level of expression is insufficient to be evident with Coomassie stain. It should be further noted that the gel comparing the pEAQ-P12A3C derived samples (figure

20) was poorly stained; lanes 4 and 5 containing known amounts, 0.39 μg and 0.20 μg of the BSA control respectively, presented no visibly discernible bands and lane 3 containing 0.78 μg BSA was faint, compared with the staining of the gel comparing pTRAc-derived samples (figure 3.19) which presented clearly distinct bands in the lanes 4 and 5 of 0.39 μg and 0.20 μg BSA. Although the amount of FMDV protein expressed using pEAQ-HT-P21A3C and staining was insufficient for densitometric quantification, expression with the pTRAc-P12A3C vector produced a yield of 75.5 μg of the antigenic structural proteins VP1 and VP3 from 60 g of fresh leaf material, equal to 1.25 $\mu\text{g/g}$, while densitometric estimates for the band of a size appropriate of VP0 amounted to a yield of only 0.155 $\mu\text{g/g}$, (note though, that VP1 and VP3 have a combined yield; both proteins, being the same size, cannot be distinguished by Coomassie staining and quantified independently as VP0 is). Densitometric yield estimates for pRIC3.0-P12A3C amounted to only 0.16 $\mu\text{g/g}$. This amount is lower than might be expected considering pRIC vector was developed from pTRAc vector and modified for higher expression (Regnard et al. 2010). In theory pRIC, with the self-replicating vector construct producing gene replicons, should provide a higher level of expression and so deliver a greater yield. This yield estimate for pRIC3.0 also does not correlate well with the abundance of VLPs observed in TEM images, given that the expression was supposedly low one would expect to see relatively few VLPs. Despite pRIC having been developed from pTRAc for improved expression, a comparatively appreciable yield estimate was achieved with pTRAc. Since this quantification experiment was only performed once, on account of time constraints, repeated experiments to quantify the level of expression with these vectors would provide more definitive results and offer more credible yield estimates. It is possible that the poor yield could indicate a problem with the gel staining rather than poor expression.

Both transient and transgenic expression of recombinant vaccine candidates in plants, have been investigated by various groups, as reviewed by Scotti and Rybicki. They reported a wide range in yield results (Scotti & Rybicki 2013); from as little as 32 mg/kg fresh leaf material with rotavirus VP7 VP4, 0.18 g/kg with BPV1L1, 0.24 g/kg with HPV-8, 0.3 g/kg with HBcAG, 0.34 g/kg with NVCP-VLP,

0.363 g/kg with HIV Pr55^{gag}, to a high yield of 3 g/kg achieved with chloroplast targeted expression of HPV 16 L1, all transiently expressed in *N. benthamiana*, and 0.2 g/kg yield was obtained with transient expression of NVC-VLP in lettuce, while a variety of plant produced vaccine candidates by transgenic expression typically achieved significantly poorer yields as low as 4×10^{-6} g/kg for HPV-16 L1 in tobacco, to 12×10^{-3} and 20×10^{-3} g/kg for human codon optimised HPV-16L1 in transgenic tobacco and potato respectively, too low to be viable for industrial production. More recently a chimeric protein of the influenza M2e peptide transiently expressed in *N. benthamiana* produced high yields of approximately 1 g/kg fresh leaf tissue (Mardanova et al. 2015). The yields obtained with plant based expression systems, cited, offer promising prospects for the potential of this technology. However, the densitometric yield estimates of FMDV capsid proteins obtained with pTRAc-P12A3C expression in this study, are at the lower end of the range for protein yields from plant expression documented in literature. This suggests appropriate optimization of this methodology, may be capable of producing higher levels of the desired FMDV capsid proteins than what was achieved in this study.

Even so, the yield obtained in this study may be sufficient for future industrial application. Standard chemically inactivated virus vaccine, currently in use, requires 2.2 μ g of 146S particles of each respective FMDV serotype per dose in order to trigger effective protection in cattle (Daoud et al. 2013). A yield of 75.5 μ g of VP1/P3 obtained from 60 g fresh leaf mass with pTRAc exceed 2.2 μ g required for protective immunization in cattle, and is easily obtained from as few as twenty *N. benthamiana* plants – approximately four to five weeks old. The term “large batch” in the context of this project would be an insignificant scale in an industrial context. Twenty of the small potted plants, approximately 30 cm in height (pot included), only occupy about 2000 cm² of space (depending on spacing arrangement of the individual plants). Such small dimensions provide immense scope for upscaling to achieve protein yield necessary for commercial production. The 2.2 μ g/dose of viral antigen required for protection, according to Daoud *et al.* (2013), measures the mass of the full 146S particle; a complete FMDV virus particle inclusive of the 8.5 kb ssRNA. By

comparison, the yields measured in these experiments estimated the combined mass of VP1 and VP3. Theoretically the yield obtained for the entire empty viral capsids would thus be possibly higher still since VP0 (VP2 and VP4) did not contribute to these quantification estimates as it is not contained in the same band of the gel densitometrically assessed by the SynGene software. This yield should also theoretically equate to a greater copy number of VLPs per unit mass than the copy number of 146S virus particles per unit mass present in the inactivated vaccine. For any given mass of the antigenic FMDV, based on the simple premise:

$$\text{viral copy number} = \frac{\text{measured total mass of all viral components}}{\text{mass of a single virus particle}}$$

The mass of a single virus particle in the case of a 75S VLP is significantly less - it lacks the RNA that contributes to the mass of a full 146S particle (K. Strohaimer 1982), hence the denominator of the equation would be significantly reduced in the case of VLPs than it would be in the case of 146S infective virus particles, and would thus represent a yield with a far greater copy number of actual particles. The greater copy number should directly correlate to better exposure of the antigenic proteins necessary to induce an immunogenic response in vaccinated animals. The copy number theoretically is thus more relevant to the efficacy of a vaccine than the mass of the antigenic component. With this considered, these yield results provide particularly positive prospects for the potential of plant expression platforms, particularly in the context of recombinant FMDV VLPs as an alternative cost effective vaccine candidate.

While this study used *N. benthamiana* for the production of FMDV structural proteins, other studies have produced FMDV derived proteins in different plants including alfalfa, (Dus Santos et al. 2005) and *Arabidopsis* (Carrillo et al. 1998). Exogenous FMDV polypeptide proteins have also been previously expressed in *N. benthamiana* (Andrianova et al. 2011). In this project FMDV capsid proteins were expressed and the self-assembling capacity of the FMDV structural polypeptide to form VLPs was also demonstrated. More specifically this study demonstrates that *N. benthamiana* presents a robust system for the expression of recombinant exogenous FMDV structural proteins

that retain the capacity to form VLPs, with appreciable yields. These works contribute to an accumulating body of research that demonstrates the scope and versatility of a plant based expression platform. In turn this provides further evidence supporting the potential of this technology to offer a viable alternative means to produce candidate vaccines against FMD.

Chapter 4

Conclusion

Foot and mouth disease continues to be the most severe threat to the agricultural livestock industry worldwide. Outbreaks of this disease are among the most costly for government and farmers.

Farmers invariably lose entire herds of livestock, while travel bans around quarantine areas, and trade restrictions, have a drastic impact on the economies of affected countries. The burden of this disease varies among countries as many regions have been free of the disease for many years. In South Africa, however, foot and mouth disease virus is endemic to the region and exists naturally in the buffalo population, an asymptomatic host of the virus, which thus acts as a natural reservoir of the virus (Thomson 1995). Constant monitoring and control is consequently an absolute necessity in the South African context in order to mitigate the spread, and burden of the disease. A vaccine is recognised as the most effective long-term solution to prevent the spread of the disease into herds of livestock.

The work in this study has demonstrated that *N. benthamiana* can be used as a plant expression platform for the development of virus-like particles (VLPs) that could serve as an effective alternative candidate vaccine to the traditional chemically inactivated FMDV virus vaccine currently in use, which carries both a high biosafety risk and high production cost. Specifically in this project, the FMDV VP1, 3, and 0 structural capsid proteins derived from the P12A gene of serotype A were expressed in combination with the 3C protease in *N. benthamiana* via an agrobacterium - mediated transient expression system.

Antibodies for these structural proteins are not readily available locally. To address this problem the P12A oligopeptide was expressed in an *E. coli* expression system for the rapid production of the protein. The 3C protease was excluded from the gene expressed in *E. coli* as the 3C protease is not conducive to *E. coli* growth. *E. coli* expressed P12A product was used to raise antibodies against the

protein in rabbits. These antibodies could then be used for the detection of the FMDV structural proteins expressed in plants by analysis with western blot.

Expression of the viral proteins in the plants could be observed three days after infiltration of the plant leaves. Furthermore, expression of the viral proteins was observed with the use of each of the three vectors used for the gene expression: pTRAc, pRIC3.0, pEAQ-HT. Densitometry estimates of 75.5 µg VP1 and VP3 protein, expressed using pTRAc-P12A3C vector, was obtained from 60 g leaf material. Virus protein yield of 1.25 mg/kg fresh leaf weight, with pTRAc-P12A3C, was higher than yields obtained with the use of the pRIC3.0-P12A3C and pEAQ-HT-P12A3C vectors. Only 2.2 µg/dose of the 146S infective FMDV virus is necessary to induce protection in cattle. Thus a protein yield of 1.25 mg/kg may be sufficient to justify testing the viability of this plant expression methodology for the industrial production of FMDV VLPs as a candidate vaccine. The auto assembly of the viral proteins into virus-like particles was also observed with each of the three vectors, as confirmed with transmission electron microscopy imaging.

Although beyond the scope of this particular project, what remains to be done in order for this research to ultimately contribute towards the establishment of a viable vaccine is to conduct animal trials to investigate the efficacy of the plant produced VLPs and the protection elicited in animals tests.

Animals vaccinated with this VLP vaccine would be distinguishable from infected animals by standard ELISA testing for FMDV non-structural proteins absent from the VLPs. This would be significant for the monitoring of livestock surrounding the Kruger National Park and other foot-and-mouth disease zones, as it is currently not possible to distinguish between the vaccinated and infected animals, since in both instances both the structural and non-structural proteins of complete 146S FMDV present. This is one of the most critically beneficial aspects of a VLP vaccine. This could also potentially have international trade legislation reconsidered and the classification of FMDV-free zones amended.

VLPs present structural mimics of the original parent virus to the immune system, incorporating all of the structural proteins. The use of VLPs as vaccines thus offer potentially better protection than using sub-unit vaccines, as the immune system is exposed to all of the structural proteins rather than a single protein or select protein motifs and epitopes. While being structural mimics of the parent virus, they do not contain any of the genomic material nor any of the non-structural proteins and hence are non-virulent, making them safer and far more appealing candidates for vaccine use than inactivated live virus particles. The ability to produce VLPs efficiently presents exciting prospects for the future of vaccine technology.

The advantages and disadvantages of the various expression systems currently available have been described and the preference towards such a plant based expression system has been highlighted. Of particular relevance to the candidate vaccine's potential as a commercial product, is the economic viability presented by the plant expression system, as is the scope for ease of upscaling necessary for industrialization of the production process, with minimal demands on upgrading infrastructure. This advantage is particularly important in sub-Saharan Africa where many countries are underdeveloped - the facilities and infrastructure necessary for large scale protein production via various alternative cell culture expression platforms, do not exist and would require huge capital expenditure. Growing plants, by comparison, can be achieved across a wider range of environments and does not require any significant infrastructure. This is possibly the most compelling advantage of this expression platform in the African context as it makes the technology far more accessible to under developed nations and more rural regions.

The prospects of this technology continue to improve with further research in the field as optimisation and discoveries reduce cost, improve efficiency, increase yield, and widen the scope of application; presenting an exciting and promising future.

The potential of this plant expression system has been effectively demonstrated by the successful production of recombinant FMDV structural protein using *N. benthamiana* in this study. The

subsequent assembly of VLPs derived from the plant expression platform was also demonstrated. These VLPs could be used as a safer candidate vaccine against FMDV in the future.

The adopted approach and technology used to develop this potential vaccine is applicable globally and would be particularly beneficial to South Africa and other developing nations. Foot and mouth disease for which the vaccine was developed, is also prevalent across the globe but is particularly relevant to the South African context.

In essence this work has demonstrated the feasibility of producing a vaccine candidate that would be more affordable, especially for farmers of developing countries here in Africa. The implementation of its production would be both more feasible and more economical than vaccine production currently is for local companies or government. This technology and its product, the potential candidate vaccine, has the potential to significantly alleviate the impact caused by the devastating disease, especially in South Africa and those countries constantly affected by FMD. The vaccine could alleviate both economic cost incurred as a result of FMD, and also the conservational hindrance of free movement of people and all animal species, through FMD infectious areas. Both prospects would be considerable socioeconomic achievements resulting from this research.

References

- Andrés, I. et al., 2006. Yeast expression of the VP8* fragment of the rotavirus spike protein and its use as immunogen in mice. *Biotechnology and Bioengineering*, 93(1), pp.89–98.
- Andrianova, E.P. et al., 2011. Foot and mouth disease virus polyepitope protein produced in bacteria and plants induces protective immunity in guinea pigs. *Biochemistry. Biokhimiia*, 76(3), pp.339–46.
- Arzt, J., Pacheco, J.M. & Rodriguez, L.L., 2010. The early pathogenesis of foot-and-mouth disease in cattle after aerosol inoculation. Identification of the nasopharynx as the primary site of infection. *Vet Pathol*, 47(6), pp.1048–1063.
- Balamurugan, V., Reddy, G.R. & Suryanarayana, V.V.S., 2007. Pichia pastoris: A notable heterologous expression system for the production of foreign proteins - Vaccines. *Indian Journal of Biotechnology*, 6(2), pp.175–186.
- BBC, 2007a. Foot-and-mouth strain identified. *BBC News*. Available at: http://news.bbc.co.uk/2/hi/uk_news/6931639.stm [Accessed February 13, 2017].
- BBC, 2007b. 'Pirbright link' to farm outbreak. *BBC News*. Available at: http://news.bbc.co.uk/2/hi/uk_news/6992466.stm [Accessed February 13, 2017].
- Blanco, E., Andreu, D. & Sobrino, F., 2017. Peptide Vaccines Against Foot-and-mouth Disease. In F. Sobrino & E. Domingo, eds. *Foot and Mouth Disease Virus : Current Research and Emerging Trends*. Norfolk, UK : Caister Academic Press. 2017, pp. 317–332.
- Botswana Vaccine Institute, 2013. BVI Annual Report 2013. , p.15.
- Bravo De Rueda, C. et al., 2014. Estimation of the transmission of foot-and-mouth disease virus from infected sheep to cattle. *Veterinary Research*, 45(1).

C. C. Brown, *H. J. Olander and R. E Meyer, 1995. Pathogenesis of Foot-and-Mouth Disease in Swine. , pp.51–58.

Canadian Food Inspection Agency, Foot-and-Mouth Disease Fact Sheet. *CFIA public website*.

Available at: <http://www.inspection.gc.ca/animals/terrestrial-animals/diseases/reportable/foot-and-mouth-disease/fact-sheet/eng/1330481689083/1330481803452> [Accessed February 13, 2017].

Cao, Y. et al., 2009. Synthesis of empty capsid-like particles of Asia I foot-and-mouth disease virus in insect cells and their immunogenicity in guinea pigs. *Veterinary Microbiology*, 137(1–2), pp.10–17.

Carrillo, C. et al., 2005. Comparative genomics of Foot-and-Mouth Disease Virus. *The Journal of Virology*, 79(10), pp.6487–6504.

Carrillo, C. et al., 1998. Protective immune response to foot-and-mouth disease virus with VP1 expressed in transgenic plants. *J Virol*, 72(2), pp.1688–1690.

Chen, Q. et al., 2012. Plant-derived virus-like particles as vaccines Plant-derived virus-like particles as vaccines. , 5515(December).

De Clercq, K. et al., 2008. FMD vaccines: reflections on quality aspects for applicability in European disease control policy. *Transboundary and emerging diseases*, 55(1), pp.46–56.

Daoud, H.M. et al., 2013. Preparation of Foot and Mouth Disease trivalent vaccine type A , O , SAT2 with determination of the Guinea pig protective dose 50 (GPPD 50). , 6(iii), pp.844–851.

DEFRA, 2007. Results of Foot and Mouth Disease Strain in Surrey, extension of zones. *Current news release, DEFRA official website*. Available at: <https://web.archive.org/web/20070927000734/http://www.defra.gov.uk/news/2007/070804a.htm> [Accessed February 17, 2017].

- Doel, T.R., 2003. FMD vaccines. *Virus Research*, 91(1), pp.81–99.
- Domingo, E. et al., 2003. Evolution of foot-and-mouth disease virus. *Virus Research*, 91(1), pp.47–63.
- Duke, Y.N. & Carolina, R.N., 1963. The Solubility of Amino in Aqueous. , 238(12).
- Dus Santos, M.J. et al., 2005. Development of transgenic alfalfa plants containing the foot and mouth disease virus structural polyprotein gene P1 and its utilization as an experimental immunogen. *Vaccine*, 23(15 SPEC. ISS.), pp.1838–1843.
- Ebert, D., 1998. Experimental Evolution of Parasites. , 282(November), pp.1432–1436.
- Escribano, M. & Borca, M. V, 1999. Induction of a Protective Antibody Response to Foot and Mouth Disease Virus in Mice Following Oral or Parenteral Immunization with Alfalfa Transgenic Plants Expressing the Viral Structural Protein VP1 1. , 353, pp.347–353.
- Grubman, M. & Baxt, B., 2004. Foot-and-mouth disease. *Clinical microbiology reviews*, 17(2), pp.465–493.
- Jamal, S.M. & Belsham, G.J., 2013. Foot-and-mouth disease: Past, present and future. *Veterinary Research*, 44(1).
- Jane Flint, S.& A.S. for M., 2009. *Principles of virology* 3rd Editio., Washington, DC : ASM Press.
- Jemberu, W.T. et al., 2014. Economic impact of foot and mouth disease outbreaks on smallholder farmers in Ethiopia. *Preventive Veterinary Medicine*, 116(1–2), pp.26–36.
- Joemat-Pettersson, M.T., 2014. speaking notes on South Africa’s good story: South Africa’s three year red meat export ban liftedNo Title. *Department of Agriculture, Forestry and Fisheries*. Available at: <http://www.gov.za/minister-tina-joemat-pettersson-speaking-notes-south-africas-good-story-south-africas-three-year-red> [Accessed March 2, 2017].
- K. Strohaimer, R.F.A.K.-H.A., 1982. Location and Characterization of the Antigenic Portion of the F M D V Immunizing Protein. , (59), pp.295–306.

- Kotecha, A. et al., 2015. Structure-based energetics of protein interfaces guides foot-and-mouth disease virus vaccine design. *Nature Structural & Molecular Biology*, 22(September), pp.788–794.
- Kumar, M. & Jalali, P.S.S.K., 2016. Expression and purification of virus-like particles (VLPs) of foot-and-mouth disease virus in Eri silkworm (*Samia cynthia ricini*) larvae. *Virus Disease*, 27(1), pp.84–90.
- Kushnir, N., Streatfield, S.J. & Yusibov, V., 2012. Virus-like particles as a highly efficient vaccine platform: Diversity of targets and production systems and advances in clinical development. *Vaccine*, 31(1), pp.58–83.
- Li, H. et al., 2016. Novel chimeric foot-and-mouth disease virus-like particles harboring serotype O VP1 protect guinea pigs against challenge. *Veterinary Microbiology*, 183, pp.92–96.
- Li, Z. et al., 2012. Development of a foot-and-mouth disease virus serotype A empty Capsid subunit vaccine using Silkworm (*Bombyx mori*) Pupae. *PLoS ONE*, 7(8), pp.1–7.
- Lico, C., Chen, Q. & Santi, L., 2008. Viral vectors for production of recombinant proteins in plants. *Journal of Cellular Physiology*, 216(2), pp.366–377.
- Liu, X. et al., 2017. Chimeric virus-like particles elicit protective immunity against serotype O foot-and-mouth disease virus in guinea pigs. *Applied Microbiology and Biotechnology*, 101, pp.4905–4914.
- Logan, D. et al., 1993. Structure of a major immunogenic site on foot-and-mouth disease virus. *Nature*, 362(6420), pp.566–568.
- Maclean, J. et al., 2007. Optimization of human papillomavirus type 16 (HPV-16) L1 expression in plants : comparison of the suitability of different HPV-16 L1 gene variants and different cell-compartment localization. *Journal of General Virology*, 16(88), pp.1460–1469.

- Mardanov, E.S. et al., 2015. Rapid high-yield expression of a candidate influenza vaccine based on the ectodomain of M2 protein linked to flagellin in plants using viral vectors. *BMC Biotechnology*, 15:42, pp.1–10.
- Martinez-Salas, E. & Belsham, G.J., 2017. Genome Organization, Translation and Replication of Foot-and-mouth Disease Virus RNA. In F. Sobrino & E. Domingo, eds. *Foot and Mouth Disease Virus : Current Research and Emerging Trends*. Norfolk, UK : Caister Academic Press. 2017, pp. 13–42.
- McKenna, T.S.C. et al., 1996. Strategy for producing new foot-and-mouth disease vaccines that display complex epitopes. *Journal of Biotechnology*, 44(1–3), pp.83–89.
- Mena, J.A., Ramírez, O.T. & Palomares, L.A., 2006. Intracellular distribution of rotavirus structural proteins and virus-like particles expressed in the insect cell-baculovirus system. *Journal of Biotechnology*, 122(4), pp.443–452.
- Merial, 2013. Aftovax inactivated vaccine against foot and mouth disease in ruminants. , p.69007.
- Mignaqui, A.C. et al., 2013. Transient Gene Expression in Serum-Free Suspension-Growing Mammalian Cells for the Production of Foot-and-Mouth Disease Virus Empty Capsids. *PLoS ONE*, 8(8), pp.1–9.
- Mohana Subramanian, B. et al., 2012. Development of foot-and-mouth disease virus (FMDV) serotype O virus-like-particles (VLPs) vaccine and evaluation of its potency. *Antiviral Research*, 96(3), pp.288–295.
- Nandi, S. et al., 2016. Techno-economic analysis of a transient plant-based platform for monoclonal antibody production. *mAbs*, 8(8), pp.1456–1466.
- Pan, L. et al., 2008. Foliar extracts from transgenic tomato plants expressing the structural polyprotein , P1-2A , and protease , 3C , from foot-and-mouth disease virus elicit a protective response in guinea pigs. *Veterinary Immunology and Immunopathology*, 121, pp.83–90.

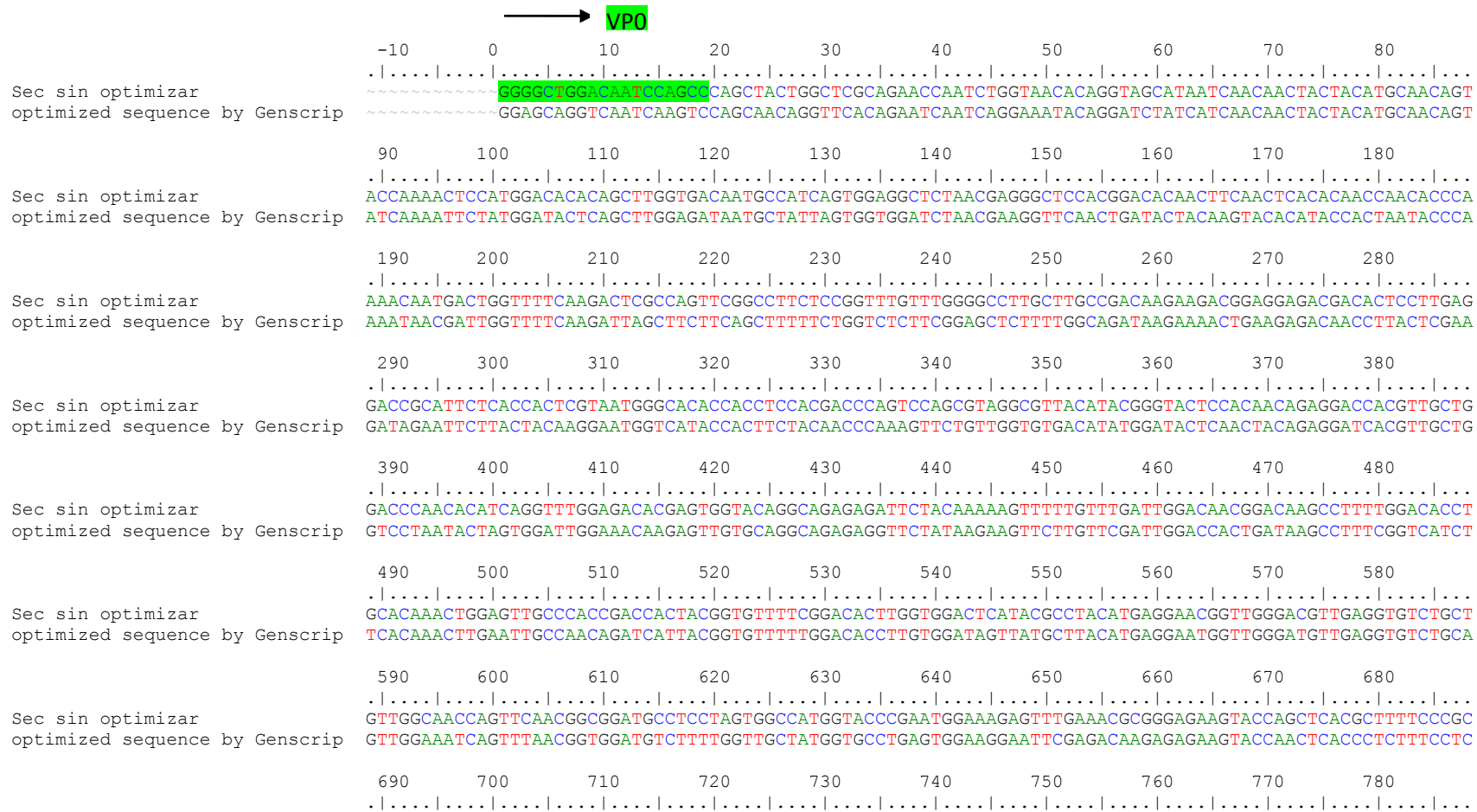
- Parthiban, A.B.R. et al., 2015. Virus excretion from foot-and-mouth disease virus carrier cattle and their potential role in causing new outbreaks. *PLoS ONE*, 10(6), pp.1–14.
- Punt, P.J. et al., 2002. Filamentous fungi as cell factories for heterologous protein production. *Trends in Biotechnology*, 20(5), pp.200–206.
- Regnard, G.L. et al., 2010. High level protein expression in plants through the use of a novel autonomously replicating geminivirus shuttle vector. *Plant Biotechnology Journal*, 8(1), pp.38–46.
- Robinson, L. et al., 2016a. Global Foot-and-Mouth Disease Research Update and Gap Analysis : 1 - Overview of Global Status and Research Needs. , 63, pp.3–13.
- Robinson, L. et al., 2016b. Global Foot-and-Mouth Disease Research Update and Gap Analysis : 3 - Vaccines. , 63, pp.30–41.
- Robinson, L. et al., 2016c. Global Foot-and-Mouth Disease Research Update and Gap Analysis : 6 – Immunology. , 63, pp.56–62.
- Robinson, L. et al., 2016d. Global Foot-and-Mouth Disease Research Update and Gap Analysis : 7 – Pathogenesis and Molecular Biology. , 63, pp.63–71.
- Rodríguez-Limas, W. a et al., 2011. Molecular and process design for rotavirus-like particle production in *Saccharomyces cerevisiae*. *Microbial cell factories*, 10(1), p.33.
- Rybicki, E.P., 2010. Plant-made vaccines for humans and animals. *Plant Biotechnology Journal*, 8(5), pp.620–637.
- Rybicki, E.P., 2009. Plant-produced vaccines: promise and reality. *Drug Discovery Today*, 14(1–2), pp.16–24.
- Sainsbury, F. & Lomonosoff, G.P., 2008. Extremely high-level and rapid transient protein production in plants without the use of viral replication. *Plant physiology*, 148(3), pp.1212–1218.

- Sainsbury, F., Thuenemann, E.C. & Lomonossoff, G.P., 2009. pEAQ : versatile expression vectors for easy and quick transient expression of heterologous proteins in plants. , pp.682–693.
- Scotti, N. & Rybicki, E.P., 2013. Virus-like particles produced in plants as potential vaccines. *Expert review of vaccines*, 12(2), pp.211–24.
- Segarra, A.E. & Rawson, J.M., 2001. CRS Report for Congress. , pp.1–6.
- Singh, A. et al., 2015. Protein recovery from inclusion bodies of Escherichia coli using mild solubilization process. , pp.1–10.
- Smitsaart, E.N. & Bergmann, I.E., 2017. Quality Attributes of Current Inactivated Foot-and-mouth Disease Vaccines and their Effects on the Success of Vaccination Programmes. In F. Sobrino & E. Domingo, eds. *Foot and Mouth Disease Virus : Current Research and Emerging Trends*. Norfolk, UK : Caister Academic Press. 2017, pp. 287–316.
- Somers, M.J. & Hayward, M.W., 2012. *Fencing for conservation: Restriction of evolutionary potential or a riposte to threatening processes?*,
- Stenfeldt, C. et al., 2014. Morphologic and phenotypic characteristics of myocarditis in two pigs infected by foot-and mouth disease virus strains of serotypes O or A. *Acta Vet Scand*, 56(1), p.42.
- Terpe, K., 2006. Overview of bacterial expression systems for heterologous protein production: From molecular and biochemical fundamentals to commercial systems. *Applied Microbiology and Biotechnology*, 72(2), pp.211–222.
- Thomson, G.R., 1995. Overview of foot and mouth disease in southern Africa *. *Revue scientifique et technique (International Office of Epizootics)*, 14(3), pp.503–520.
- Veerapen, V.P. et al., 2018. Novel expression of immunogenic foot-and-mouth disease virus-like particles in Nicotiana benthamiana. *Virus Research*, 244(November 2017), pp.213–217.

- Wei, H., Fan, Y. & Gao, Y.Q., 2010. Effects of Urea , Tetramethyl Urea , and Trimethylamine N -Oxide on Aqueous Solution Structure and Solvation of Protein Backbones : A Molecular Dynamics Simulation Study. , pp.557–568.
- Wernery, U. & Kaaden, O.R., 2004. Foot-and-mouth disease in camelids: A review. *Veterinary Journal*, 168(2), pp.134–142.
- Wigdorovitz, A. & Pe, D.M., 1999. Protection of Mice against Challenge with Foot and Mouth Disease Virus (FMDV) by Immunization with Foliar Extracts from Plants Infected with Recombinant Tobacco Mosaic Virus Expressing the FMDV Structural Protein VP1. *Virology*, 91, pp.85–91.
- Xiao, Y. et al., 2016. Large-scale production of foot-and-mouth disease virus (serotype Asia1) VLP vaccine in Escherichia coli and protection potency evaluation in cattle. *BMC Biotechnology*, pp.1–9.
- Zou, Q., Habermann-rottinghaus, S.M. & Murphy, K.P., 1998. Urea Effects on Protein Stability : Hydrogen Bonding and the Hydrophobic Effect. , 115(September 1997), pp.107–115.

Appendices

Appendix A: P12A3C Nicotiana optimised DNA sequence by GenScript



Appendix B: Composition of Buffers and Solutions

GROWTH MEDIA: (1 L)

LB-Lennox:

10 g tryptone
5 g yeast extract
5 g NaCl
15 g of agar added*
Volume brought to ≤900 mL with distilled water
pH adjusted to 7
Volume brought to 1 L with distilled water
Autoclaved
*Used only when making LB-agar plates

Infiltration Medium: (1 L)

1.952 g MES
2.03 g MgCl₂ (4.34g hydrated)
30 g Sucrose
Make up to 800mL with distilled water
pH adjusted to 5.6 with HCl
Add distilled water to 1 L
1 mL 0.2 M acetosyringone (final conc 200 μM) added just before use

BUFFERS FOR SDS-PAGE and coomassie stain:

1.5 M Tris, pH 8.8; Resolving Buffer for separating gels (200 mL for 4 gels)

36.3 g Tris base dissolved in 180 mL of distilled water
pH adjust to 8.8 with concentrated HCl
volume raised to 200mL with distilled water

1.5 M Tris, pH 6.8; Stacking Buffer for stacking gels (50 mL for 4 gels)

3g Tris base dissolved in around 40 mL of distilled water
pH adjusted to 6.8 with concentrated HCl
volume raised to 50mL with distilled water

10x Electrophoresis running buffer (1L)

30.3g Tris base
144.2g glycine
10g SDS
Dissolved with heat and pH adjusted to 8.5 with HCl

Volume raised to 1L with distilled water

1% Coomassie Blue stock solution: (100 mL)

Dissolve 1 g Coomassie Brilliant Blue G-250 in 100mL dH₂O

Coomassie Blue Stain: (500 mL)

62.5 mL 1% Coomassie Blue Stock solution

250 mL Methanol

80 mL Glacial Acetic Acid

127 mL distilled water

Stain/destain solution: (1L)

450 mL Methanol

450 mL distilled water

100 mL Glacial Acetic acid

5x sample loading buffer: (5mL)

470 µL 1M TrisCl pH7.5

940 µL 10% SDS

19 µL 0.5M EDTA

2.45 mL glycerol

545 µL ddistilled water

205 µL Mercaptoethanol

0.02 g of bromophenol blue

BUFFERS FOR WESTERN BLOTTING:

10x Phosphate Buffered Saline (PBS): (1L)

17.8 g Na₂HPO₄·2H₂O

2.4 g KH₂PO₄,

80 g NaCl ,

2 g KCl,

Dissolved in 800 mL distilled water

pH adjusted to 7.4 with 10 M NaOH

distilled water added to 1 L

Autoclaved

1x Transfer buffer: (1 L)

5.82 g Tris base
2.93 g Glycine
200 mL methanol
cold distilled water to 1 L
pH 9.2

10% Tween-20: (100 mL)

10 mL Tween-20 added to 90 mL distilled water
Filter sterilized
Stored in the dark

Blocking Buffer: (100 mL)

5 g Milk Powder dissolved in around 70 mL distilled water
10 mL 10x PBS and 1 mL 10% Tween 20 added
distilled water added to 100 mL

GENERAL USE BUFFERS:**1% Bovine Serum Albumin:** (10 mL)

100 mg BSA (Pentax Fraction v) dissolved in 10mL ddH₂O, Filter sterilized, stored at – 20

6x DNA loading buffer: (10 mL)

4 g sucrose and 24.04 g bromophenol blue dissolved in 8mL distilled water
400 µL 0.5 M EDTA added
Volume brought to 10 mL with distilled water, Filter sterilized

1% Agarose: (100mL),

1 g Agarose added to 100 mL 1 X TBE buffer
2.5 µL 10 mg/mL EtBr added per 50 mL agarose after melting

Buffer QBT (equilibration buffer):

750 mM NaCl

50 mM MOPS pH 7.0

15 % Isopropanol (v/v)

0.15% Triton X-100 (v/v)

Buffer QC:

1.0 M NaCl

50 mM MOPS pH 7.0

15 % (v/v) isopropanol

Buffer QF:

1.25 M NaCl

50m M Tris.Cl pH 8.5

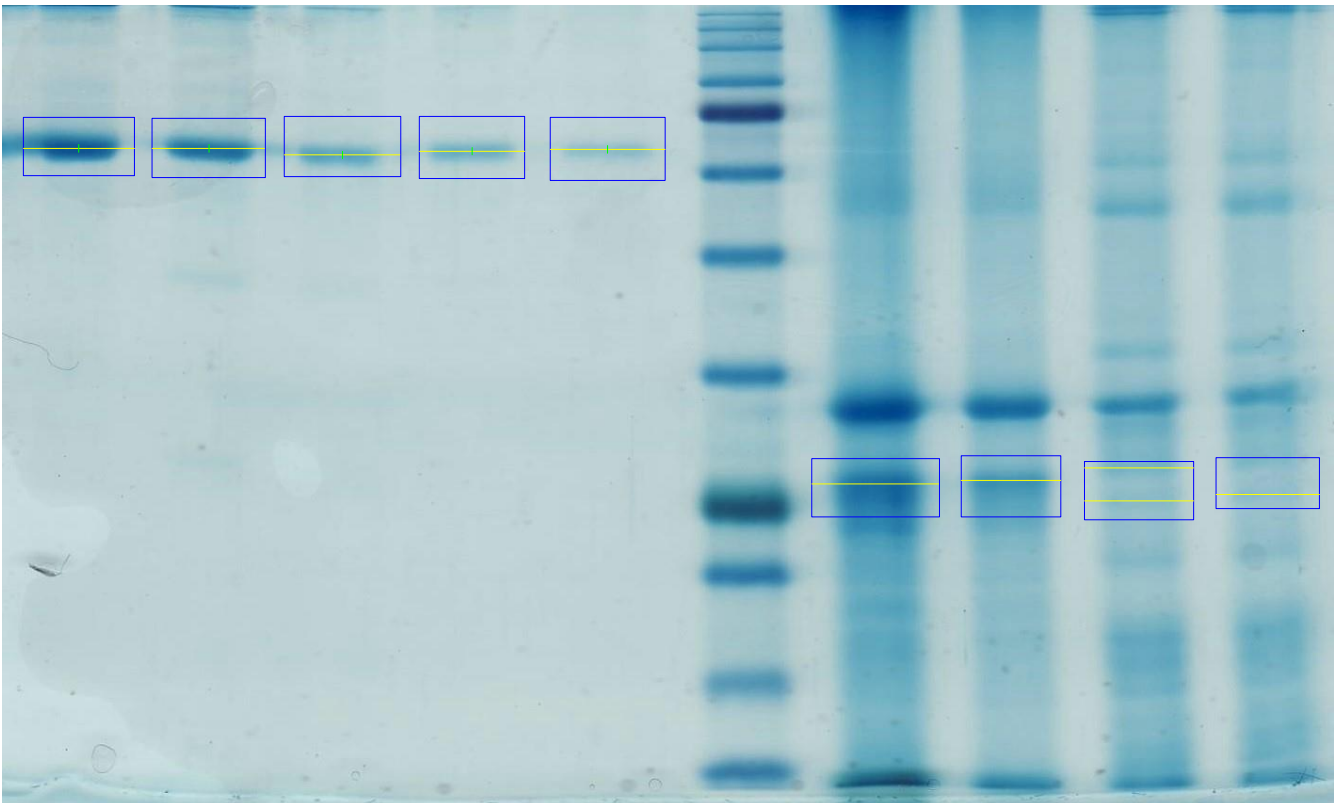
15% (v/v) isopropanol

Appendix C: FMDV capsid protein quantification

SynGene™ software yield calculations for protein produced via pTRAC-P12A3C.

Bovine Serum Albumin quantity calibration details

gels loaded with 30 μ L sample + 6 μ L SAB



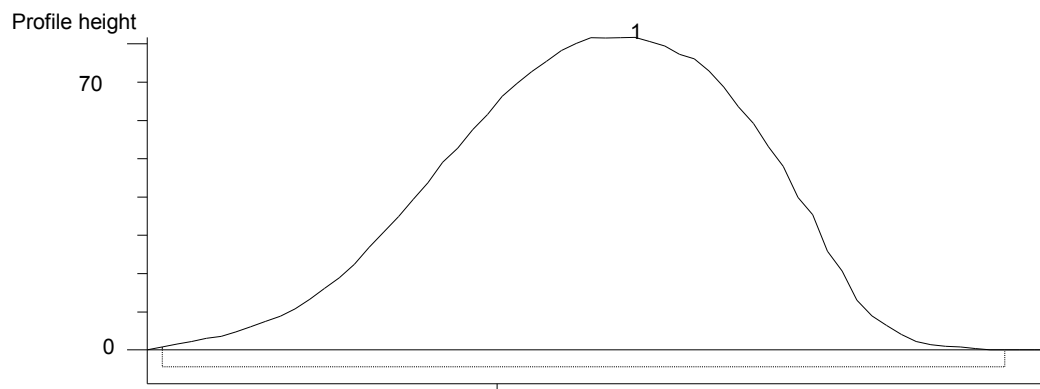
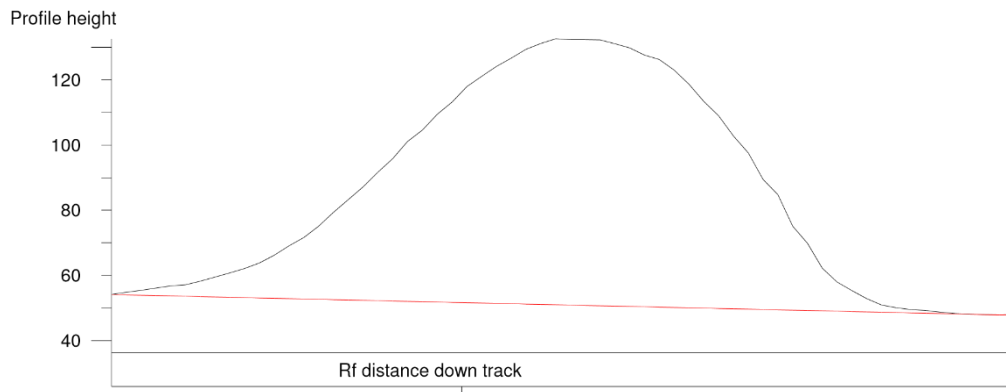


Figure A1: Track 1; BSA = 3.13 μg , Profile height = 81.681

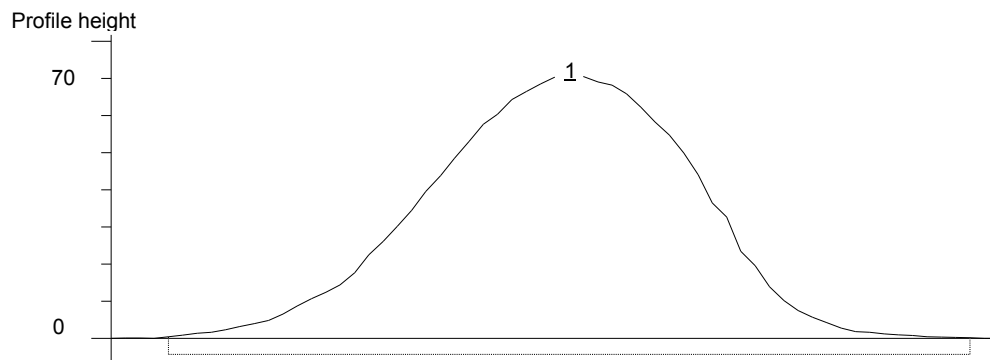
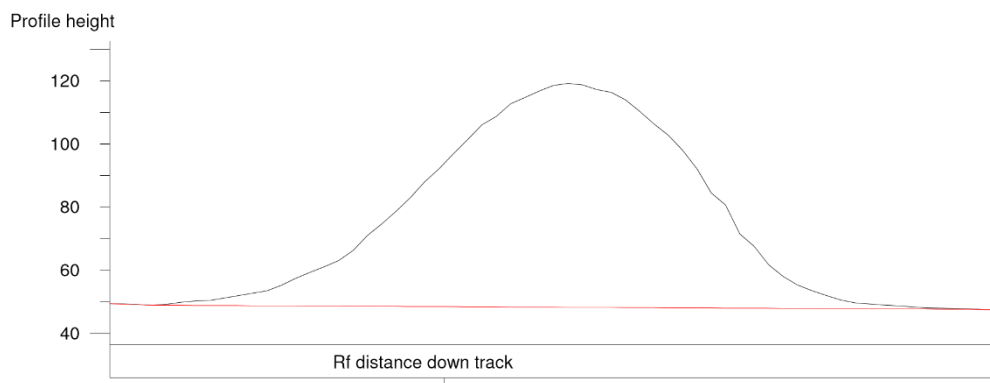


Figure A2: Track 2; BSA = 1.56 μg , Profile height = 70.982

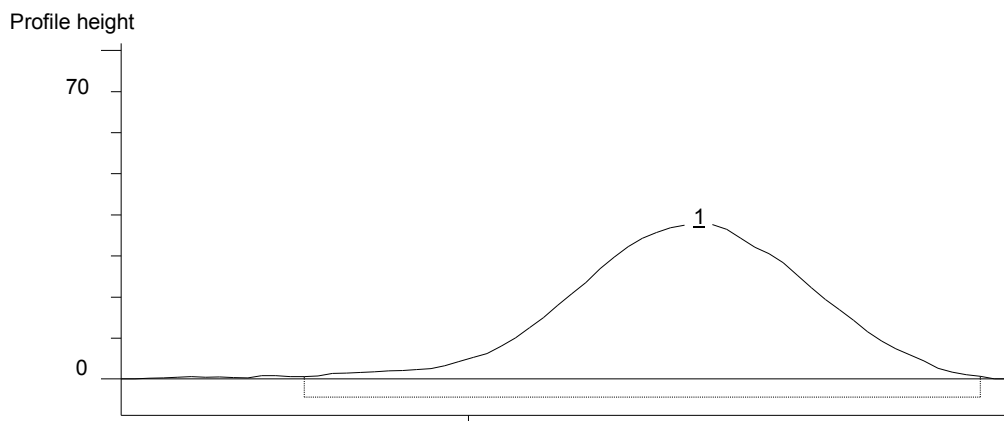
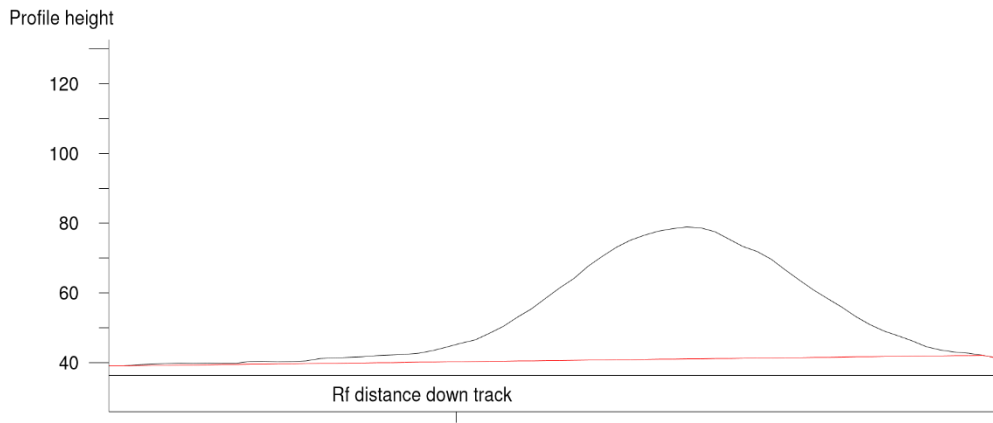


Figure A3: Track 3; BSA = 0.78 μg , Profile height = 37.875

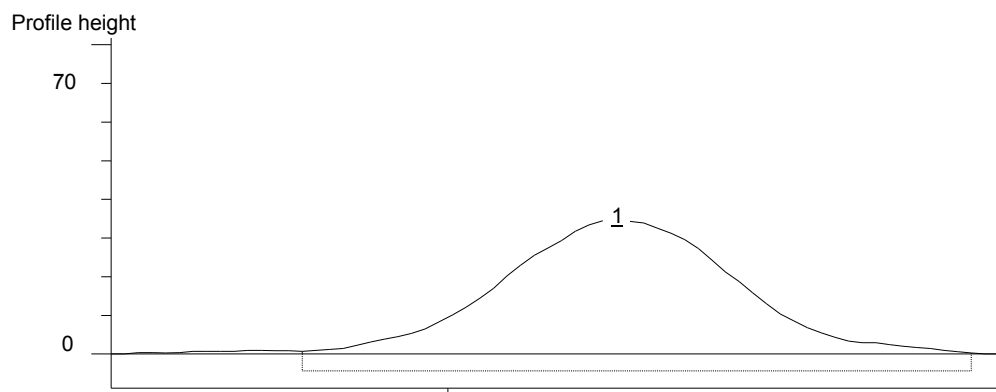
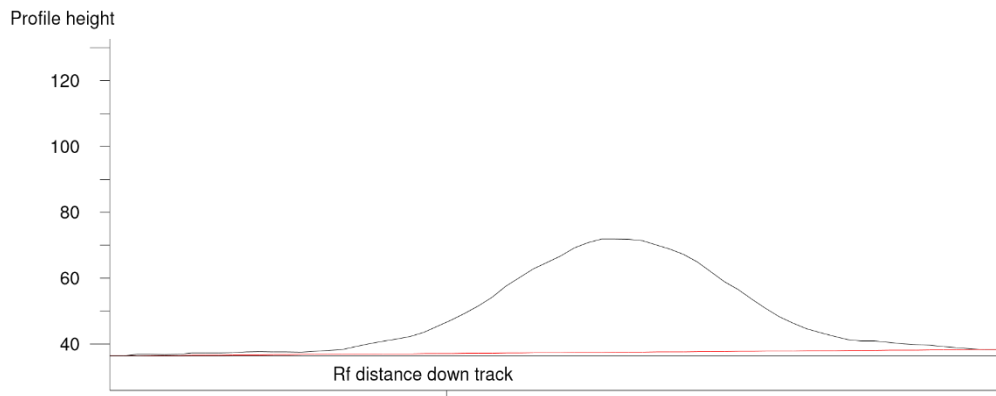


Figure A4: Track 4; BSA = 0.39 μg , Profile height = 34.448

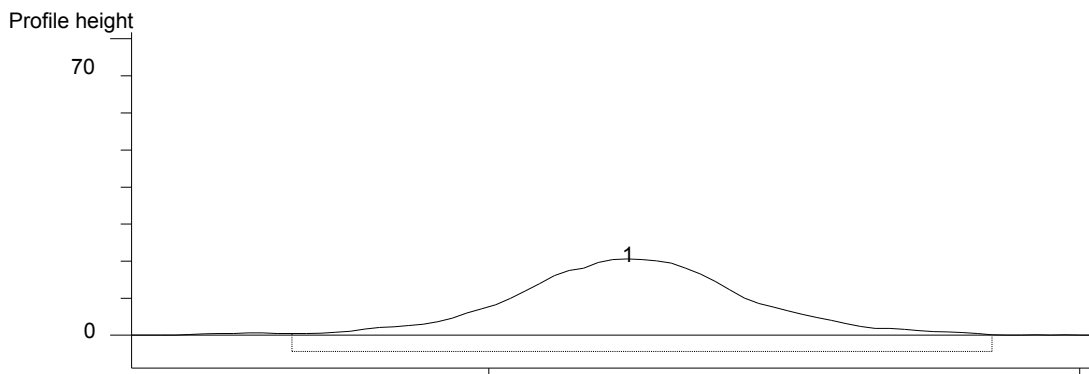
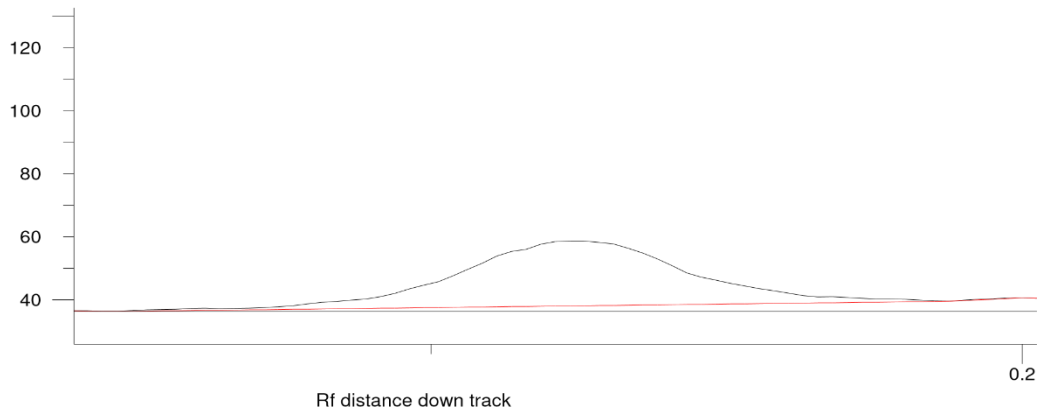
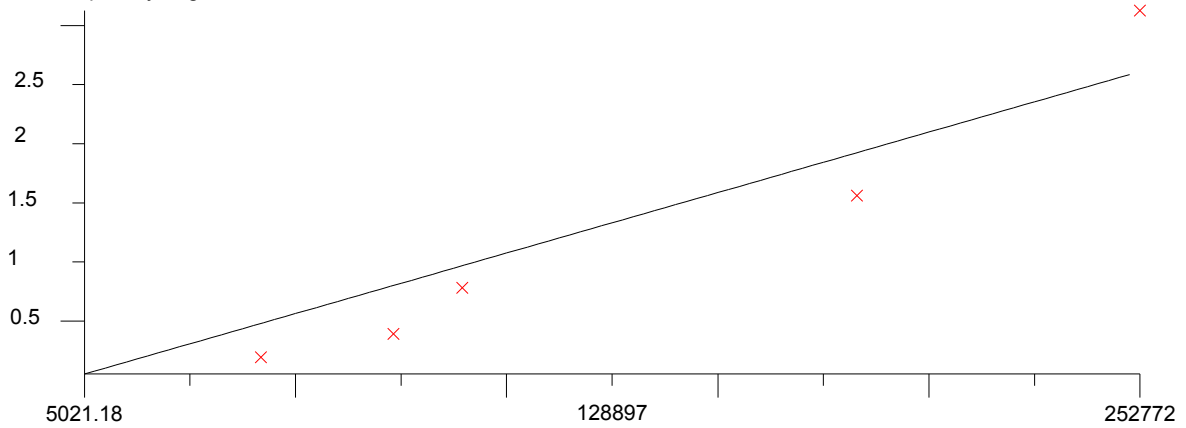


Figure A5: Track 5; BSA = 0.20 µg, Profile height = 20.758

Curve type Linear through origin (multiple standard values)
 Calibrate All tracks to a single curve. Units µg

Calibrated quantity - ug



Raw volume ($Y = 0 + 1.03e-005 * x$; $R = 0.967$)

VP1/3 produced by pTRAc-P12A3C; 15 – 40 % sucrose gradient purification

gels loaded with 30 μ L sample + 6 μ L SAB

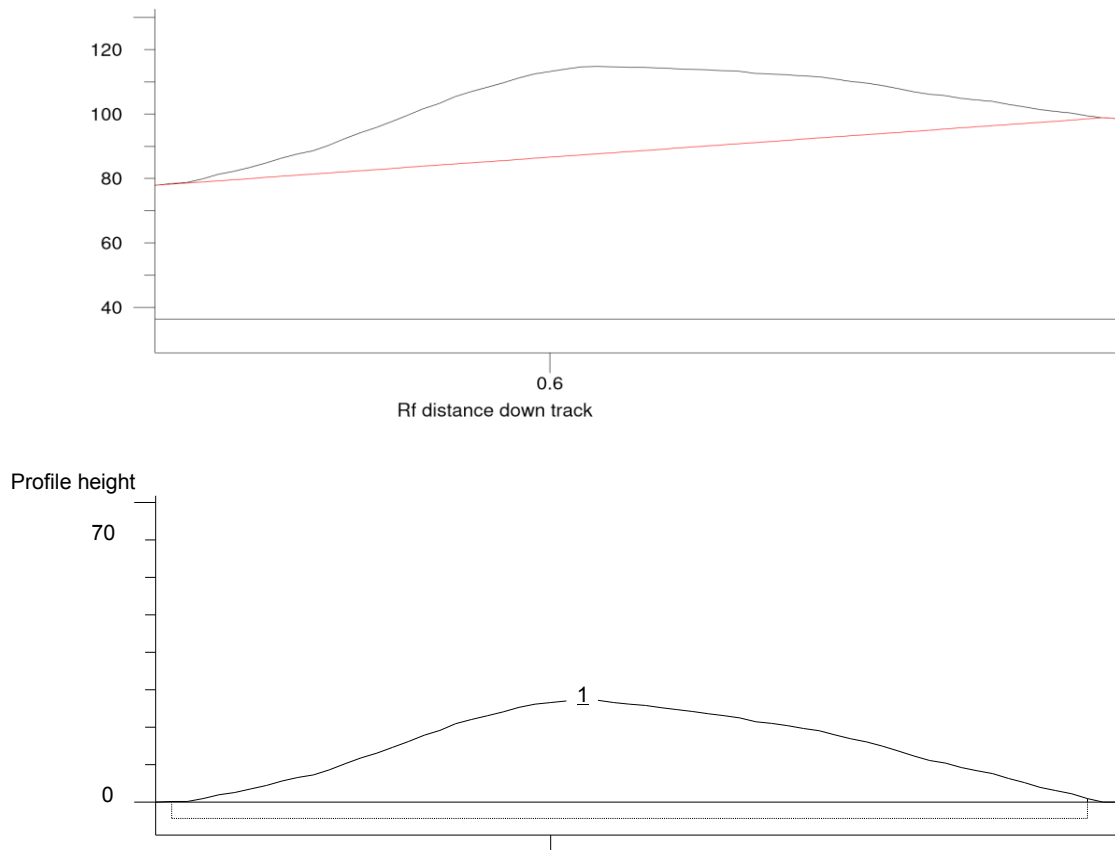


Figure A6: Track 6; VP1/3 = 1.23 μ g, Profile height = 27.391

lane 7, fraction 24, densitometry quantity estimate of VP1/VP3 25 kDa band = 1.23 μ g

$$1.23 \mu\text{g} \times (1\text{mL} / 0.03\text{mL})$$

= 41 μ g of desired FMDV VP1/VP3 capsid protein in total 1 mL fraction 24

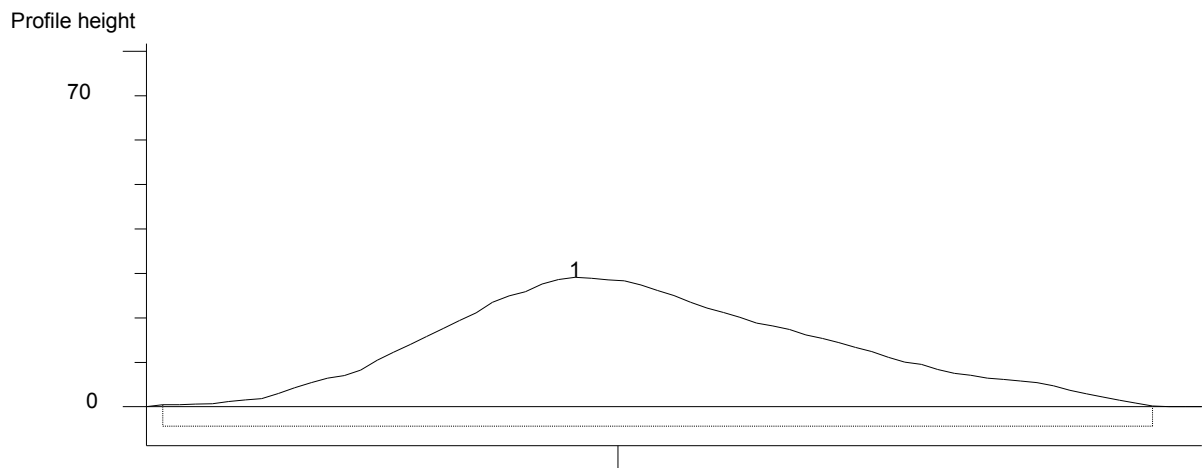
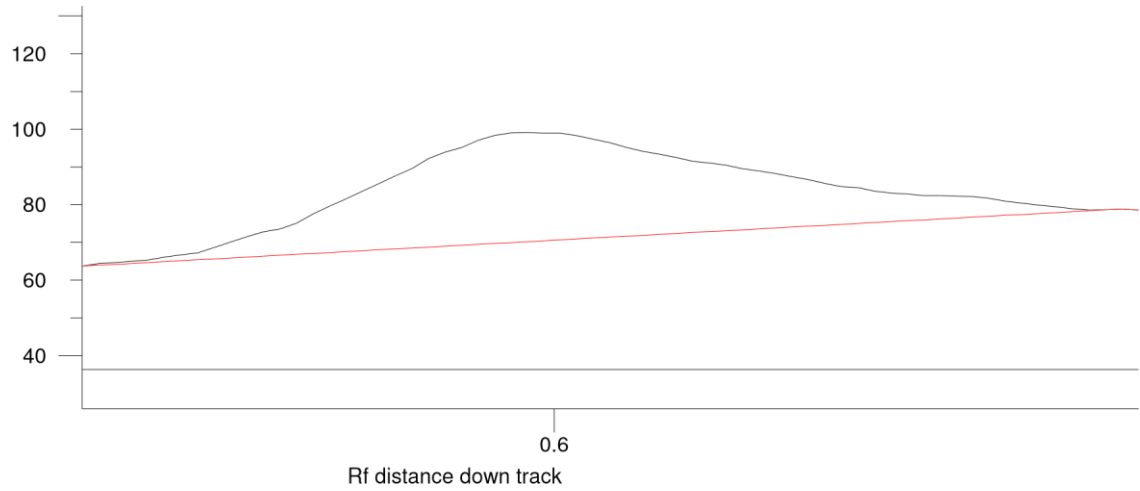


Figure A7: Track 7; VP1/3 = 0.86 μg , Profile height = 11.398

lane 8, fraction 25, densitometry quantity estimate of VP1/VP3 25 kDa band = 0.86 μg

$0.86 \mu\text{g} \times (1\text{mL} / 0.03\text{mL})$

= 28.6 μg of desired FMDV VP1/VP3 capsid protein in total 1 mL fraction 25

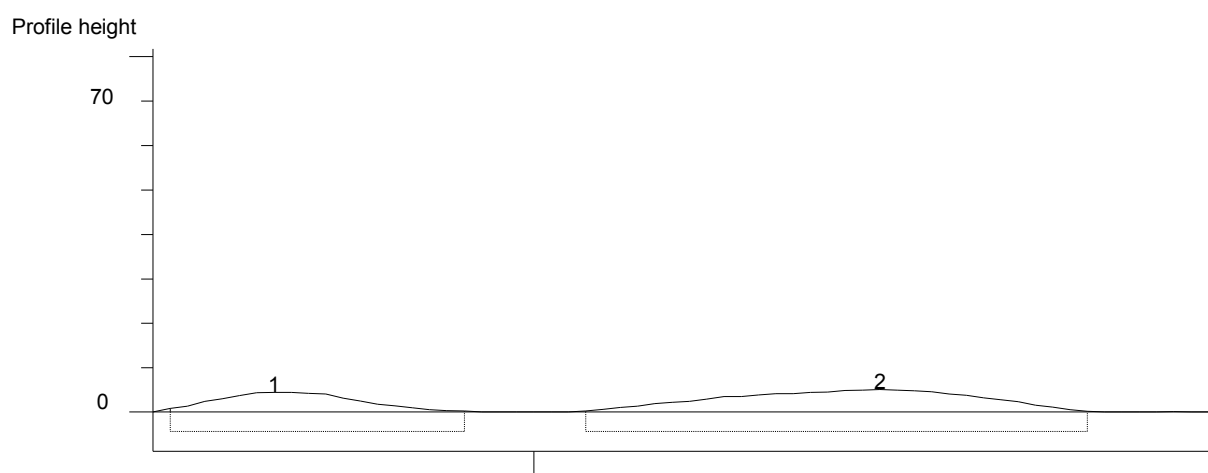
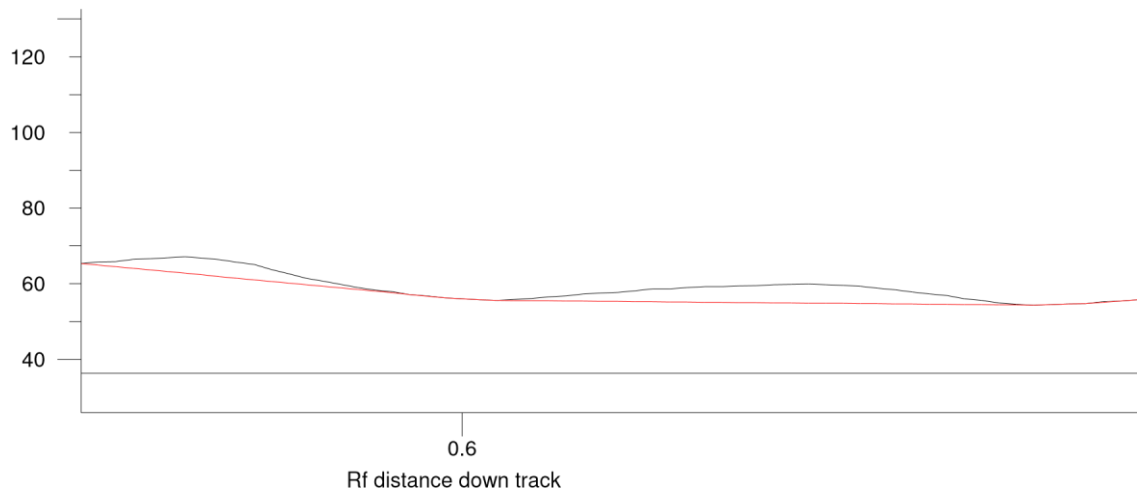


Figure A8: Track 8; VP1/3 = 0.11 µg, Profile height = 5.069

lane 9, fraction 27, densitometry quantity estimate of VP1/VP3 25 kDa band = 0.11 µg
 0.11 µg × (1mL /0.03mL)
 = 3.6 µg of desired FMDV VP1/VP3 capsid protein in total 1 mL fraction 27

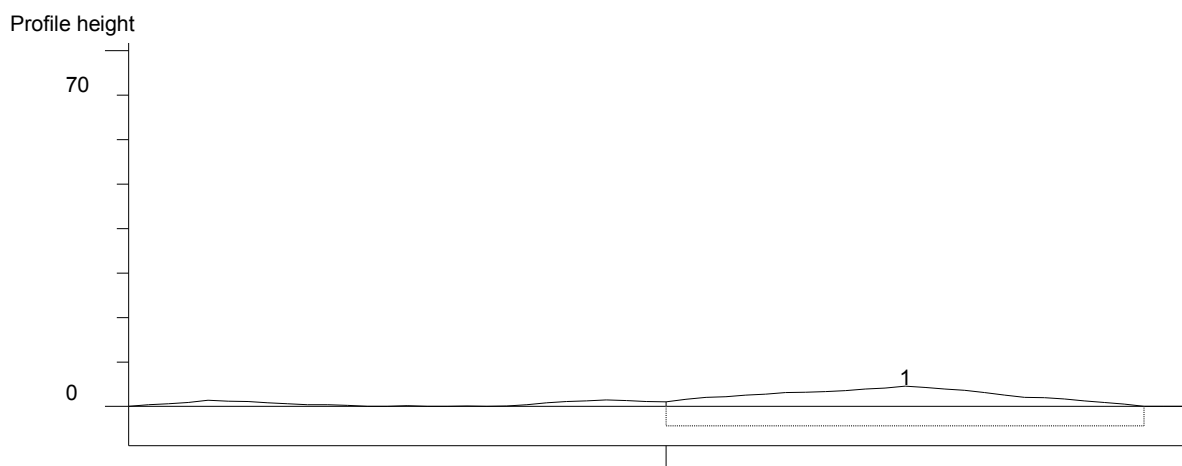
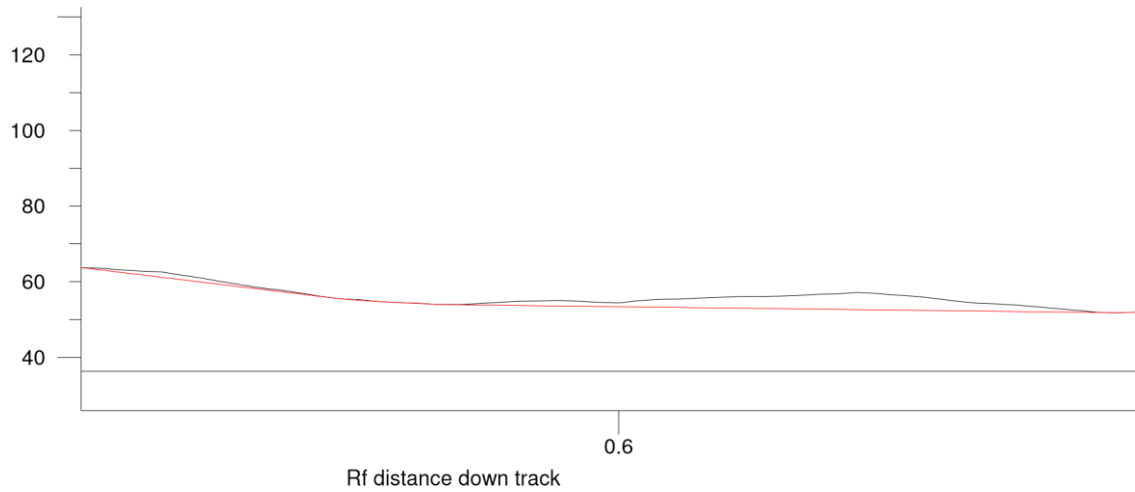


Figure A9: Track 8; VP1/3 = 0.07 μg , Profile height = 4.579

lane 10, fraction 28, densitometry quantity estimate of VP1/VP3 25 kDa band = 0.07 μg

$$0.07 \mu\text{g} \times (1\text{mL} / 0.03\text{mL})$$

= 2.3 μg of desired FMDV VP1/VP3 capsid protein in total 1 mL fraction 28

Total yield $\approx \sum$ fractions 24, 25, 27, 28

$$41 \mu\text{g} + 28.6 \mu\text{g} + 3.6 \mu\text{g} + 2.3 \mu\text{g}$$

= **75.5 μg** yield from 60 g fresh leaf mass

$$= 1.25 \times 10^{-6} \text{ or } 0.000125 \%$$

mystery band produced by pTRAc-P12A3C; 15 – 40 % sucrose gradient purification

gels loaded with 30 μ L sample + 6 μ L SAB

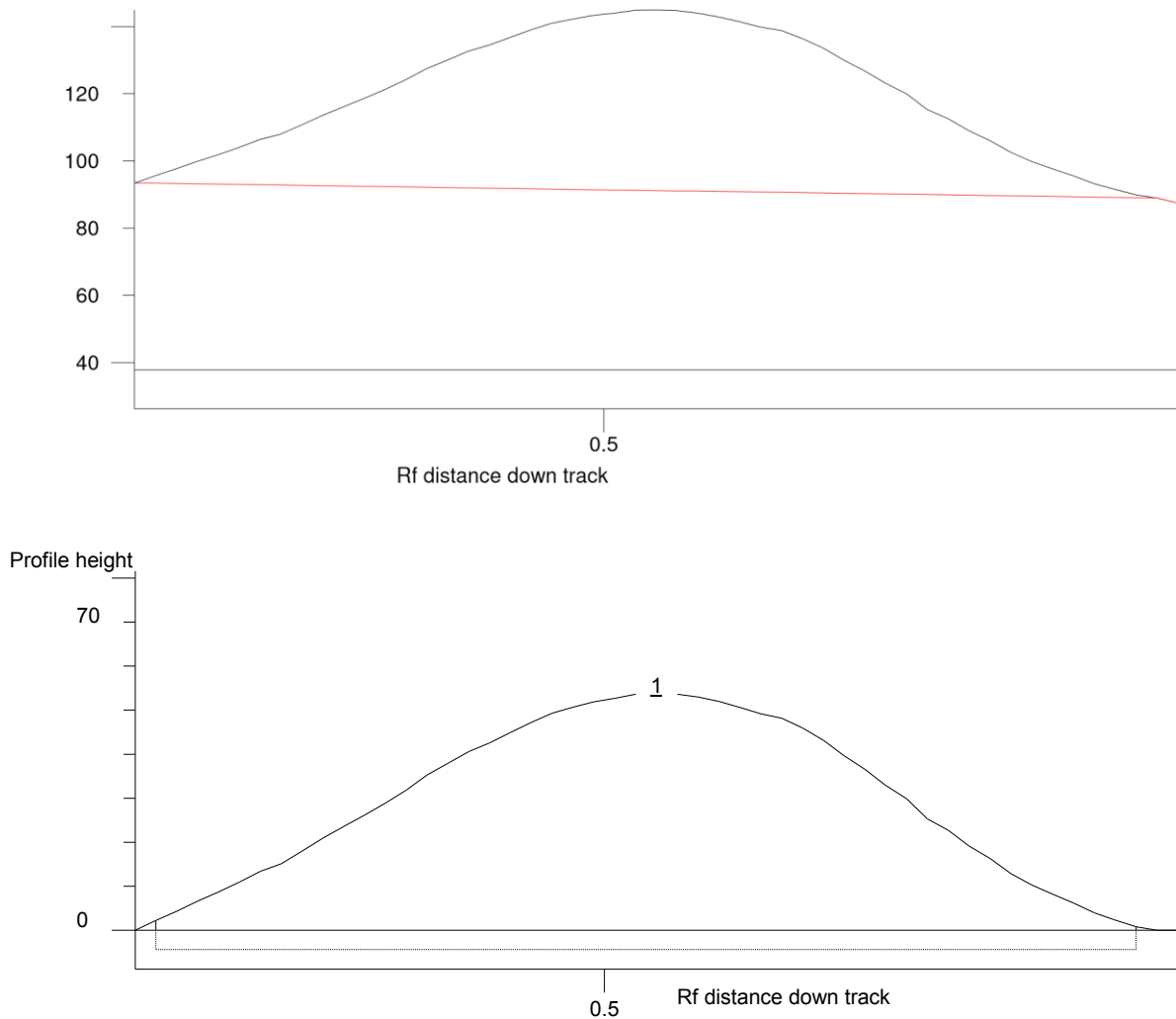


Figure A12: Track 6; mystery = 1.87 μ g, Profile height = 53.709

lane 7, track 6, fraction 24, densitometry quantity estimate of mystery <32 kDa band = 1.87 μ g

$$1.87 \mu\text{g} \times (1\text{mL} / 0.03\text{mL})$$

$$= 62.3 \mu\text{g of desired FMDV mystery protein in total 1 mL fraction 24}$$

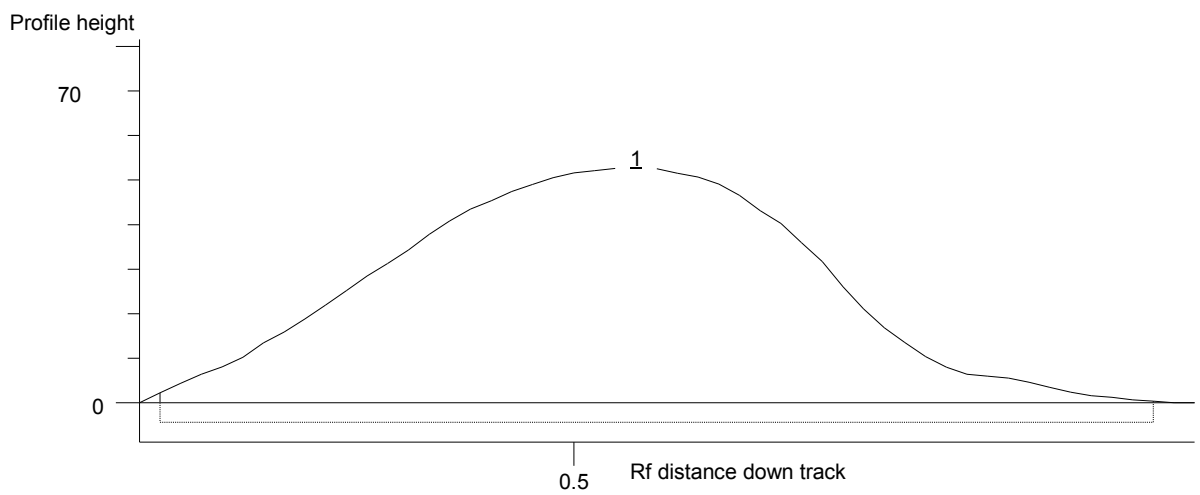
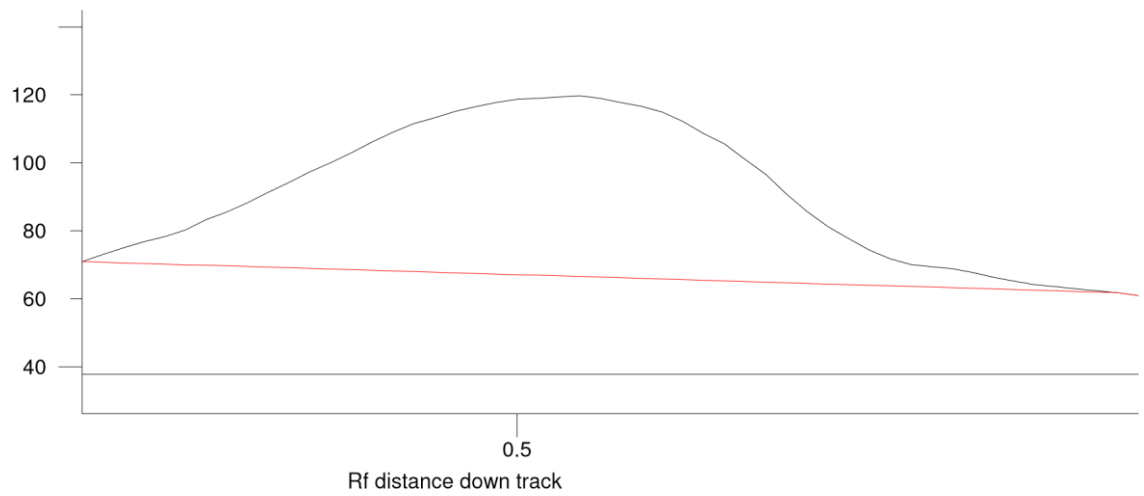


Figure A13: Track 7; mystery = 1.17 μg , Profile height = 53.171

lane 8, track 7, fraction 25, densitometry quantity estimate of mystery <32 kDa band = 1.71 μg

$$1.71 \mu\text{g} \times (1\text{mL} / 0.03\text{mL})$$

= 57 μg of desired FMDV mystery protein in total 1 mL fraction 25

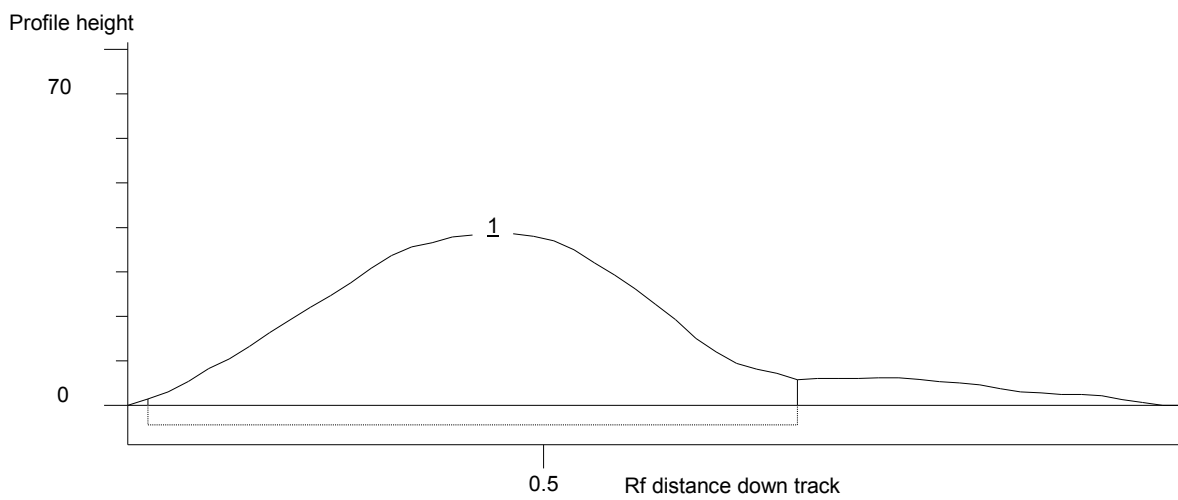
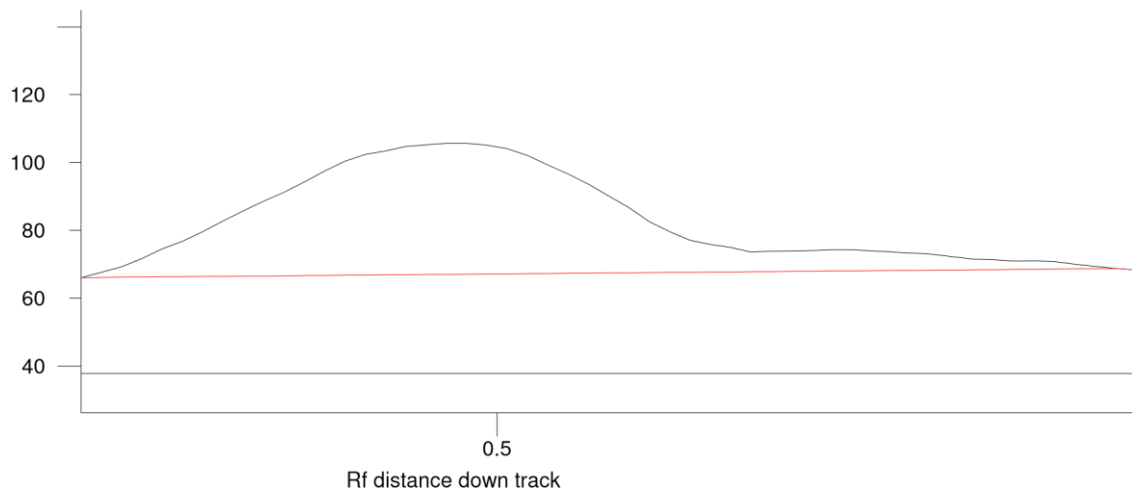


Figure A14: Track 8; mystery = 0.89 μ g, Profile height = 38.669

lane 9, track 8, fraction 27, densitometry quantity estimate of mystery <32 kDa band = 0.89 μ g

0.89 μ g \times (1mL /0.03mL)

= 29.6 μ g of desired FMDV mystery protein in total 1 mL fraction 27

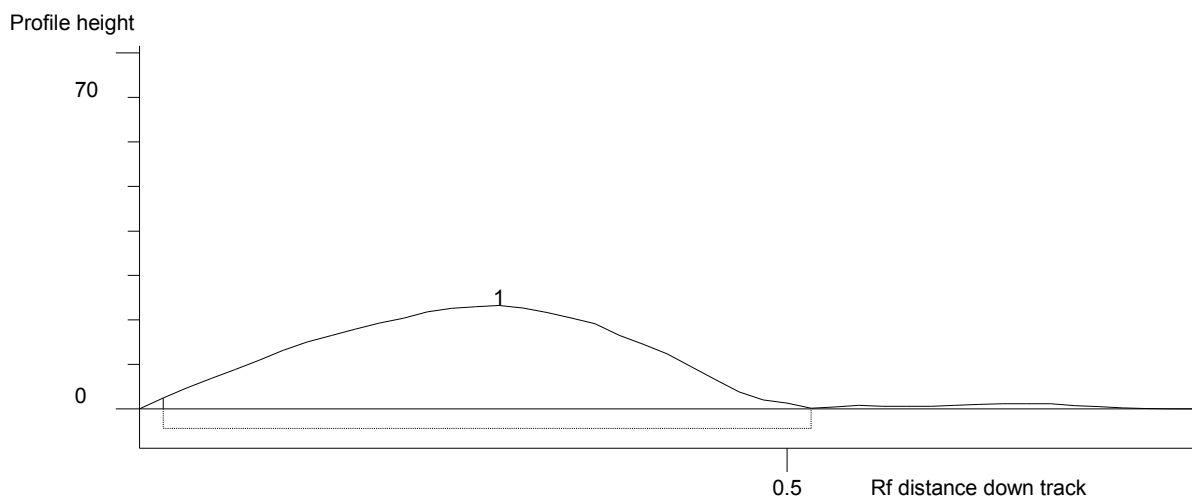
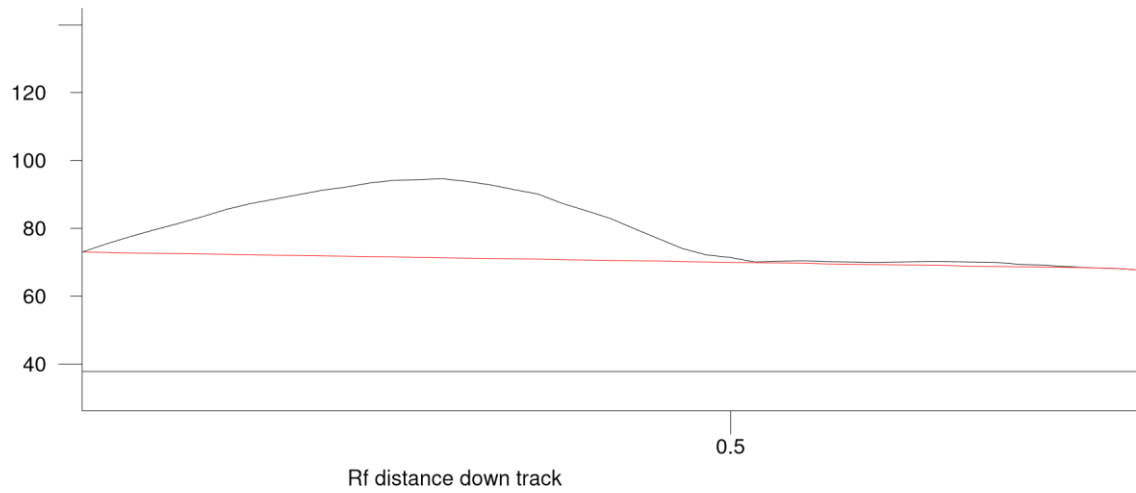


Figure A15: Track 9; mystery = 0.42 μg , Profile height = 23.621

lane 10, track 9, fraction 28, densitometry quantity estimate of mystery <32 kDa band = 0.42 μg

$$0.42 \mu\text{g} \times (1\text{mL} / 0.03\text{mL})$$

= 14 μg of desired FMDV mystery protein in total 1 mL fraction 28

Total yield $\approx \sum$ fractions 24, 25, 27, 28

$$62.3 \mu\text{g} + 57 \mu\text{g} + 29.6 \mu\text{g} + 14 \mu\text{g}$$

= 162.9 μg yield from 60 g fresh leaf mass

$$= 2.715 \times 10^{-6} \text{ or } 0.0002715 \%$$

VP0 produced by pTRAc-P12A3C; 15 – 40 % sucrose gradient purification

gels loaded with 30 μ L sample + 6 μ L SAB

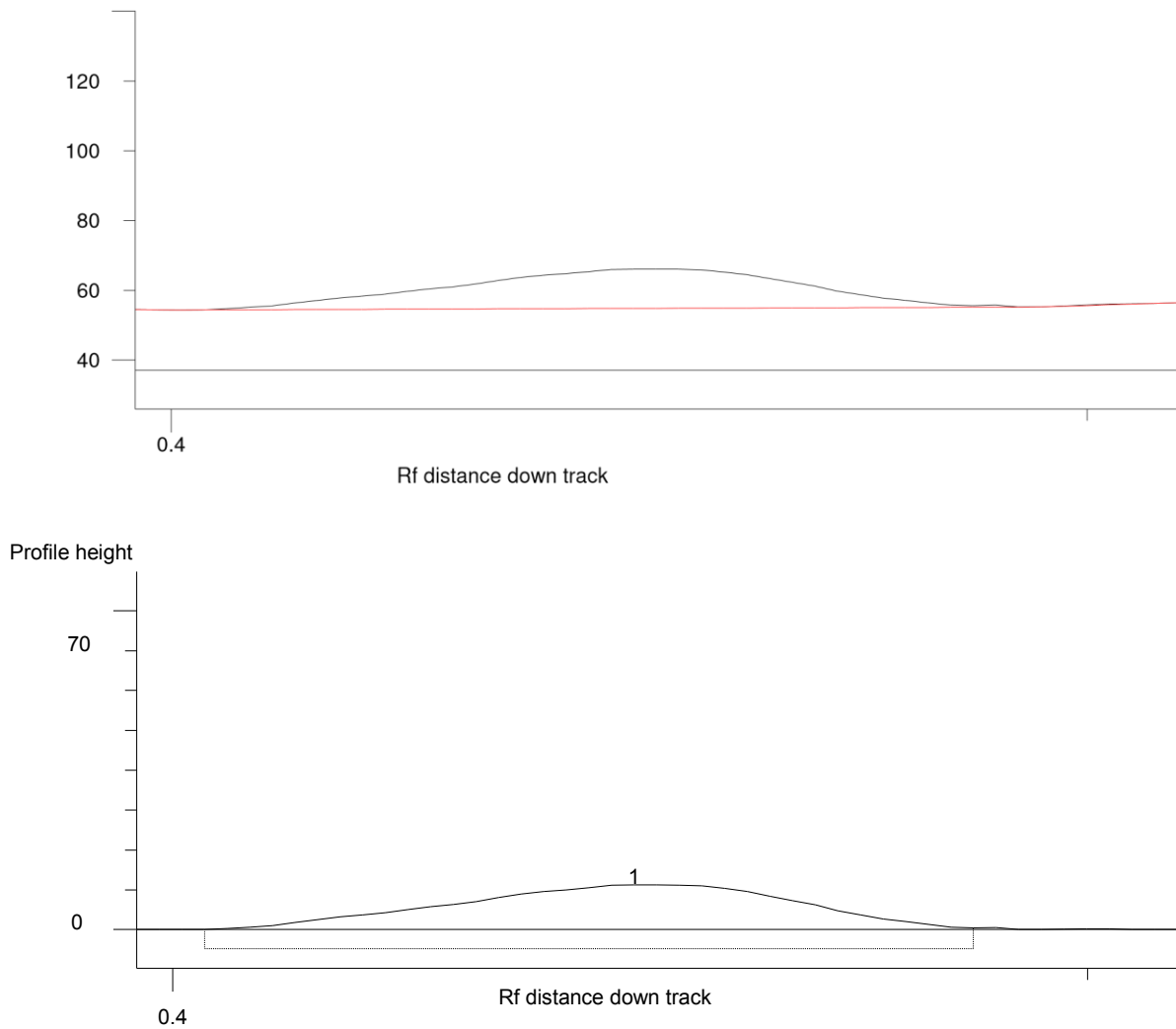


Figure A16: Track 6; mystery = 0.18 μ g, Profile height = 11.258

lane 9, track 6, fraction 27, densitometry quantity estimate of VP0 37 kDa band = 0.18 μ g

$0.18 \mu\text{g} \times (1\text{mL} / 0.03\text{mL})$

$= 6 \mu\text{g}$ of desired FMDV VP0 capsid protein in total 1 mL fraction 27

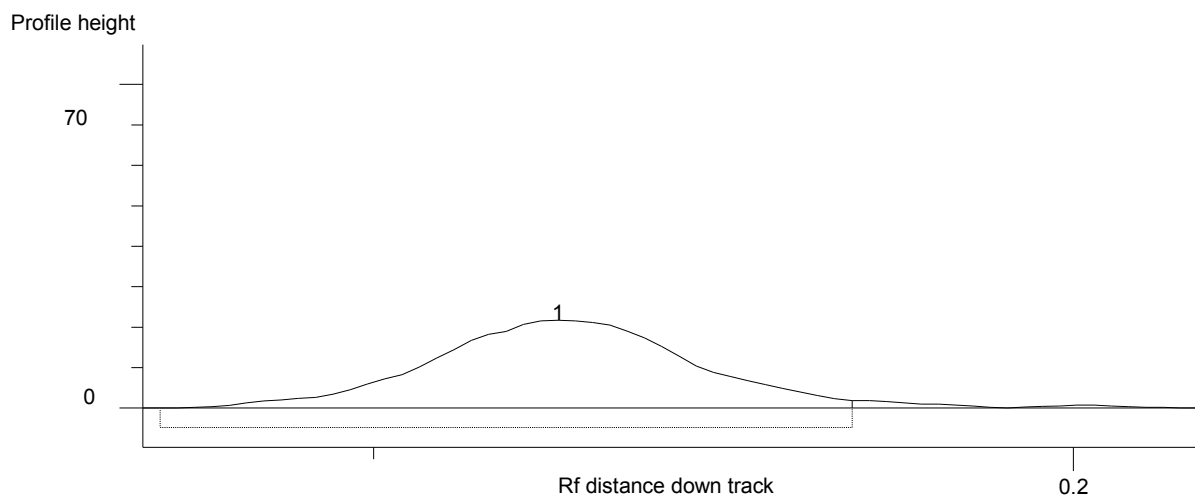
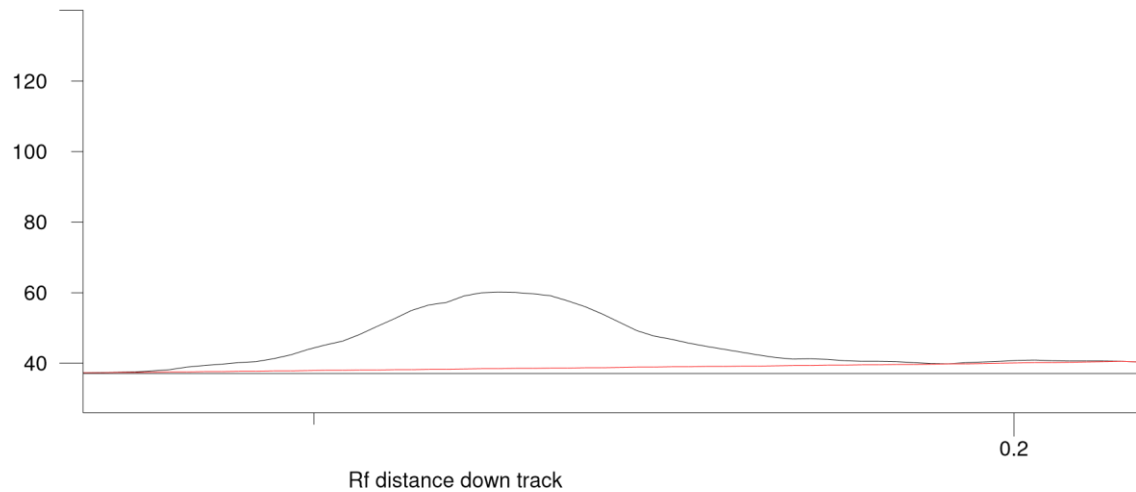


Figure A17: Track 7; mystery = 0.10 μg , Profile height = 8.434

lane 10, track 7, fraction 28, densitometry quantity estimate of VP0 37 kDa band = 0.10 μg

$$0.10 \mu\text{g} \times (1\text{mL} / 0.03\text{mL})$$

= 3.3 μg of desired FMDV VP0 capsid protein in total 1 mL fraction 28

Total yield $\approx \sum$ fractions 27, 28

$$6 \mu\text{g} + 3.3 \mu\text{g}$$

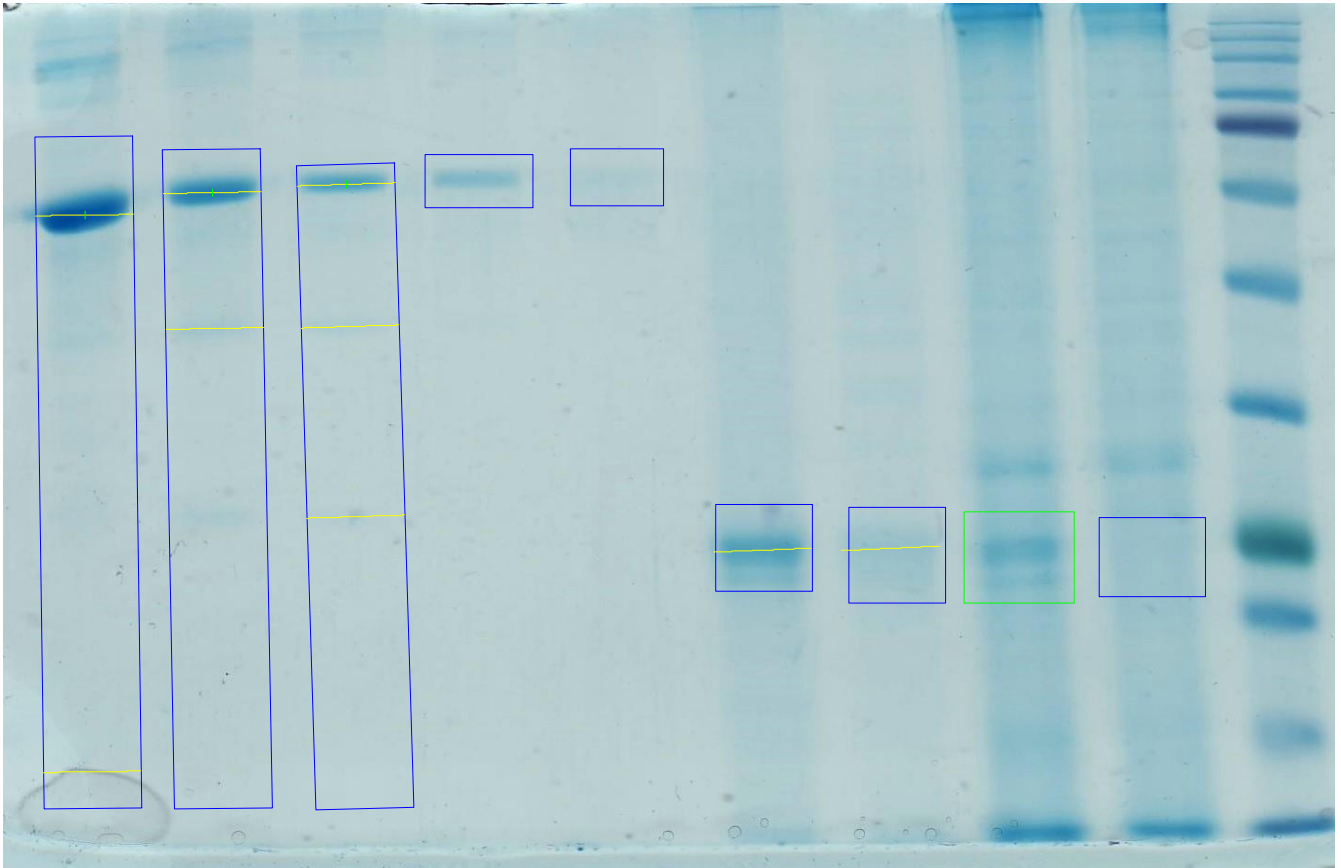
= 9.3 μg yield from 60 g fresh leaf mass = 0.155 $\mu\text{g/g}$

$$= 1.55 \times 10^{-7} \text{ or } 0.0000155 \%$$

SynGene™ software yield calculations for protein produced via pRIC3.0--P12A3C

Bovine Serum Albumin quantity calibration details

gels loaded with 30 μ L sample + 6 μ L SAB



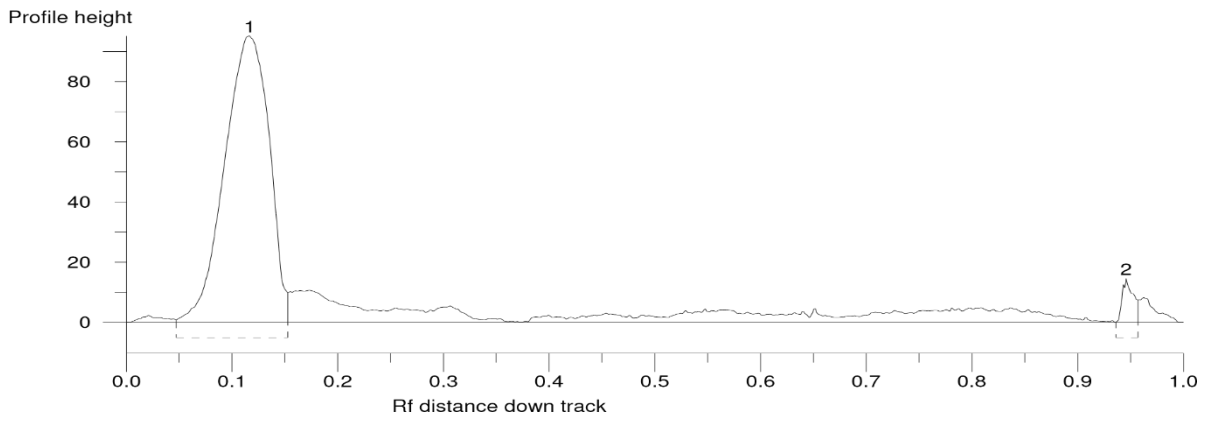
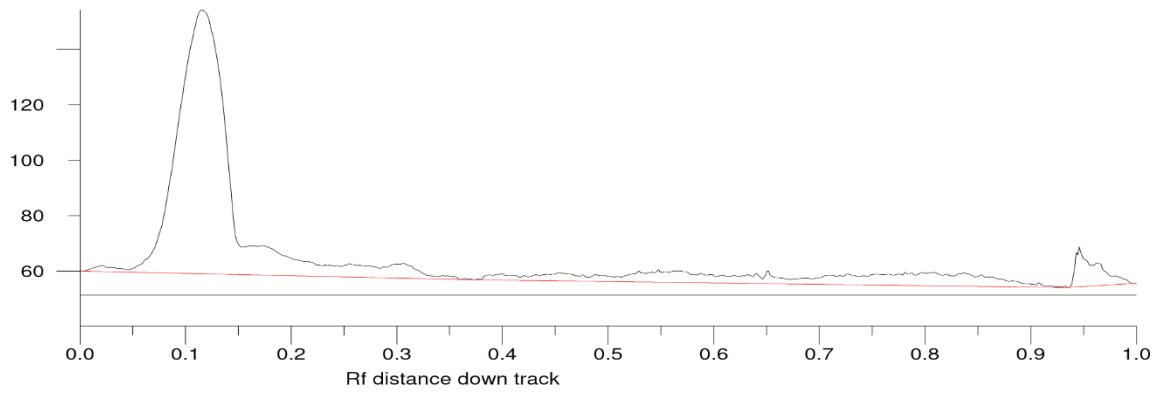


Figure A20: Track 1; BSA = 3.13 μg , Profile height = 95.131

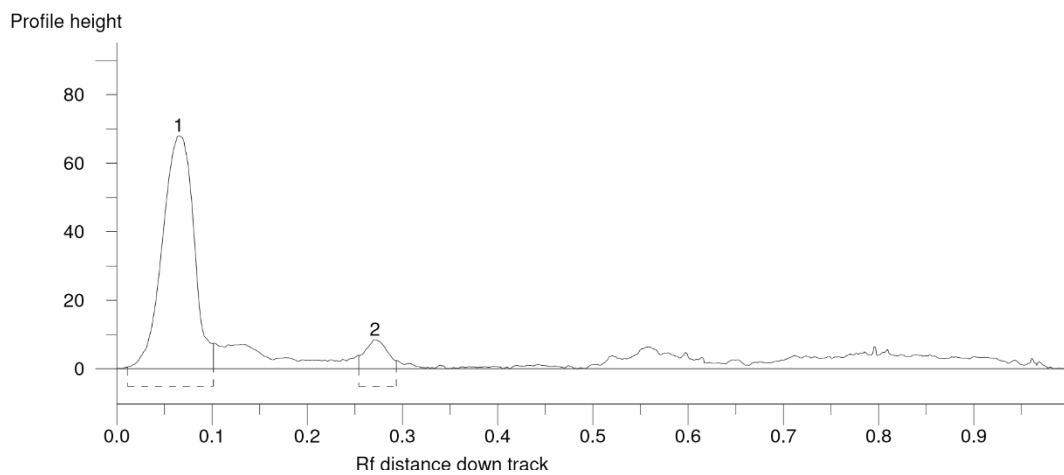
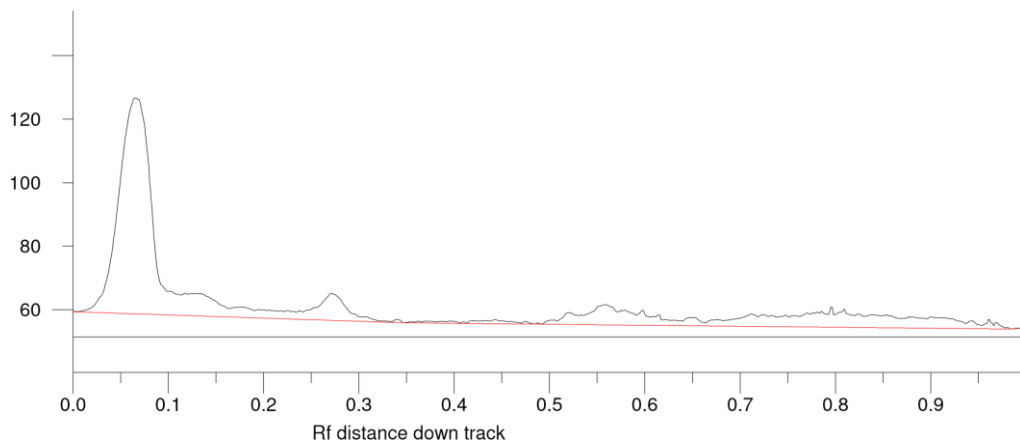


Figure A21: Track 2; BSA = 1.56 μg , Profile height = 68.035

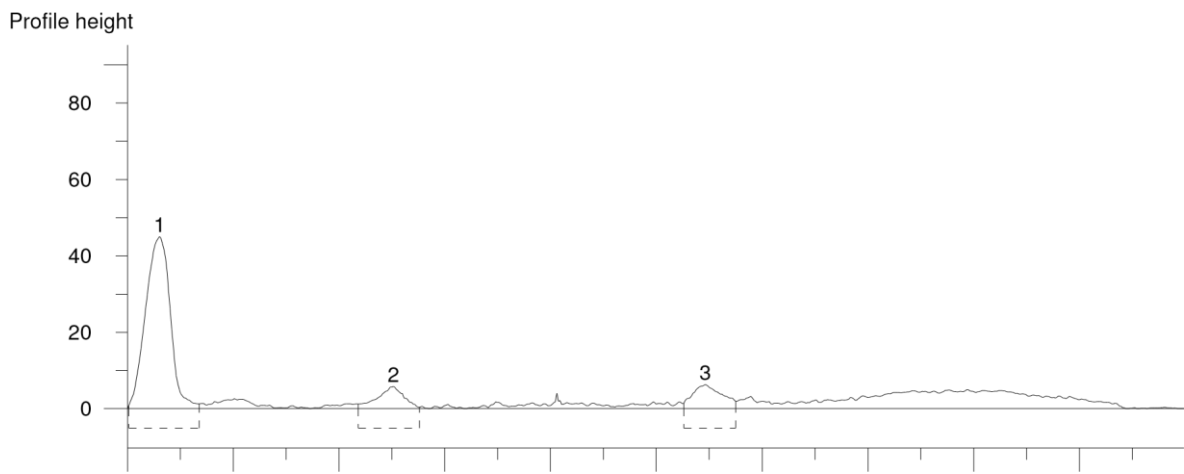
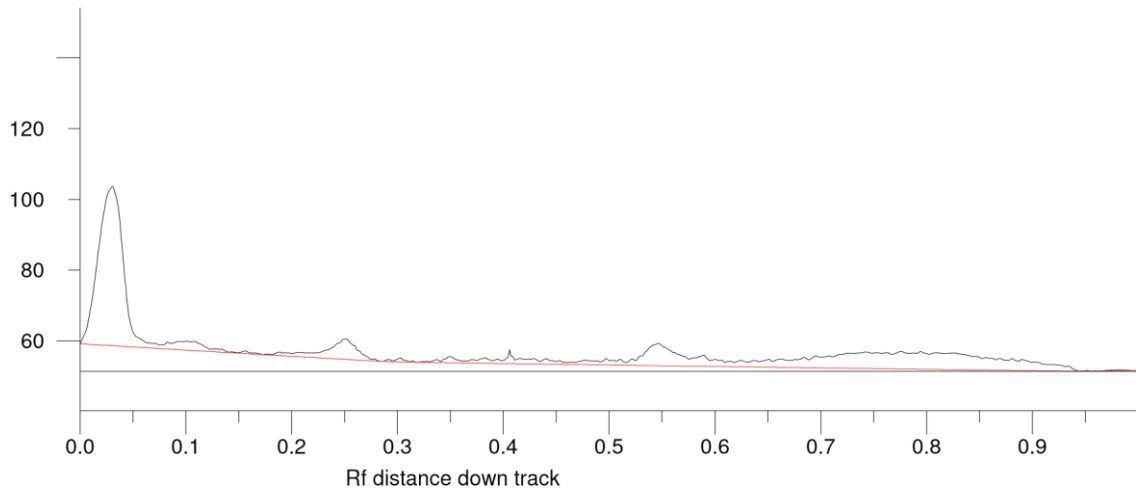
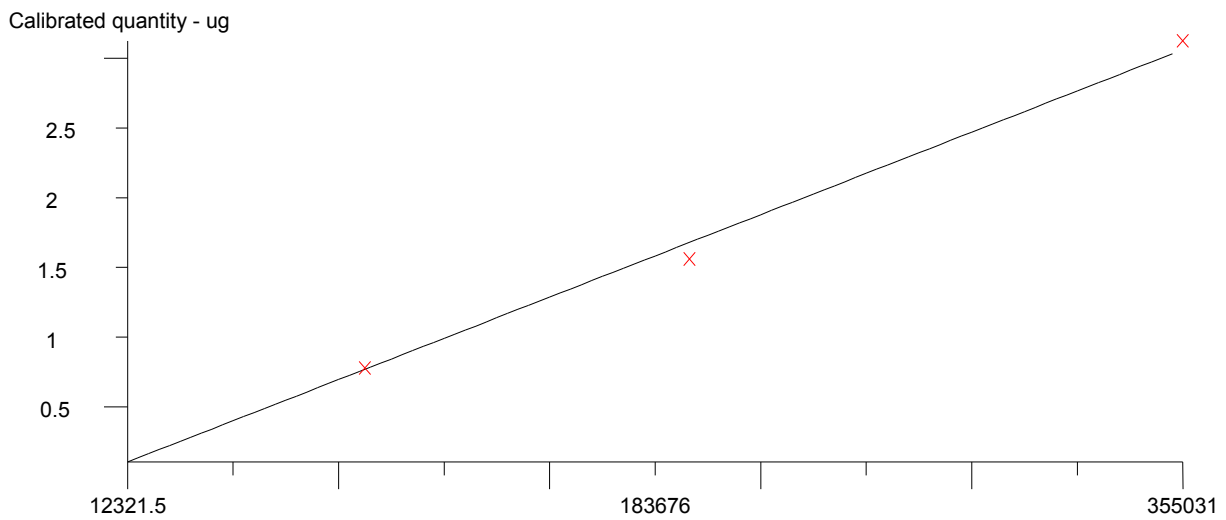


Figure A22: Track 3; BSA = 0.78 μ g, Profile height = 45.086

Curve type Linear through origin (multiple standard values)
 Calibrate All tracks to a single curve. Units μ g



Raw volume ($Y = 0 + 8.63e-006 * x$; $R = 0.998$)

gels loaded with 30 μL sample + 6 μL SAB

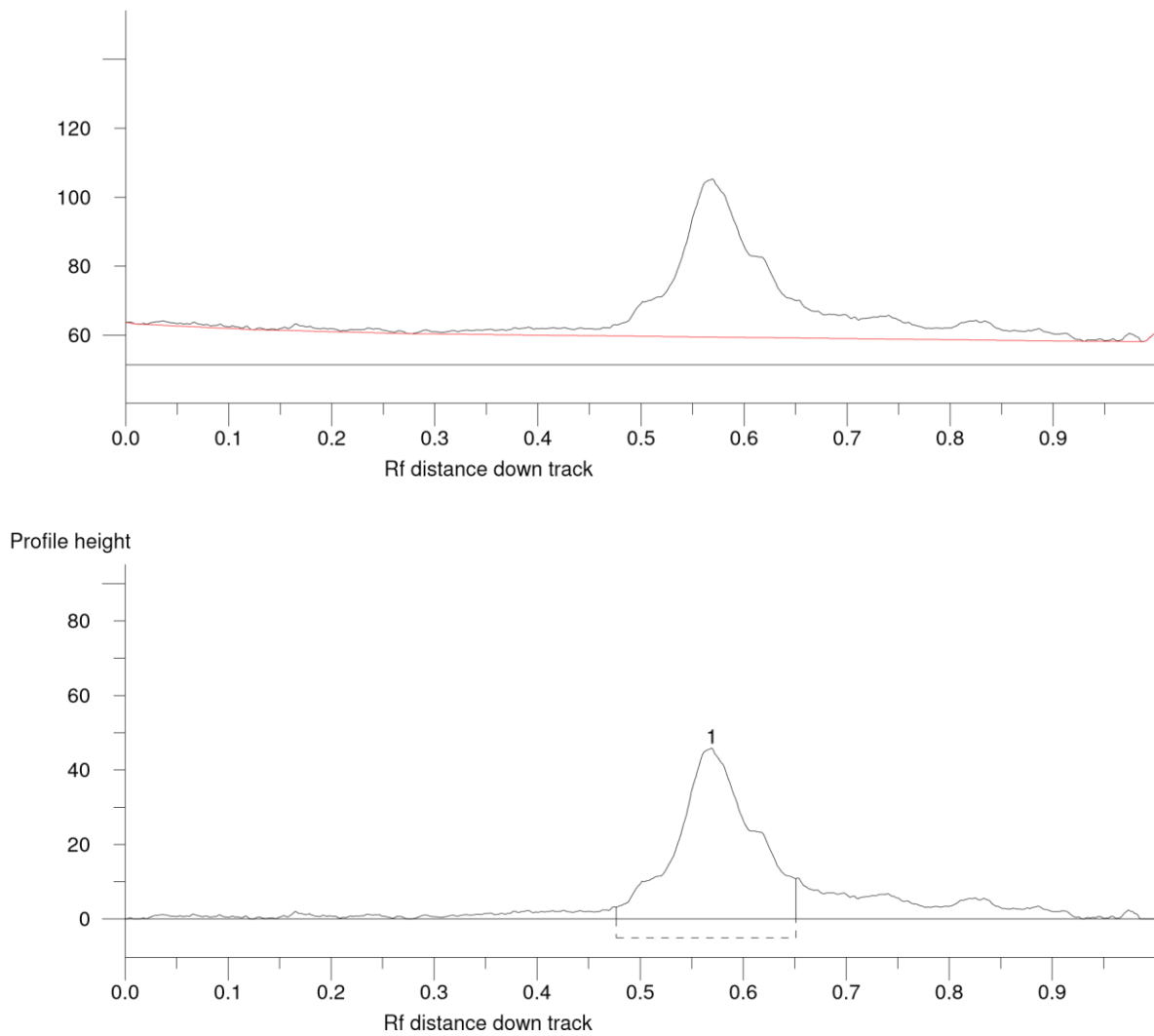


Figure A23: Track 6; VP1/3 = 2.28 μg , Profile height = 45.862

lane 6, track 6, fraction 24, densitometry quantity estimate of VP1/VP3 25 kDa band = 2.28 μg

2.28 μg \times (1mL / 0.03mL)

= 7.6 μg of desired FMDV VP1/VP3 capsid protein in total 1 mL fraction 24

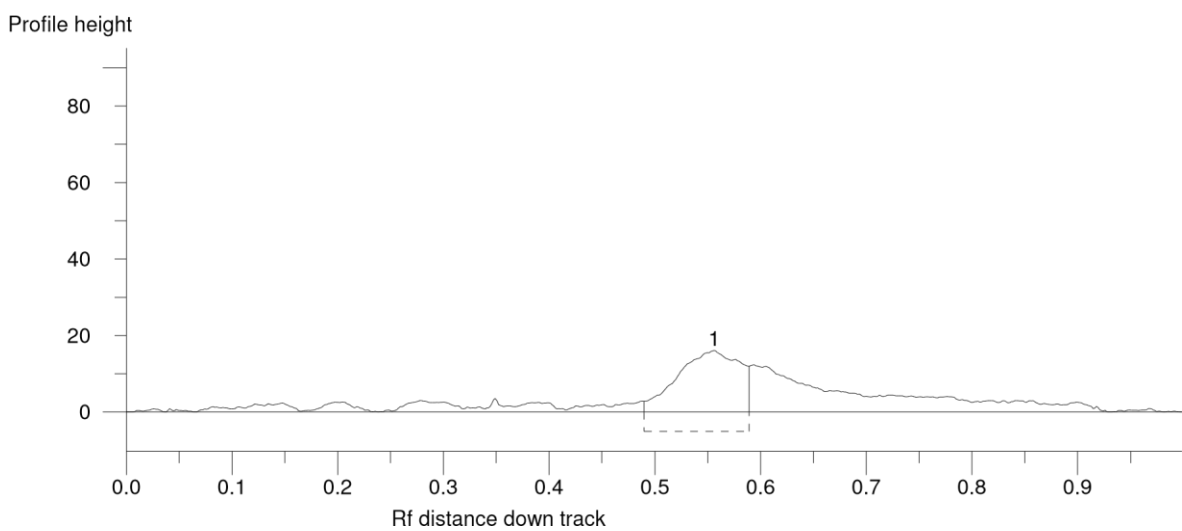
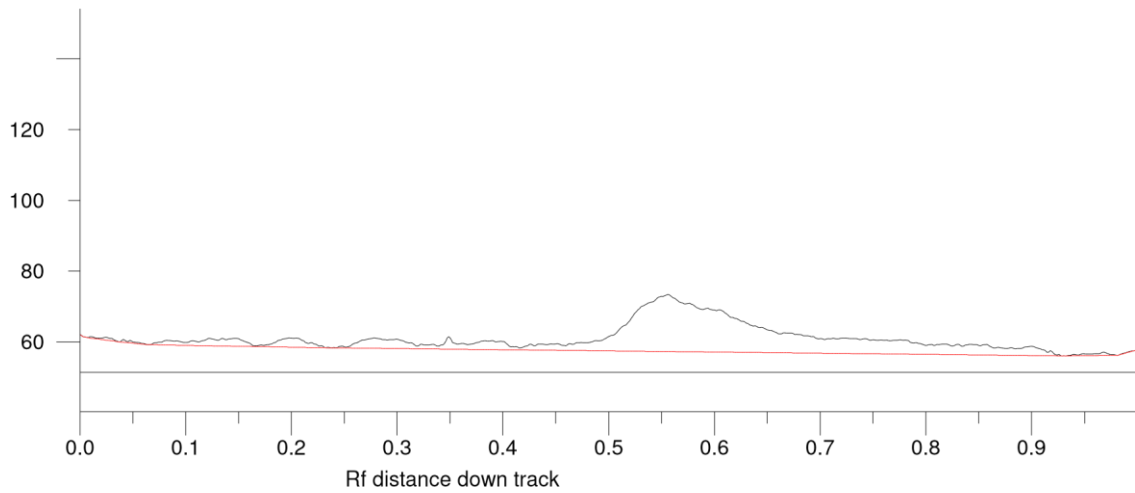


Figure A24: Track 7; VP1/3 = 0.63 μ g, Profile height = 16.111

lane 7, track 7, fraction 25, densitometry quantity estimate of VP1/VP3 25 kDa band = 0.63 μ g

$$0.63 \mu\text{g} \times (1\text{mL} / 0.03\text{mL})$$

$$= 2.1 \mu\text{g of desired FMDV VP1/VP3 capsid protein in total 1 mL fraction 25}$$

Total yield $\approx \sum$ fractions 24, 25

$$7.6 \mu\text{g} + 2.1 \mu\text{g}$$

$$= 9.7 \mu\text{g yield from 60 g fresh leaf mass}$$

$$= 1.616 \times 10^{-7} \text{ or } 0.00001616 \%$$

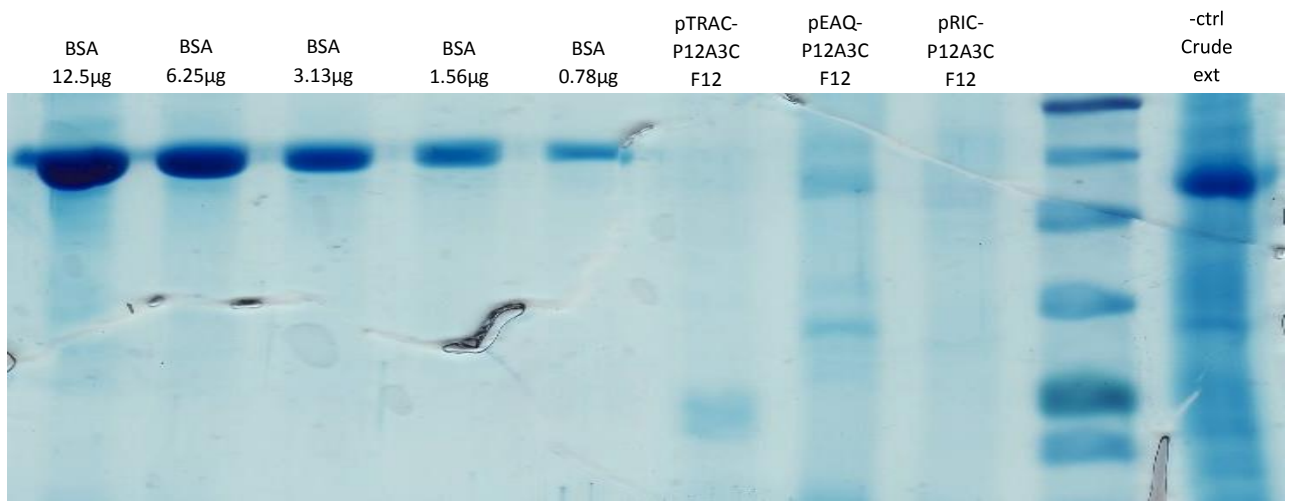


Figure C. Coomassie stain of gel comparing P12A3C expressed in *N. benthamiana*, via pTRAC,, pEAQ and pRIC; lanes 6 – 9 respectively, purified with a 5% - 20% sucrose gradient. Against Bovine Albumin Standard dilution series. Lane 1 = BAS 12.5 µg; Lane 2 = 6.25 µg; lane 3 = 3.13 µg; lane 4 = 1.56 µg; lane 5 = 0.78µg; lane 6 = pTRAc-P12A3C Fraction 12; lane 7 = pEAQ-P12A3C Fraction 12; lane 8 = pRIC-P12A3C Fraction 12; lane 10 = pTRAc-empty crude extract. Ladder used = NEB # P7712S boad range protein marker.